1-1-2007

Study of scour caused by obliquely impinging plunging and non-plunging turbulent jets.

Piyali Chaudhuri
University of Windsor

STUDY OF SCOUR CAUSED BY OBLIQUELY IMPINGING PLUNGING AND NON-PLUNGING TURBULENT JETS

by

Piyali Chaudhuri

A Thesis
Submitted to the Faculty of Graduate Studies
through Civil and Environmental Engineering
in Partial Fulfillment of the Requirements for
the Degree of Master of Applied Science at the
University of Windsor

Windsor, Ontario, Canada

2007

Your file Votre référence
ISBN: 978-0-494-35045-4
Our file Notre référence
ISBN: 978-0-494-35045-4

ABSTRACT

In this research an effort is made to better understand the scour caused by obliquely impinging square turbulent jets in a cohesionless bed for both plunging and non-plunging conditons. The variables of interest are time and the jet impinging angles. Experiments were carried out at different test durations, five jet impinging angles and two tailwater conditions corresponding to the plunging and the non-plunging cases. Velocity measurements were conducted using a laser Doppler anemometer for jet impinging angle of 0°. The densimetric Froude number was maintained at ten, while the jet expansion ratio was held greater than ten. The results indicate that jet impinging angles and tailwater depths, both have an influence on the extent of scour caused by three-dimensional jets. Empirical equations to describe the scour depth are proposed for the asymptotic state and are found to be valid for a wide range of impinging angles.

DEDICATION

To Almighty, my parents and husband

ACKNOWLEDGEMENTS

I would like to express my great and sincere gratitude to my advisors Dr. Nihar Biswas and Dr. Ram Balachandar for their invaluable guidance, advice, thoughtful insights, continuous support, and encouragement throughout my work on this thesis.

I would also like to offer my thanks to graduate committee, Dr. G. Rankin, and Dr. E. Carriveau for their helpful comments, suggestions and advice.

I wish to extend my sincere thanks to Mr. Mathew St. Louis and Mr. Lucian Pop for their prompt help and assistance during my work.

Special thanks to Dr. Shineeb, Mr. M.A.A Faruque, Vesselina and Arjun for their assistance during writing the thesis.

Finally, great appreciation is expressed to my parents and my husband for their encouragement and support throughout my life.

TABLE OF CONTENTS

LIST OF TABLES

LIST OF FIGURES

LIST OF APPENDICES

LIST OF SYMBOLS

A	Area of the nozzle
b_o	Width of the nozzle
B	Width of the flume
d	Diameter of the jet
d_{16}	Sand diameter, 16 % of which is finer by weight
d_{50}	Median size of bed material
d_{84}	Sand diameter, 84 % of which is finer by weight
D	Sand diameter
F_o	Densimetric Froude number [$= Uo/\{g(\Delta\rho/\rho)d_{50}\}^{0.5}$]
F_r	Flow Froude number [$=U_o/(gb_o)^{0.5}$]
g	Acceleration due to gravity
h_o	Ridge height
h_{imp}	Vertical impingement distance
H	Tailwater depth
LDA	laser Doppler anemometer
L_i	Angular impingement distance
L_{off}	Distance from nozzle bottom to the start of the scour hole
L_s	Length of scour hole
L_T	Distance of the ridge end from the nozzle bottom
Re	Reynolds number [$= U_o b_o/\nu$]
t	Time
U_o	Average jet velocity

V_o	Volume of scour hole
w	Width of scour hole
x	Longitudinal distance
x_m	Distance of maximum depth of scour hole from the nozzle
y	Vertical distance
z	Lateral distance
α	Jet impinging angle
β	Percent of air content
$\Delta\rho$	Difference between the mass densities of water and bed material
ρ_s	Mass density of bed material
ρ	Mass density of water
ε_m	Maximum scour depth
σ_g	Geometric standard deviation of bed material $[=(d_{84}/d_{16})^{0.5}]$
ν	Kinematic viscosity

CHAPTER 1
INTRODUCTION

1.1 Introduction

Scour is a topic of importance in hydraulic engineering practice. It is a natural process that takes place as part of the morphologic changes of rivers and also as an outcome of man-made structures. Scour is the removal of soil or fill material from streambeds and stream banks when the hydrodynamic shear stresses exceed the sediment critical shear stress. Scour also occurs in cohesive materials, like clay and even in deeply weathered rock. Scouring can progressively undermine the foundation of a structure. Erosion near dam outlet works, spillways, or foundation threatens the operation or safety of hydraulic structures. As complete protection against scouring is usually prohibitively expensive, and engineers often seek ways to guide and control the process so as to minimize the risk of failure. This guidance comes both from controlled studies in laboratories and from field experience. Despite much study, the principles of analysis of scouring are not well established and the results of various investigations often show differing trends.

When a water jet enters a water body away from the boundary there is intense turbulent action at the point of entry. If the same jet enters a water body near a boundary the turbulent action results in the state of dynamic scour and the hole deepens until a quasi-equilibrium state is reached. At this state, usually denoted as an asymptotic state, the size of the hole or other geometric parameters does not change with time. Such type of scenario is relevant in many applications of hydrology, geomorphology and hydraulic engineering. Thus, the study of scour by high speed impinging flows are important for

assessing the stability of hydraulic structures, such as vertical gates, flip bucket spillways, hydraulic jump type stilling basins and culverts that may be affected by erosion of the downstream bed.

1.2 Plunge Pool Scour

Occurrence of plunge pools (scour holes) is a common feature near hydraulic structures. Plunge pools serve as significant stream energy dissipaters, increasing flow resistance and enhancing stream channel stability. These features may also improve habitat diversity and serve as refugia for stream biota during low flow periods.

As applied to hydraulic engineering, plunge pools are common features of dam structures (Figure 1.1). The plunge pool is a widened and deepened section of the downstream channel into which the spillway discharges flow. They are an economic means to dissipate hydraulic energy of high speed flows and are located at the end of trajectory spillways or bottom outlets as applied in dam engineering. The flood discharge for surface spillways is first conveyed over a gated or ungated spillway crest which is followed by a chute. Once the discharge has reached a level close to the dam foot it is directed into a flip bucket and ejected in the air. The air-water jet travels through the atmosphere and strikes a plunge pool where the hydraulic energy is dissipated and a level of tailwater travels in the downstream watercourse. The energy in the jet after striking with the plunge pool gets dissipated by the turbulence in the pool and by shear with the surrounding water and with the boundaries of the pool (Pagliara et al., 2004). Plunge pool scour at the foot of hydraulic structures like trajectory spillways may cause structural undermining which may endanger the dam foundation and destabilization of the adjacent

valley slopes. Thus, scour due to plunging jets are significant concerns both for structural foundation and are also causes of backwater due to the ridge formation, where the scour material is deposited.

The main concerns of the plunge pool are its structural stability, tailwater submergence and ridge geometry which is aggravated by the impinging high-speed jet. The reason that the plunge pool by trajectory spillway jets has received only limited attention until today is the complex experimental arrangement (Hager et al., 2004). Hence, limited information is available on the scour from these types of jets (Afify and Urroz, (1994); Minor et al., (2002); Canepa and Hager, (2003); Pagliara et al., (2006).

1.3 Scour Categories

Scour has been defined as the enlargement of a flow section by the removal of material composing the boundary by the action of the fluid motion (Laursen, 1952).

Scour can be divided into the following types (Breusers and Raudkivi, 1991):

General Scour: It occurs in a river or stream as a result of natural processes irrespective of whether a structure is present.

Constriction Scour: It occurs if a structure causes the narrowing of a watercourse or the rechanneling of berm or flood plain flow.

Local Scour: It results directly from the impact of the structure on the flow. This scour is a function of the type of structure and is superimposed on the general and constriction scour.

Scour can be divided based on different conditions of transport (Breusers and Raudkivi, 1991):

Clear-water scour: It occurs if the bed material in the natural flow upstream of the scour area is at rest. The shear stresses on the bed some distance away from the structure are thus not greater than the critical or threshold shear stresses for the initiation of particle movement.

Live-bed scour: It is referred to as scour with bed material sediment transport, and occurs when the flow induces a general movement of the bed material, i.e the shear stresses on the bed are greater than the critical one. Equilibrium scour depths are reached when the amount of material removed from the scour hole by the flow equals the amount of material supplied to the scour hole upstream.

1.4 Jet Classification

Flow through hydraulic structures often issues in the form of a jet. Jet is the flow of fluid of higher velocity emitting into the surrounding fluid of lower or no velocity (Rajaratnam 1976). The characteristics of jets can be influenced by the design of nozzle geometry (nozzle shape, nozzle cross- section) and the ambient conditions surrounding the jet. A jet is commonly classified as a free jet (unconfined) when it is not influenced by any physical/fluid structures surrounding the jet. It should be remarked that the characteristics of jets in confined situations have been studied to a lesser extent even though a number of practical situations reflect a confined three-dimensional analysis.

Depending on the density of the surrounding fluid, the jet can be classified into two types:

i) Non-buoyant: Jet and surrounding fluid have the same density.

ii) Buoyant: Jet density is less than that of the surrounding fluid.

Based on the geometric configuration, jets are classified into four types:

i) Free Jet: The fluid flow is far from any solid boundary.

ii) Wall Jet: The fluid flow takes place at the boundary of the location of the jet.

iii) Horizontal offset Jet: The jet axis is at some distance away from the bed/boundary but the jet initially flows parallel to the bed.

iv) Impinging Jet: The jet flows at some angle towards the bed or boundary.

A distinction can also be made between two-dimensional, three-dimensional jets (based on their aspect ratios) and circular jets. Non-circular jets can have enhanced entrainment properties relative to comparable circular jets, due to axis rotation of the jet cross section resulting from deformation of vortex rings with non-uniform curvature (Sankar, 2005). As a result of their enhanced mixing properties non-circular jets find their applications in devices where mixing is a subject of vital importance. Jets are said to be submerged when they exit into the fluid of equal or higher density, otherwise they are said to be unsubmerged jets. Based on the type of flow jets are also classified as laminar or turbulent jets. Another distinction can be made depending on whether jet plunges into a waterbody. Jets are said to be plunging when they travel through air and fall into a water body, whereas they are called non-plunging when the jets are ejected from within the waterbody.

Literature provides very little information about the characteristics of a jet emanating from a square cross-section that interacts with a sand surface. The present study aims to investigate clear water local scour of cohesionless soil caused by non-buoyant, three-dimensional (square) turbulent jets under plunging and non-plunging conditions.

1.5 Objectives

The present study aims to investigate and compare the scour caused by plunging of a three-dimensional (square) turbulent water jet with that of a non-plunging jet. In particular, the dynamic scour resulting from the interaction of a three-dimensional jet with cohesionless sand in unsubmerged/plunging and submerged/non-plunging conditions will be investigated.

The specific objectives of this study are:

1) To study the time development of scour on cohesionless sediments.
2) To study the effect of jet impinging angles.
3) To study and compare the scouring effects of the plunging jet with a non-plunging jet for a constant impinging distance.

1.6 Scope

The scope of the study was as follows:

1) A well-designed square nozzle was used to carry out the experiments.
2) One type of cohesionless uniform fine sand grain was used as the bed material.
3) The impinging height of the jet was held constant for both plunging and

non-plunging conditions.

4) The time variations of the scour geometry were studied for different test conditions up to the asymptotic state.
5) At the end of each test the centerline scour profiles, perimeter of the scour hole, the perimeter of the ridge and the volume of the scour hole were measured.
6) The centreline velocity profiles at different downstream locations of the nozzle were measured by laser Doppler anemometry (LDA) measuring technique during the experiment for an impinging angle of 0°.
7) In order to study the effect of jet impinging angles both the sets of plunging and non-plunging jet experiments were done for different impinging angles (0°, 15°, 30°, 45°, 90°).

1.7 Organization of the Thesis

This thesis is organized into five chapters. Chapter 1 refers to the scour problem and the issues that lead to the objectives of the thesis. Chapter 2 consists of a review of previous studies done by different researchers on scour caused by turbulent jets in cohesionless soil. Chapter 3 provides a description of the experimental setup and test program. Chapter 4 presents the results and analysis of data. Chapter 5 provides the conclusion from the present study and the recommendations for future work.

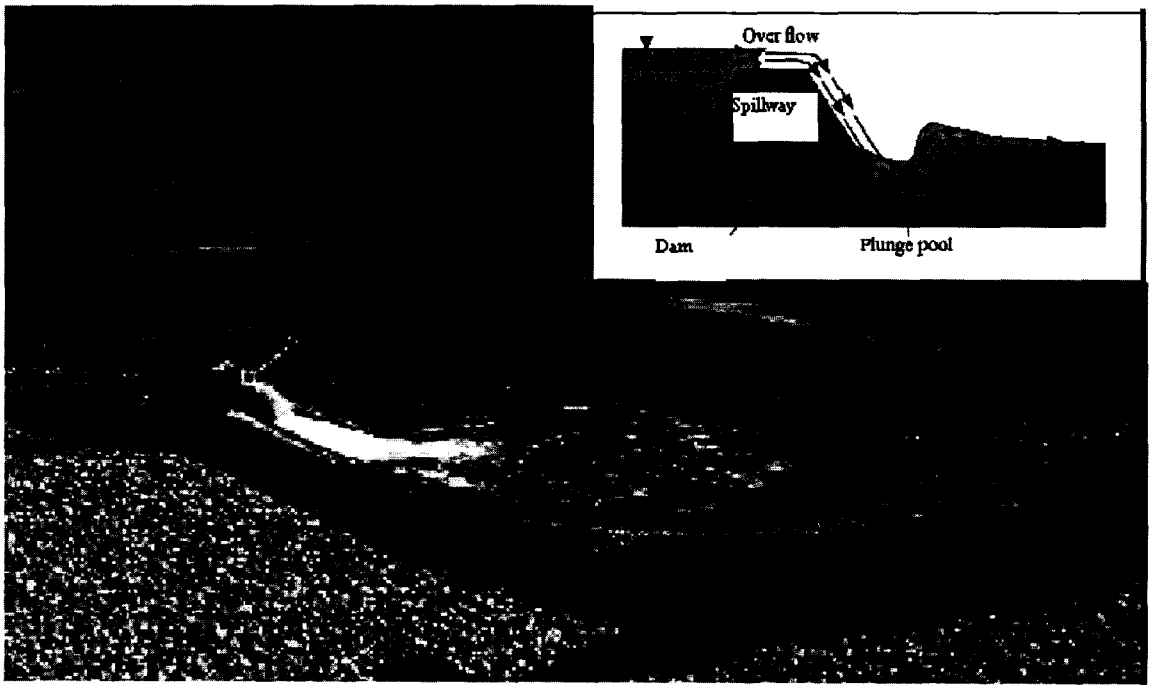

Figure 1.1: Photograph showing the plunge pool from spillway, photo taken from the 7-Oaks dam in California; top right shows the schematic diagram of the plunge pool, photo taken from Azuma et al., 2006

CHAPTER 2
LITERATURE REVIEW

2.1 Introduction

In this chapter, the previous study on the scour due to jets interacting with the cohesionless soils has been discussed. In this review, the research carried out on scour caused by different types of jets has been emphasized in order to illustrate the need for investigation on the specific area. In this literature review, studies conducted on scour caused by plane wall jets, three-dimensional wall jets, offset jets as well as plunging jets has been discussed. The focus of this thesis is to study the scour caused by plunging jets at different jet impinging angles, hence special emphasis has been given to the details of the plunging jet case which is the area that needs further investigation.

2.2 Previous studies on scour by jets:

2.2.1 Scour by Plane Turbulent Wall Jets:

The plane wall jet is defined as a rectangular jet (having a large aspect ratio) that initially flows tangentially along a boundary surrounded by stationary (or moving) fluid (Rajaratnam, 1976). A plane turbulent wall jet, as defined by Rajaratnam (1976), is a jet of thickness b_o and uniform velocity U_o issuing from a rectangular slot tangentially to a flat plate surrounded by stationary (or moving) fluid. As soon as the jet leaves the slot or nozzle, it possesses tremendous scouring potential created by the high incoming velocity resulting in sediments immediately being dislodged from the initial flat erodible bed, lifted and held in suspension due to counter clockwise eddies, and then transported downstream at a rapid rate. Most of the jet scour studies have been carried out with plane

turbulent wall jets interacting with cohesionless soils (Tarapore, 1956; Rajaratnam, 1981; Rajaratnam and MacDougall, 1983; Aderibigbe and Rajaratnam, 1998, Balachandar et al. 2000). Most of these studies have been conducted at high degree of submergence. Scour development was found to vary logarithmically with time up to a certain time until asymptotic state is reached when no significant change occur (Tarapore, 1956). The rate of scouring seems to decrease with time. However studies by Balachandar and Kells (1997) have indicated the absence of an asymptotic state even at the end of 144 hours of testing. Balachandar and Kells (2000) have showed a cyclic behaviour of jets with alternate digging and refilling of the scour hole at relatively lower submergence but at high submergence no alternate flicking of the jet was noticed (Deshpande et al., 2007). Bey et al., (2006) have noted the importance of turbulent eddies in influencing scour, especially at the latter stages of development of scour. Rajaratnam (1981) and Ali and Neyshabouri (1991) found that the equilibrium maximum scour depth was mainly a function of densimetric Froude number (F_o). At the end of every section importance of each variable is discussed and the evaluation of each of the parameter is carried out.

2.2.2 Three-dimensional Wall Jets:

Scour caused by three-dimensional wall jets has not been studied as extensively as plane jets. Rajaratnam and Berry (1977) have studied scour produced by circular wall jets and concluded that the main geometric characteristics of the scour hole are functions of the F_o. Rajaratnam and Diebel (1981) has also performed experiments using a similar set-up at low tailwater depths. They concluded that relative tailwater depth and relative width of the channel do not affect the maximum depth of scour but the location of

maximum scour was affected. The effect of tailwater depth (H) has been studied by Ali and Lim (1986) on two-and three-dimensional wall jets with shallow tailwater depths and noted that tailwater depth had an influence on the maximum depth of scour at asymptotic conditions for $2.9 < F_o < 12$. They found a critical tailwater depth beyond which any increase or decrease in tailwater causes an increase in the maximum depth of scour. This critical value increases with increase of F_o and the effect of tailwater is insignificant when $H/b_o > 16$.

Lim (1995) has studied the effect of channel width to nozzle width ratio (expansion ratio, B/b_o) on scour development and concluded that scour depth was unaffected when $B/b_o \geq 10$ but affected when B/b_o was 5.

Faruque et al., (2006) studied the effect of tailwater depth on local scour by three-dimensional (square) wall jets interacting with cohesionless soil and his results showed that scour depth tends to be larger at lower submergence. Importantly, he concluded that the densimetric F_o, tailwater depth and grain size-to-nozzle size ratio, all have an influence on the scour development for three dimensional wall jets. Sarathi et al., (2007) has studied local scour caused by square jets interacting with cohesionless sand bed to investigate the role of nozzle size-to-grain size ratio and tailwater depth. He has observed that at a certain F_o, the evolution of scour with time depends on nozzle size-to-grain size ratio, however, at asymptotic state, the scour hole parameters were found to be less dependent on grain size. Sarathi et al., (2007) has also found that the maximum depth of the scour hole depends on the tailwater depth but it is limited to $H/b_o \leq 1$ for $F_o = 3.9$, at $F_o = 6.6$ it is limited to $H/b_o \leq 3$. However, tailwater has a minimal effect on the

maximum width of the scour hole though the length of scour hole seemed to be sensitive to tailwater depth at shallower conditions.

2.2.3 Offset Jets:

Ali and Neyshabouri (1991) studied scour caused by two-dimensional deeply submerged turbulent offset jets. Due to the plunging nature of the jet and impingement on the sand bed, the bed particles were found to move upstream and downstream directions forming two dunes. In the beginning the dimensions of the upstream dune increases faster than the downstream dune but after a long duration the rate of erosion became reduced. The maximum depth of scour has been considered to be functions of particle size, F_o and offset height.

Chiew and Lim (1996) also studied local scour by deeply submerged circular offset jets. They concluded that maximum depth of scour hole reduces with increase of the offset distance and attributed this to the phenomena of jet diffusion. This trend is because the kinetic produced by the jet is farther away from the sediment bed reducing its scouring ability. Thus it can be concluded that the formation of an offset scour hole is not only dependent on F_o but also on the offset distance.

Karki et al., (2007) has studied scour by two-dimensional offset jets and concluded that there was no formation of two dunes as mentioned by Ali and Neyshabouri (1991). Karki et al., (2007) has also studied scour by three-dimensional offset (square) jets and found that the shape of the geometry of the scour hole and the corresponding ridge are elongated longitudinally and decreased laterally as the offset distance is increased. The

offset length (L_{off}), defined as the distance between nozzle and the point of beginning of scour hole was found to increase with increasing offset distance.

2.2.4 Impinging Jets

Figure 2.1 shows the schematic diagram of a jet impinging on a sand bed. All the geometric parameters and symbols used in the following sections have been defined in the figure. A dimensional analysis by Buckingham's pi theorem yields:

$$\frac{\varepsilon_m}{b_o} = f\{\mathrm{Re} = \frac{U_o b_o}{\nu}, F_o, \frac{H}{b_o}, \frac{d_{50}}{b_o}, \frac{B}{b_o}, \frac{U_o t}{b_o}, \frac{L_i}{b_o}, \frac{h_{imp}}{b_o}, \alpha, \beta\} \tag{2.1}$$

Here, t is the time from the start of the test, B is the width of the channel, L_i is the impingement distance and β is the percent of air content. Based on previous studies and the test conditions used in the present study, the effect of Reynolds number is considered small.

2.2.4.1 Effect of Impingement height (h_{imp} or L_i)

Most of the studies dealing with jet impingement on sand beds have been empirical due to the complex nature of the process. For obliquely impinging jets, the two limiting cases are the perpendicularly impinging (α = 90°) and the wall jet (α = 0°), see Figure 2.1. A number of investigations have been carried out to study erosion in cohesionless bed by vertically impinging circular jets (Westrich and Kobus 1973, Rajaratnam and Beltaos 1977; Aderibigbe and Rajaratnam 1996, Rajaratnam and Mazurek 2003), and horizontal circular wall jets (Rajaratnam and Berry, 1977; Lim, 1995; Chiew and Lim, 1996; Ade and Rajaratnam, 1998). However, relatively few

studies have been published on the more complicated case of erosion produced due to oblique impingement of turbulent jets (Mih and Kabir, 1983; Pagliara et al., 2006).

It is observed that the erosion characteristics of a scour hole produced by a non-plunging circular turbulent jets impinging at 90° to the bed at large impingement height h_{imp} (height of the nozzle exit above the soil bed) is different from the scour produced when the jet is close to the bed. For large impingement heights where the jet is fully developed before impinging on the bed, the maximum depth of the scour hole (ε_m) is properly scaled with h_{imp}, and ε_m / h_{imp} is mainly a function of $F_o = \frac{U_o}{\sqrt{gD(\rho_s - \rho)/\rho}}$.

However, for small impingement heights where the potential core of the jet impinges on the bed, the maximum depth of scour scales with d (diameter of the jet) as ε_m/d and is a function of F_o (Rajaratnam and Beltaos 1977; Aderibigbe and Rajaratnam, 1996). For non-plunging circular turbulent jets flowing tangentially to the bed ($\alpha = 0°$), ε_m/d was found to be a function of only F_o (Rajaratnam and Berry, 1977) and described by the equation:

$$\frac{\varepsilon_m}{d} = 0.39F_o - 0.78 \qquad (2.2)$$

For the study on erosion of polystyrene bed by obliquely impinging circular turbulent air jet at large impingement height (Rajaratnam and Mazurek, 2002), shows that the asymptotic scour depth, total scour length and width of scour hole in terms of the impingement height as a function of $F_o/(L_i/d)$. It is seen that the maximum scour depths produced by obliquely impinging jet is larger than would be produced by perpendicular impinging jet as in the latter case much of the sand stays suspended in a recirculating

flow within the scour hole, which settles out when the jet is stopped (Aderibigbe and Rajaratnam, 1996). However, the obliquely impinging jet has a component of flow that is parallel to the bed, allowing greater potential for the movement of particles out of the scour hole. For the jet impact angle 30° to 60° the maximum scour depth (Rajaratnam and Mazurek, 2002) can be described by:

$$\frac{\varepsilon_m}{L_i} = 0.73\frac{F_o}{(L_i/d)} - 0.10 \tag{2.3}$$

and for jet impact angle 7.5° and 15° the maximum scour depth can be described by:

$$\frac{\varepsilon_m}{L_i} = 0.77\frac{F_o}{(L_i/d)} - 0.20 \tag{2.4}$$

An experimental investigation on the study of erosion of sand beds by obliquely (10°, 30°, 45°, 60°) impinging submerged circular turbulent jets has been done by Rajaratnam et al., (1995). They has concluded that the main characteristics of the eroded bed profile such as maximum scour depth, height of ridge, length of scour hole are functions of parameter $\frac{F_o}{\sqrt{h_{imp}/2b_o}}$, where $2b_o$ is the thickness of the jet at the nozzle.

One can conclude that the impingement height is an important geometric parameter for plunging jets. In the present study the vertical impingement height has been held constant ($11b_o$) for both the plunging and non-plunging cases and the height is greater than the length of the potential core of the jet.

2.2.4.2 Effect of Tailwater depth (H)

Some investigations have been performed to examine the erosion of cohesionless material by submerged impinging jets, where the tailwater depth is large, including those of Westrich and Kobus (1973), Rajaratnam and Beltaos (1977), Mih and Kabir (1983),

Aderibigbe and Rajaratnam (1996) and Rajaratnam and Mazurek (2003). The outcomes found in the literature are usually related to circular impinging jets in submerged condition, whereas investigations in the unsubmerged condition are quite rare. It is considered that the tailwater depth is yet another important variable to understand scour caused by jets.

Rajaratnam and Mazurek (2003) have carried out an experimental study on the erosion of loose cohesionless sand beds by a plunging vertical impinging circular water jets at a small tailwater depth. They concluded that the maximum depth of erosion increases linearly with the logarithm of time for a longer time of erosion process and eventually reaches an asymptotic state. The asymptotic scour depths as well as the radius of the scour hole in terms of the diameter of the impinging jet at the level of the original uneroded sand bed are mainly functions of the densimetric Froude number. They also made a comparative study between the two distinct states of erosion, the dynamic scour that exists when the jet is on and the static scour that exists after the jet is turned off, and concluded that dynamic scour is three times the static scour in the asymptotic state. Also included are the results that the maximum depth of scour produced by a plunging jet is less than that for a non-plunging jet for $0.4 < F_o/(h_{imp}/d) < 2.1$ but for larger values of $F_o/(h_{imp}/d)$, the plunging jet produces deeper scour than non-plunging jet. The scour hole radius of the plunging jet is less than that produced by a non-plunging jet for $F_o/(h_{imp}/d) <1$.

The effect of tailwater ratio (Height of water level above sand bed/Diameter of jet=H/d) was investigated for the case of plane plunge pool scour using circular

impinging water jets for H/d=0.7-10 (Pagliara et al., 2006). The results shows that for impact angle 30°; H/d >5 maximum scour depth is small due to relatively high ridge, 3< H/d < 4.5, ridge height increases to its absolute maximum along with small increase of scour depth. When H/d = 2 the ridge is eroded and the scour hole deepens, depending upon the grain size and water velocity. But the erosion of ridge has not been thoroughly analysed as sediment motion depends on other additional parameters.

Literature also shows that the ratio between static and dynamic scour depth depends on the jet impact angle whereas the effect of jet submergence is relatively small except for small angles (Pagliara et al., 2004). Thus, a thorough investigation is needed to study the effect of scour due to obliquely impinging water jets on sand beds with varying degrees of submergence. The present study investigates and compares the scour caused by the plunging with the non-plunging jets such that the distance from the nozzle opening to the free surface is held constant at $1b_o$, while the impingement height is also constant. This results in H/b_o being slightly greater for the non-plunging jets.

2.2.4.3 Effect of Time (t)

Many of the previous studies were interested only in the scour hole dimension due to an impinging circular turbulent jet (Rajaratnam and Beltaos 1977; Rajaratnam 1981; Blaisdell and Anderson 1991; Borman and Julien 1991). It seems that during a significant portion of the erosion process, the maximum depth of erosion varies linearly with the logarithm of time (Rajaratnam, Beltaos 1977) and departs from this trend to approach an asymptotic state. Empirical equations to predict the quasi-equilibrium depth of scour hole have been summarized based on the experimental data by these researchers. Blaisdell et al. (1991) expressed the scouring process using semi-log, log-log, and

hyperbolic functions and discussed how an equilibrium scour depth is achieved. He also indicated that the time scale of the scour is related to the quasi-equilibrium scour hole depth. On the other hand, fewer studies concentrate on the process of scour hole development. As has been pointed out by Blaisdell et al. (1991), that the sediment transport process in a plunge pool shows that sediment particles are detached and entrained by turbulent burst or fluctuations of flow properties caused by the impinging jet, even when the mean shear stress is smaller than the critical shear stress for a given bed material.

Rouse (1939) has studied the scour under two-dimensional vertical jets, and obtained that, for a given flow geometry, sand bed, and duration of scour, follow a relationship between scour depth and the logarithm of time as:

$$\frac{ds}{dt} = K(\frac{V}{W} - 1) \tag{2.5}$$

where V is the velocity, W is the fall velocity of particles and K is a constant.

Sarma and Sivasankar (1968) has done a study of scour of sand under vertical circular jets of water and found that for a given flow geometry, the limiting scour depth is proportional to $\frac{V}{W}$. The scour depth for a given discharge, jet diameter and duration of scour reduces with depth of water over the sand bed and the limiting scour depth is unaffected by the depth of flow. Thus their study further supported that progress of scour is not strictly follow a logarithmic rule but is only approximate to it and the scour depth and time relationship is a $\tan^{-1}$ function.

Thus, one can conclude that time is one of the most important parameters of scour. The present study would investigate the time variation of the scour process for both the plunging and the non-plunging jets up to the asymptotic condition.

2.2.4.4 Effect of Air Entrainment (β)

Effect of air entrainment on the depth of scour of plunge pool scour has been studied by various researchers like Blaisdell and Anderson (1991); Afify and Urroz, (1994); Minor et al., (2002); Canepa and Hager, (2003); Pagliara et. al, (2006) and their results show that for air-water mixture velocity, scour depth decreases significantly due to the addition of air to the jet.

To show the effect of entrained air on the scour depth, Afify and Urroz, (1994) has done a series of experiments in a sand bed plunge pool by means of circular jets at different jet impact angles and flow velocities. It was found that air entrainment reduces the scour depth as the jet dissipates more energy due to the formation of bubbles in the plunge pool resulting in the decrease of the scour depth.

In order to investigate the effect of air concentration of a water jet on plunge pool scour, Minor et al., (2002) have used a pre-aerated pressurized flow with a pipe, instead of using the complete arrangement involving chute and bottom aerators to create an aerated jet. It was demonstrated that the maximum scour depth due to pure water jet varies linearly with the F_o and an increasing air concentration of the jet impinging on the tailwater and underlying sediment reduces the maximum scour depth.

The effect of air discharge on plunge pool scour was investigated by Canepa et al., (2003) using an air-water jet from a circular pipe impinging on a sediment surface.

The result shows that for air-water mixture velocity, the scour depth decreases significantly due to the addition of air to the jet.

The effect of jet air content plays an important role in case of plunge pool scour. In order to understand this effect Pagliara et al.,(2006) performed experiments in a rectangular channel using a circular pipe of water in which air was added uniformly to compare with the prototype conditions with the air discharge decreasing from the jet contour towards the jet core. Four jet impact angles were chosen (α = 30°, 45°, 60°, 90°) and tests were done for submerged as well as unsubmerged conditions. The results show that effect of jet air content is slightly larger for unsubmerged jet than for submerged jets. But more detailed investigations are necessary to produce the final design criteria.

The present study deals with the scour caused by clear water jet both for the plunging and the non-plunging conditions.

2.2.4.5 Effect of jet impinging angle (α)

An experimental program to study the plane plunge pool scour of a completely disintegrated rock surface was conducted by Pagliara et al.,(2006) and it was seen that the maximum scour depth both for submerged and unsubmerged case (α = 30°, 45°, 60° and 90°) may be fitted as:

$$\varepsilon_m = -0.38 \sin(\alpha+22.5°) F_{d90},\ 2< F_d <20,\ 30° \leq \alpha \leq 90°\ \text{and}\ H \approx 3.5\ d. \qquad (2.6)$$

The effect of the jet impinging angle was originally assumed to be following a sine function, but the data sets indicated that the scour depth is larger for α = 60° than 90°. This was explained due to the deposition/ridge height is significantly larger for α = 60° than 90° because less sediment is suspended in the more confined scour hole of a vertical

jet. Another reason was that the ridge erosion is larger for $\alpha = 60°$ than 90° jets (Pagliara et al., 2006).

Previous studies carried out by Westrich and Kobus (1973) on vertical jet classified asymptotic scour holes as either "scour form I" or "scour form II", depending on the interaction of the flow field with the bed. Aderibigbe and Rajaratnam (1996) classified the flow patterns over the asymptotic scour holes as either the Strongly Deflected Jet Regime (SDJR) or the Weakly Deflected Jet Regime (WDJR). However, WDJR or SDJR were found to be similar to the earlier defined scour form I and scour form II respectively. As defined by Aderibigbe and Rajaratnam (1996) in this flow regime the jet penetrates the bed and gets strongly deflected, transporting eroded material out of the scour hole by suspension. Due to the reduced transport capacity of the deflected jet at larger radial distances, the bed material is deposited in the inner sides of the scour hole and thus slides towards the center of erosion and thereby causes renewed erosion. This flow regime is quite distinctive due to the re-circulatory flow and its interaction with the sand surface. On the other hand in case of WDJR, the jet has a weak penetration into the bed and as a result there is reduced interaction with the bed. The jet is weakly deflected, travelling the boundary of the scour hole as far as the crest of the ridge. This flow transports the eroded material out of the scour hole along the bed, as a result the scour hole slope varies significantly.

The present study aims to investigate the effect of the jet impinging angles (0°,15°, 30°, 45° and 90°) kept at a constant impinging distance for both the plunging and non-plunging conditions.

2.3 Evaluation from Previous Studies

A review of the literature reveals that scour caused by circular plunging jets have been studied with respect to different influencing hydraulic parameters, whereas scour problem due to the square turbulent plunging jets is almost absent. Most of the literature shows vertical impingement whereas results on oblique impingement of water jets on sand beds seem to be limited.

Local scour is a time-dependent process that results from the high velocity flow through or over hydraulic structures. There have been a numerous studies of scour, particularly in cohesionless materials, but due to the complex nature of the flow and its interaction with sediment bed, the problem remains not well understood. Most studies of scour have concentrated on scour in deep water, hence the effect of varying tailwater has not been fully studied. Hence, the role of tailwater depth and also the time variation of the scour process needs further detailed study.

The effect of the submergence of jet and the effect of the jet impinging angle needs further investigation. There is also a need to understand the flow behaviour of the spatial plunge pool scenario and the three-dimensional pattern of the flow. In addition there is a need to obtain empirical expressions for the better prediction of scour hole parameters considering the effects of jet impinging angle, tailwater depth, jet plunging height, time and the air content in the jet both for the plunging and the non-plunging cases.

In the present study the parameters F_o, U_o, d_{50}, b_o, ν, B and h_{imp} are held constant whereas t, H, L_i, α are varied. The jet air-content has not taken into account in the present study.

Thus, the functional relationship in (2.1) reduces to:

$$\frac{\varepsilon_m}{b_o} = f\{\frac{H}{b_o}, \frac{U_o t}{b_o}, \frac{L_i}{b_o}, \alpha\} \tag{2.7}$$

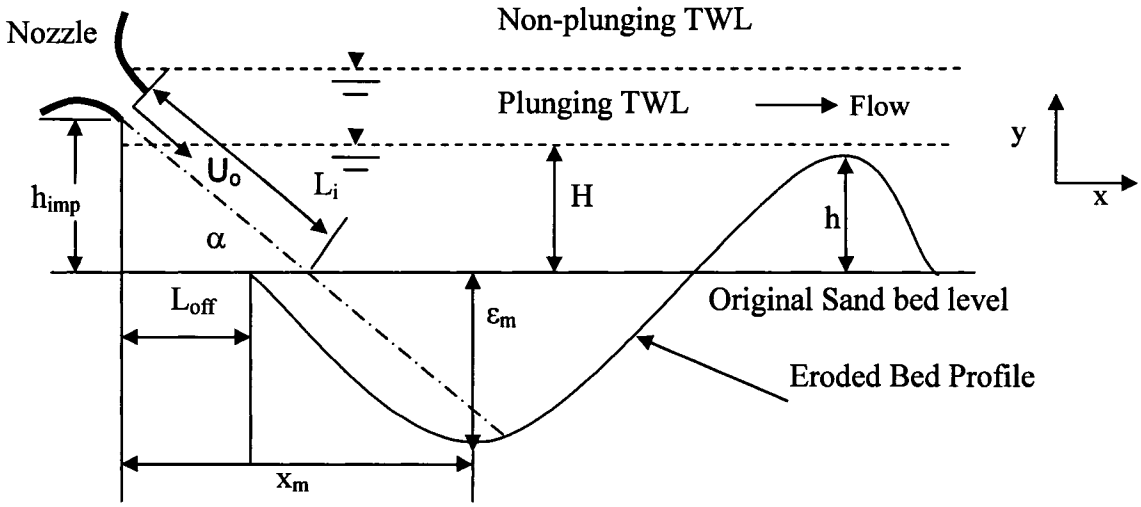

SECTION VIEW

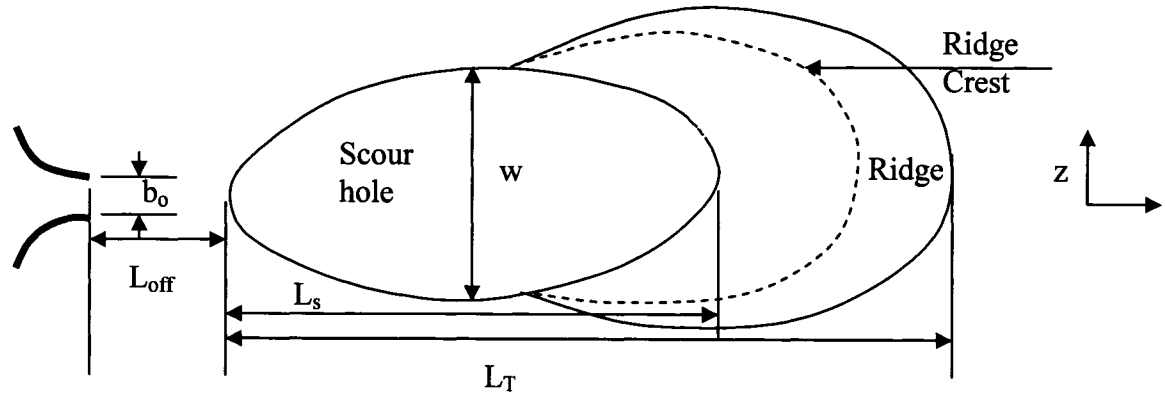

PLAN VIEW

Figure 2.1: Definition of the scour parameters

CHAPTER 3
EXPERIMENTAL SETUP AND PROCEDURES

3.1 Introduction

An open channel flume has been used in carrying out the experiments of the present study of scour caused by obliquely impinging square turbulent jet. The schematic drawing of the open channel flume and the experimental setup is shown in Figure 3.1. The experimental setup, the nozzle, the properties of the bed materials and the laser Doppler anemometer that is used to measure the velocity distribution has been described in this chapter.

3.2 Experimental setup

The experiments have been conducted in a recirculating 10 m long, 0.9 m deep and 0.625 m wide open channel flume at the University of Windsor. The sides and the bottom of the flume is made up of transparent tempered Plexiglas, which facilitates the optical access for measuring the velocity using laser Doppler anemometer (LDA). The flume is permanent equipment and the quality of flow has been confirmed in previous studies. The bottom slope of the flume is adjustable but it was kept horizontal for the present study. The header tank is mounted on the top of the flume by means of scaffoldings which helps in the removal of the air in the flow and also facilitates in keeping the constant head of water throughout an experiment. The constant flow rate is also monitored by means of the flow meter installed in the set up. The header tank is 24 inch square and 20 inch deep, made up of plexiglass and wood. Only one side of the header tank is made up of plexiglass for optical view of the water level and all other sides including the bottom is

made of wood. A fine sand bed, 0.26 m deep, 0.625 m wide and 2 m long was prepared in the flume and levelled properly below the nozzle invert. At the end of the sand bed a sand trap was provided to prevent any accidental transport of sand into the recirculating water and the pump assembly. A digital point gauge with a resolution of 0.01 mm was mounted on a traversing system for measuring the scour profiles.

3.2.1 The Nozzle:

A well designed nozzle with a 10 mm x 10 mm exit cross-sectional area (b_o) was used to generate the three-dimensional impinging jet, exiting onto a sand bed. Details are shown in Figure 3.2. The nozzle and supporting structures allow for the desired change of the jet impact angle. Turbulence reducing screen and flow straightners are installed at the entrance to the nozzle to minimize large scale turbulence. The ratio of the width of the channel to the nozzle width is 62.5 which are well above the recommended value of ten (Lim, 1995) to avoid side wall effects. Prior to the start of each experiment, the quality of the flow was verified by calibrating the flow meter every time to ensure accuracy of the flow rate.

3.2.2 Sand Bed:

A bed made up of sand particles was used to prepare the bed. Grain size analysis was carried out and the grain size distribution curves are shown in the Figure 3.3. The gradation measurements of the sand particles are tabulated in Table 3.1. From hydraulic point of view, Breusers and Raudkivi (1991) noted that if $d_{95}/d_5 < 4$ or 5, then the sand is uniform, and similarly if the geometric standard deviation, σ_g defined as $(d_{84}/d_{16})^{0.5} <$ 1.35, then the sand may be considered uniform. For mixtures which do not meet these

criteria, the non-uniformity of grain size reduces the resistance to flow and transport of sediment. The 50 % diameter on the grain size distribution plot is called the geometric mean diameter d_g, hence the use of d_{50} is adequate for relatively narrow grain size distributions. The characteristics of the sand particles indicate that the sand can be considered to be uniform from hydraulic point of view. The specific gravity of the present sand type has been considered as 2.65.

3.3 Measurements

The desired velocity required for every experiment was set by adjusting the valve on the pipe from the header tank and by setting the desired tailwater height. For measuring velocity, a single-component fiber-optic laser Doppler anemometer, or LDA (Dantec Measurement Technologies Inc.) was used. This technique has been well used and several researchers have used the same system (Faruque et al., 2006, Bey et al., 2006 and Sarathi et al., 2007)

The present LDA system has been powered by 300-mW argon-ion laser. The optical systems include a Bragg cell, a beam expansion unit and a 500 mm focussing lens. The LDA system was operated in backward scatter mode. The measuring volume for the present configuration was 0.124 x 0.123 x 1.65 mm^3. Tracer particles were added during the velocity measurements. Hollow glass spheres of size 12 microns were used as tracer particles. Due to restrictions imposed by the geometry of the transmitting optics and the channel support structures, no measurements were possible at locations closer than $2b_o$ (20mm) downstream of the nozzle exit. Measurements were conducted along the centreline of the channel at different stations ($5 \leq x/b_o \leq 55$). Typical data rates of 10 ~

150 Hz were obtained and the maximum data acquisition at each measurement location was set to 5000 particles.

At the end of the test the scour profiles were measured by the digital point gauge after draining the water out of the flume by opening the tailwater control gate. To measure the volume of the scour hole at the end of the experiment, the procedure suggested by researchers like Ali and Lim (1986), Faruque et al., (2006) and Sarathi et al., (2007) was used. This involved neatly spreading out a thin sheet of plastic in the scour hole region and pouring known volumes of water until the water surface touched the tip of the point gauge, which was adjusted to the original sand bed level.

3.4 Test Conditions

A summary of the test conditions is presented in Table 3.2. In total 30 experiments were conducted under unsubmerged or plunging conditions (water level is $1b_o$ below the nozzle bottom) with a tailwater depth of $10b_o$ and 30 more experiments for submerged condition or non-plunging condition (water level is $1b_o$ above the nozzle top) with a tailwater depth of $13b_o$. One type of sand sample (d_{50} = 0.71 mm) has been used for all experiments. Few experiments have been repeated to ensure repeatability. The jet exit velocity was kept constant at 1.09 m/s which corresponds to a jet exit Reynolds number ($Re= U_ob_o/\nu$) of 1.1 x 10^4. This value can be considered to be high enough for fully turbulent conditions to prevail. The flow Froude number $F_r = \frac{U_o}{\sqrt{gb_o}}$ is 3.5 and the densimetric Froude number $F_o = \frac{U_o}{\sqrt{g(\Delta\rho/\rho)d_{50}}}$ is 10. Both the plunging and non-plunging cases were examined for jet plunging angles of 0, 15, 30, 45 and 90 degrees by

adjusting the nozzle accordingly. For each angle the tests were run for 1, 3, 6, 24, 48 and 72 hours and it was observed that there was no considerable change in scour hole geometry after about 48 hours. However, all the experiments were conducted for 72 hours as well.

3.5 Test Procedure

The sand surface is levelled to provide zero slope and saturated prior to the start of the test. Water is filled in the flume and the pump is started to fill up the constant head tank. Prior to the start of the test the required flow velocity is adjusted using the inline calibrated flowmeter. Then each test as indicated in the Table 3.2 was continued for the required duration. In all test cases, the final equilibrium scour condition was also obtained (t = 72, 96 hours). Following a test run, the geometric profiles of the scour hole and the ridge are obtained using a digital point gauge with an electronic display unit after stopping the flow and slowly draining the water from the bed. The point gauge is set on a traverse which could be moved in the longitudinal as well as the traverse direction. The digital point gauge has a resolution of ±0.01 mm. Important scour parameters include the centreline scour profile, plan view of the scour hole, ridge perimeter, maximum scour depth, width, length of scour, maximum ridge height, location of maximum ridge height, maximum ridge width, location of maximum ridge width and the distance of the end of the ridge from the nozzle exit. Maximum scour dimensions are measured with respect to the original bed level. Volume of the scour hole is calculated by the method of Ali and Lim (1986) and used by previous researchers like Faruque et al., (2006) and Sarathi et al., (2007). Digital photographs are also taken after each test run.

Quantity	Sand Bed
d_{50}(mm)	0.71
d_{84} (mm)	0.82
d_{16} (mm)	0.60
$\sigma_g = (d_{84}/d_{16})^{0.5}$	1.17

Table 3.1: Gradation measurements of the sand bed

Test #	Test Case	F_o	F_r	h_{imp}/b_o	Li/b_o	H/b_o	d_{50}/b_o	α (deg)	Test Duration (hrs)
A	Plunging	10	3.5	11	∞	10	0.071	0	1, 3, 6, 24, 48, 72
B	Non-plunging	10	3.5			13	0.071	0	1, 3, 6, 24, 48, 72
C	Plunging	10	3.5		42.5	10	0.071	15	1, 3, 6, 24, 48, 72
D	Non-plunging	10	3.5			13	0.071	15	1, 3, 6, 24, 48, 72, 96
E	Plunging	10	3.5		22.0	10	0.071	30	1, 3, 6, 24, 48, 72
F	Non-plunging	10	3.5			13	0.071	30	1, 3, 6, 24, 48, 72
G	Plunging	10	3.5		15.6	10	0.071	45	1, 3, 6, 24, 48, 72
H	Non-plunging	10	3.5			13	0.071	45	1, 3, 6, 24, 48, 72
I	Plunging	10	3.5		11.0	10	0.071	90	1, 3, 6, 24, 48, 72
J	Non-plunging	10	3.5			13	0.071	90	1, 3, 6, 24, 48, 72

Table 3.2: Summary of test conditions

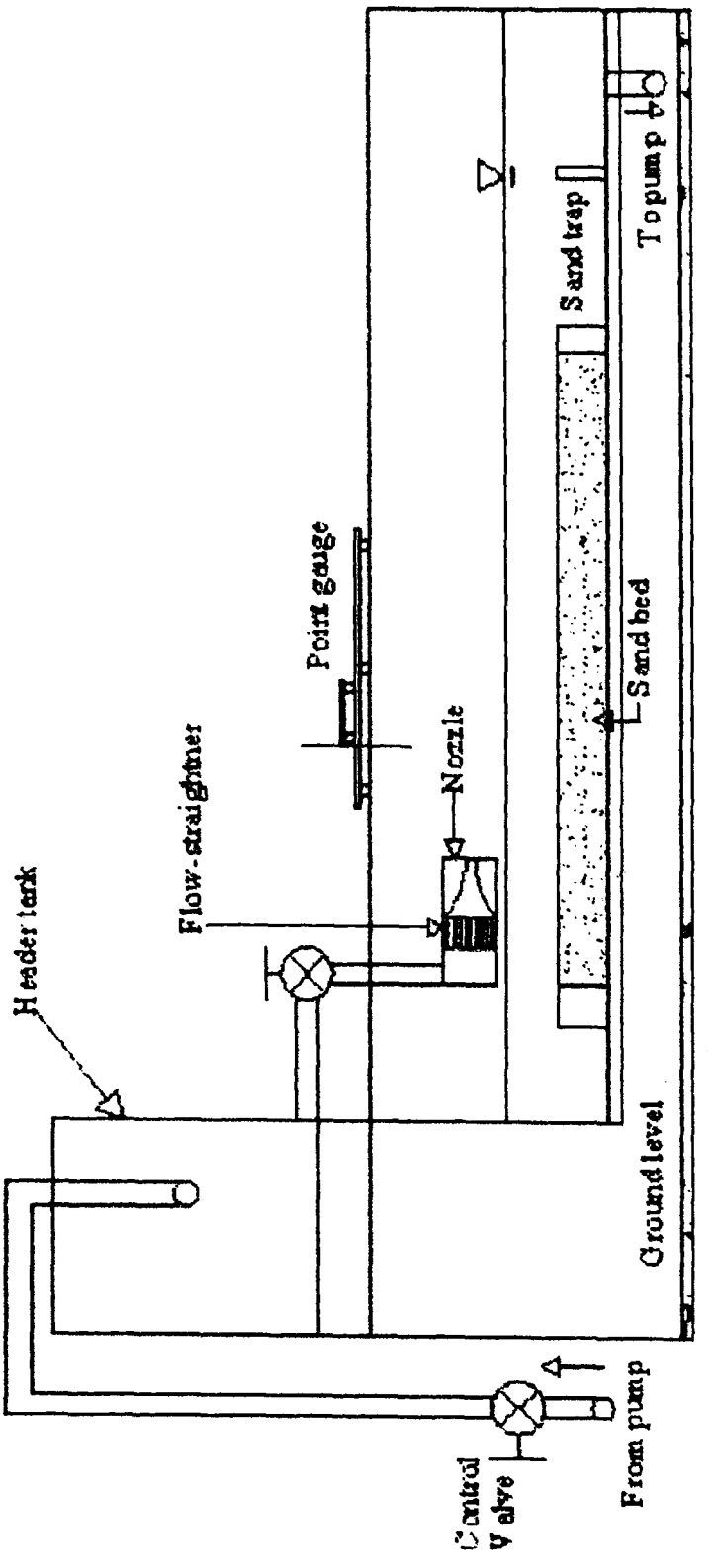

(not to scale)

Figure 3.1: Schematic diagram of the experimental set-up

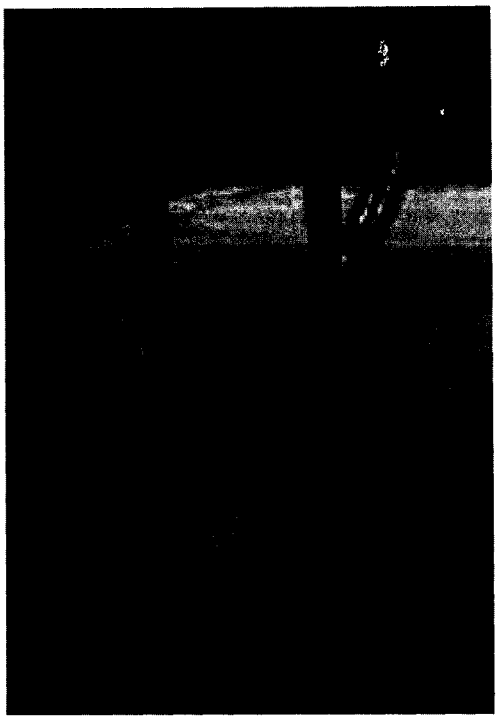

(a)

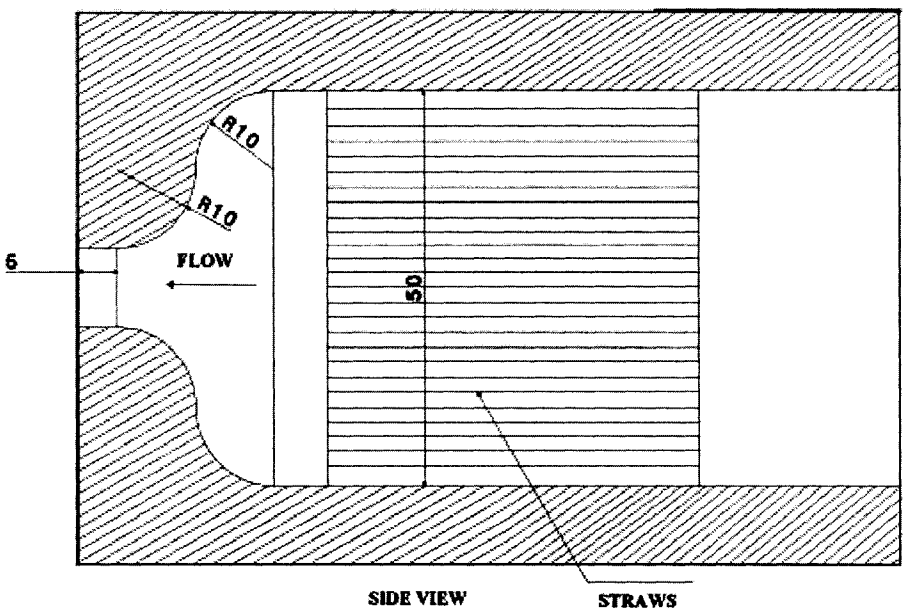

(b)

Figure 3.2: (a) Photograph of the square nozzle
(b) Side view of the square nozzle (measurements given in mm)

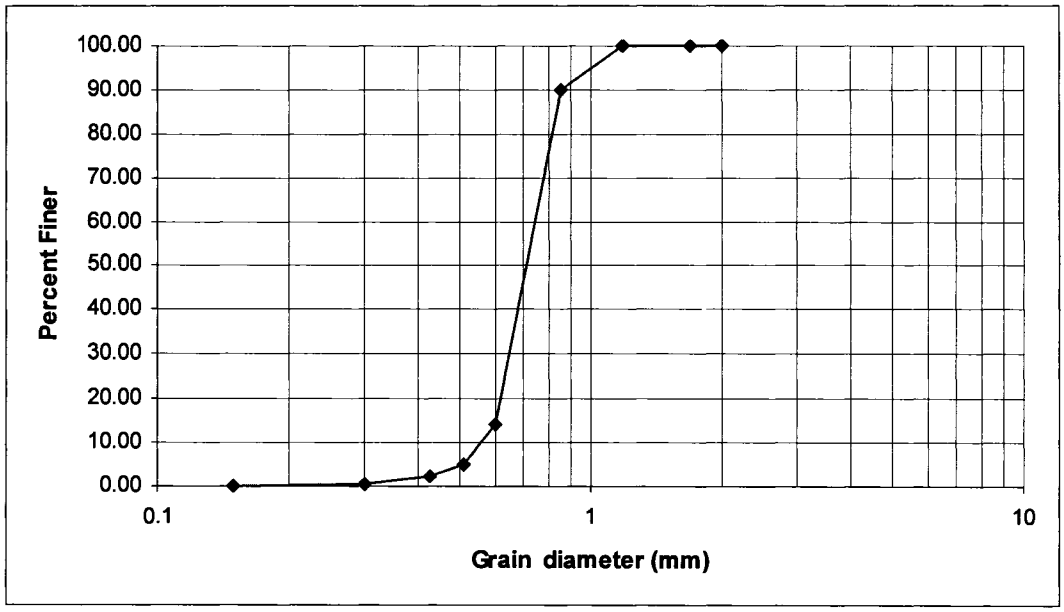

Figure 3.3: Sand grain size distribution

CHAPTER 4
RESULTS AND DISCUSSION

4.1 Introduction

In this chapter, the results of the experiments are discussed. A qualitative description of the flow field is first provided. This is followed by the discussion on the evolution of the scour process both for the plunging and the non-plunging cases. Quantitative comparisons between the plunging and the non-plunging cases are also presented.

4.2 Non-plunging case

4.2.1 Stages of Scour process

At $\alpha = 0°$, as the jet exits the square nozzle into the ambient fluid, it expands in all directions. Due to the proximity of the free surface the tendency to expand laterally is higher. This has been noticed in previous studies dealing with jets near free surfaces (Sankar et al., 2007). There is no sign of bending of the jet towards the sand bed even after 24 hours of testing. Consequently no scour of the bed material occurs. At $\alpha = 15°$, when the jet exits the nozzle into the waterbody, the jet strongly interacts with the free surface and after traveling farther, it interacts with the sand bed. Scouring action is not initiated immediately and after the first few minutes ($t \approx 300$ secs), some sand motion commences, at a considerable streamwise distance away from the nozzle. With time the scour hole tends to take an elongated streamlined shape. For $t > 600$ secs, the jet energy causes the sand particles to lift, forming the scour hole while the transported sand forms a ridge all around the scour hole. With increasing time, the depth of scour increases while

retaining the same elongated shape of the hole. For example, at t = 1 hr, the scour hole shape shows a streamlined shaped scoured region with small ridge all around the scour hole (Figure 4.1a). At t = 6 hours, the scour geometry takes on an elliptical shape which continues to persist up even at an asymptotic state. The jet expansion is primarily in the direction of the jet axis thus, the scour hole has a streamwise extension resulting in an elliptical scour hole. Figure 4.1 presents the time development of the scour geometry for α = 15°.

With the increase of the jet impinging angles (α = 30° and 45°), the jet impinges on the sand surface immediately and the jet expands in both lateral and longitudinal directions. For α = 90°, the jet diffusion takes place exactly below the nozzle bottom. One can note that for α = 30°, 45° and 90°, the interaction of the jet with the sand bed takes place soon after the jet flow is commenced. A scour hole is formed and gradually grows in size. With the progress in time, the depth of scour increases while retaining the same general shape of the hole which is nearly circular for 30° and 45° and circular for 90°. As the angle increases from 30° to 90°, a vortex develops upstream of the jet impact zone which results in the flow to diffuse radially from the jet impact zone. Thus, the tendency of the jet to expand laterally increases and the scour hole shape changes consequently. A typical set of photographs at t = 6 hours clearly illustrates this trend (Figure 4.2). With time, the jet expands into a larger volume and as such diffuses at a faster rate. Gradually, an asymptotic state is reached. Further, for α = 45° and 90°, at all times during the flow, one can note large amounts of sand to remain in suspension within the scour hole during the jet flow and is deposited in the hole when the jet is stopped.

4.2.2 Scour Profiles

Figure 4.3 shows a comprehensive summary of the time development of the scour geometry along the nozzle axis for all jet impinging angles for t = 1 to 72 hours. In each row, the centerline scour profiles, plan view of the perimeter of scour hole and the corresponding plan view of the ridge are presented for a given time. Each column shows the change in profiles over time. For example, the middle column shows the variation of the perimeter of scour hole from t = 1 to 72 hours.

From Figure 4.3a, one can note that for $\alpha = 15°$ and t = 1 hr, the scour profile is elongated in shape. This is because the flow is mostly in the direction of the jet axis. Further, the distance of the start of the scour hole from the nozzle (L_{off}) is $21b_o$, the location of the maximum depth of scour hole (x_m) is $34b_o$ and the maximum depth of the scour hole (ε_m) is $16b_o$. On increasing the jet impinging angle to $\alpha = 30°$ and 45°, respectively, the distance of the scour hole from the nozzle is reduced and the location of the maximum depth of scour hole gets closer to the nozzle. At $\alpha = 90°$ they occur right below the nozzle. This is because on increasing the jet impinging angle, the jet impact zone comes nearer to the nozzle and it is directed more towards the bed. The maximum depth of scour hole increases while the angle increases from 15° to 45° while it is smaller at α = 90°. For obliquely impinging jets (15° to 45°), there is a component of flow parallel to the bed allowing greater potential to cause scour. For α = 90° the reduction of scour depth is due to suspension of sand within the scour hole while the jet is flowing. When the jet is stopped these suspended sands settle down in the scour hole. Similarly, the ridge height (h_o) increases from 15° to 45° and decreases for 90°. The asymptotic

state of scour is reached at t = 72 hours in all cases except for $\alpha = 15°$, where the asymptotic state is attained at t = 96 hour (Figure 4.3f).

Figure 4.3g shows that at t = 1 hour, the shape of the scour hole perimeter changes from elliptical for $\alpha = 15°$ to a nearly circular shape for $\alpha = 30°$ and 45°, while the shape of the scour hole is exactly circular for $\alpha = 90°$. At $\alpha = 15°$, as the jet exits the nozzle, there is a tendency to have a larger sized hole in the direction of jet flow. With the increase of jet impinging angle from α = 15° to 45°, the tendency to expand laterally increases and the size of the scour hole changes consequently. In addition, with the increase of the jet impinging angle, a vortex develops upstream from the jet impact zone resulting in a less elongated scour hole. Between α = 30° and 45°, the jet flow is no longer axial and water flows more radially from the jet impact zone. This is also reflected in the change of the scour hole length and width. The length of the scour hole (L_s) decreases from $\alpha = 15°$ to 90°, whereas the width of scour hole (w) increases from $\alpha = 15°$ to 45°.

Figure 4.3m shows that at t = 1 hour, the shape of the ridge perimeter changes from an elongated shape for $\alpha = 15°$ to a nearly circular shape for $\alpha = 30°$ and 45°, while the shape of the ridge perimeter is circular for $\alpha = 90°$. This phenomenon happens during all test runs lasting from 1 to 72 hours (Figure 4.3m-r). The reasons stated earlier for the scour hole geometry are considered to be applicable in this case as well.

4.3 Plunging case

4.3.1 Stages of Scour Process

As the jet exits the nozzle and plunges into the waterbody, the jet expands rather quickly in the streamwise direction for $\alpha = 0°$. Following this, the jet expands in the

lateral direction, albeit slower. With the increase in the jet impinging angles (α = 15° to 45°), the tendency of the jet to expand laterally increases. For α = 90°, the jet expands uniformly in radial directions.

For all flow conditions except for α = 90°, as the jet plunges into the waterbody and interacts with the sand bed, vigorous scour action starts immediately and the scour hole progresses rather quickly in the longitudinal direction. The scour hole expands in the lateral direction as well but at slower rate. The jet energy causes the sand particles to lift forming the scour hole and the transported sand forms the ridge downstream of the scour hole. In few minutes, the scour hole and the ridge take on a definite shape. With time, the depth of scour increases while retaining the same general shape of the hole, which is more or less elliptical for a jet impinging angle of 0° and 15°, tending to be nearly circular for 30° and 45°, and circular for 90°. A typical set of photographs at t = 6 hours clearly illustrates this trend (Figure 4.4). Following the scour hole, flow has to negotiate a ridge of significant size and particles could be seen to be slowly rolling down the ridge past the crest. The particles would clearly require a significant amount of energy to go past the ridge which has to be drawn from the mean motion of the jet. This energy decreases as the jet expands and interacts with the bed. With further passage of time, the dimensions of the scour hole do not change significantly and a quasi-equilibrium stage is reached. It has been seen that for all jet impinging angles, the asymptotic state is reached at about t = 72 hours. A typical set of photographs at α = 15° clearly illustrates the development of the scour hole geometry with time (Figure 4.5).

For tests with the jet impinging at 0°, for t > 1 hour, in addition to the longitudinal growth of the scour hole and the formation of the ridge, occasionally some sand particles

near the ridge crest tends to roll down towards the scour hole while some particles are rolled up the ridge crest. This occasional rolling of sand particles near the ridge crest continues upto t ~ 21 hours but at a reduced rate. Turbulent bursts can be seen to occur near the scour hole contributing to the transport of sand particles after about t = 48 hours. For t > 48 hours, bursts are the only mechanism inducing sand grain motion in the vicinity of the maximum depth. The importance of the turbulent bursts is described by Bey et al., 2006. These bursts occur quite frequently and the frequency of occurrence decreases with the progress of time. The phenomena of the rolling down of the sand grains near the ridge crest and the sand motion due to turbulent bursts are not observed for any other jet impinging angles.

For an impinging angle of 15°, 30 and 45°, there is vigorous scouring due to the oblique impingement of the jet towards the sand bed. The obliquely impinging jet has a component of flow that is parallel to the bed, allowing a greater capacity for transport of particles out of the scour hole (Rajaratnam and Mazurek, 2003). Upstream of the jet plunging zone, sediment is not scoured but slides by avalanches into the scour hole, from where it is entrained by the jet and moved up the scour hole towards the ridge crest. Further at all times during the flow, for the jet impinging at α = 45° and 90°, large amounts of sand to remain in suspension within the scour hole during the jet flow and is deposited in the scour hole when the jet is stopped.

4.3.2 Scour Profiles

Figure 4.6 shows the development of the scour geometry along the nozzle axis for all jet impinging angles with time. Similar to Figure 4.3, in each row, the centerline scour

profiles, perimeter of scour hole and the corresponding ridge perimeter are presented for a given time. Each column shows the change in profiles over time.

Figure 4.6a shows that for $\alpha = 0°$ and at t = 1 hr, the distance of the scour hole from the nozzle bottom (L_{off}) is $17b_o$ and the location of the maximum depth of scour hole (x_m) is 31.5 b_o. On increasing the jet impinging angle from 15° to 45°, L_{off} and x_m get closer to the nozzle (for example at $\alpha = 45°$, $L_{off} = 4.1b_o$, $x_m = 11.1b_o$) and are right below the nozzle for $\alpha = 90°$. The maximum depth of scour hole increases as α increases from 0° to 30° and it decreases when the jet impinging angle is between 45° and 90°. For α = 45°, a part of the flow gets deflected by the sediment ridge in the upstream direction and transports the eroded material out of the scour hole by suspension. For α = 90°, as the jet penetrates the bed, it gets strongly deflected towards itself which causes much of the sand to remain suspended in the within the scour hole and is deposited when the jet is stopped. This accounts for the decrease in the scour depth. Further, the ridge height increases from 0° to 30° and decreases for 45° and 90°. This description is similar at all time instants for t = 1 to 72 hours (Figures 4.6a-f).

Furthermore, Figure 4.6g, shows that for t = 1 hr and $\alpha = 0°$ to 90°, the length of the scour hole decreases with the increase of angles. This is due to the lateral diffusion of the jet with the increase of jet impinging angles. However, the width of the scour hole increases from $\alpha = 0°$ to 30° and decreases for 45° and 90°. Thus, the length to width ratio of the scour hole decreases from $\alpha = 0°$ to 45° and it is almost equal for 90°. This length to width ratio is reflected in the change of shape of the scour hole from more or less elliptical to a circular shape. Thus, one can note that this description is similar at all time instants for t = 1 to 72 hours (Figures 4.6g-l).

Figure 4.6m, shows that at t = 1 hour, except for $\alpha = 90°$, the shape of the ridge perimeter does not show any noticeable change of shape for $\alpha = 0°$ to 45°. This description is similar at all time instants from t = 1 to 72 hours (Figure 4.6m-r).

4.4 Non-plunging v/s Plunging scour process

Figures 4.7, 4.8, 4.9 and 4.10 show the comparison between the time development of the scour geometry for all jet impinging angles $\alpha = 15°$ to 90° for both the plunging and the non-plunging jet conditions. Since there is no scour formation for $\alpha = 0°$ for the non-plunging case, it is not included in the description. From Figure 4.7a, for α = 15° at t = 1 hr, the distance of the start of the scour hole from the nozzle bottom (L_{off}) for plunging case is $13.5b_o$ whereas it is $21b_o$ for the non-plunging case. The variation of L_{off} with the progress of time is more or less constant for all time instants. This is similar for all jet impinging angles α = 15° to 45° and for all time instants (Figures 4.7 a-f, 4.8 a-f and 4.9 a-f). For α = 90°, the scour hole occurs exactly below the nozzle for both the non-plunging and the plunging conditions (Figure 4.10 a-f).

Futhermore, Figure 4.7a shows that for α = 15° at t = 1 hr, the maximum depth of the scour hole for non-plunging jet is found to be less ($\varepsilon_m = 1.56\ b_o$) than the plunging jet ($\varepsilon_m = 4.15\ b_o$). The same observation is also reflected in the height of the ridge (h_o) which is greater for the plunging case than the non-plunging case. The asymptotic state for the plunging condition for α = 15° is attained at t = 72 hours whereas the asymptotic state for the non-plunging condition is reached at t = 96 hours (Figure 4.3f).

Figure 4.8a shows that for α = 30° at t = 1 hr, the maximum depth of the scour hole for non-plunging jet is found to be less than the plunging jet. The height of the ridge (h_o)

is greater for the plunging case than the non-plunging case. The same description continues for all time instants t = 1 to 72 hours (Figure 4.8 a-f).

Figures 4.9a and 4.10a show that for $\alpha = 45°$ and 90° at t = 1 hour, the maximum scour depth for the plunging case is less than the non-plunging case. This behaviour is opposite to that stated for Figure 4.7 and 4.8. At low values of $F_o/(h_{imp}/b_o)$ i.e $0.4 < F_o/(h_{imp}/b_o) < 2.1$, the submerged/non-plunging jet is weakly deflected, and there is not much sediment in suspension within the scour hole while the jet is flowing and consequently, when the jet is stopped, there is no significant change in the scour hole geometry, which has been also observed by Rajaratnam and Mazurek, 2003. The same difference in the maximum scour depth is noticed for all run times (t = 1 to 72 hours) for both the plunging and the non-plunging conditions. However, the asymptotic state for the 90° plunging condition is reached much earlier ($t > 24$ hours) when compared to the non-plunging condition ($t > 48$ hours).

Figure 4.7g shows that for $\alpha = 15°$, at t = 1 hour, the perimeter of the scour hole shows a change in shape from an elliptical one in the case of non-plunging condition to a more or less circular shape for the plunging condition. The length of the scour hole is greater for non-plunging condition than plunging condition, whereas the width of the scour hole is greater for plunging condition than the non-plunging condition. The same is also observed for $\alpha = 30°$, at t = 1 hour (Figure 4.8g) between the plunging and the non-plunging condition. This phenomenon is similar for all time instants (t = 1 to 72 hours) for both the jet impinging angles, $\alpha = 15°$ and 30° (Figure 4.7 g-l, 4.8 g-l).

Further, for $\alpha = 45°$ (Figure 4.9g-l), it is noticed that the scour hole shape is more or less circular for both the test conditions for t = 1 to 72 hours. This is because the flow direction over the scour hole is radial from the jet impact zone.

For $\alpha = 90°$ (Figure 4.10g), the shape of the scour hole is circular for both flow conditions. Furthermore, the radius of the scour hole is slightly greater for the non-plunging condition than the plunging condition. This is because the plunging jet is more strongly deflected than the non-plunging jet resulting in a smaller scour hole radius (Rajaratnam and Mazurek, 2003). This description of the shape of the scour hole is similar for all time instants (Figure 4.10 g-l).

The perimeter of the ridge for $\alpha = 15°$ at t = 1 hour (Figure 4.7m) shows a change of shape from an elongated one in case of the non-plunging condition to a more or less circular shape for the plunging condition. With time ($t \geq 24$ hours) the shape of the ridge perimeter gradually changes to a more or less circular shape for both the flow conditions. For α ranging between 30° and 90°, and for t = 1 to 72 hours, the shape of the ridge perimeter does not show any noticeable change of shape for the two test conditions (Figures 4.8m-r, 4.9 m-r, 4.10m-r). Further, for $\alpha = 90°$ (Figure 4.10m-r) the radius of the ridge for the non-plunging condition is slightly greater than the plunging condition for all time instants.

Overall, for small jet impingement angles ($15° < \alpha < 30°$), the difference in the scour geometry between the non-plunging and the plunging condition is more prominent. It is observed that for $\alpha > 45°$, the difference in the scour geometry is further reduced. In order to investigate whether the tailwater depth has an influence on the scour geometry for $\alpha > 45°$, some additional tests are done for $\alpha = 90°$ and the tailwater depth of $12b_o$.

The results show that for vertical jet case, the tailwater depth has minimal effect (Figure 4.11) on scour geometry. In addition, the vertical jet flow shows some distinct characteristics for both the plunging and non-plunging conditions.

In the present study, the vertical jet flow in the plunging condition behaves as Strongly Deflected Jet Regime (SDJR) as defined by Aderibigbe and Rajaratnam (1996). In this flow regime the jet penetrates the bed and gets strongly deflected, transporting eroded material out of the scour hole as suspension. Due to the reduced transport capacity of the deflected jet at larger radial distances, the bed material is deposited in the inner sides of the scour hole and thus slides towards the center of erosion and thereby causes renewed erosion. On the other hand, under non-plunging condition for the vertical jet shows behaviour similar to the Weakly Deflected Jet Regime (WDJR) as defined by Aderibigbe and Rajaratnam (1996) where the jet has a weak penetration into the bed and as a result there is reduced interaction with the bed. The jet is weakly deflected, travelling the boundary of the scour hole as far as the crest of the ridge. This flow transports the eroded material out of the scour hole thereby increasing the scour depth.

4.5 Velocity Profiles

The velocity distribution in the region above the scour hole and the ridge was investigated at the near asymptotic state of the scour process. Figure 4.12 shows the longitudinal mean velocity measurements at ten different sections taken for the plunging condition. The asymptotic bed profile is also shown for better understanding of the physical locations of the velocity measurements. The velocity measurements are carried out along the plane containing the nozzle axis for the jet impinging angle of 0°.

For the plunging case (Figure 4.12) at section x/b_o= 5, the velocity profile shows that there is very little flow in this section as it lies behind the jet impinging zone. From x/b_o = 20 to x/b_o = 25, the jet expands and interacts with the sand bed. At x/b_o > 30, negative values of velocity occur at farther distances from the bed indicating the presence of reverse flow closer to the free surface.

Figure 4.13 shows the longitudinal mean velocity measurements at ten different sections taken during the test for the non-plunging condition for $\alpha = 0°$. As there is no scour formation hence no scour profile has been shown in the figure. The velocity measurements are carried out along the plane containing the nozzle axis. From the velocity profiles of the non-plunging case (Figure 4.13), it is observed that there is no sign of the bending of the jet towards the sand bed.

4.6 Proposed scour prediction equations

4.6.1 At asymptotic condition:

In the following section an attempt has been made for better prediction of scour profile at the asymptotic condition. In the present study for the obliquely impinging jet set at fixed impingement height, the functional relationship (2.7) shows the dependence of the maximum depth of scour on time (t), angular impingement distance (L_i), height of tailwater (H) and the jet impinging angle (α). However, the tailwater depth ratio is held constant for the plunging and non-plunging conditions respectively, which reduces the equation to:

$$\frac{\varepsilon_m}{b_o} = f\{\frac{U_o t}{b_o}, \frac{L_i}{b_o}, \alpha\} \tag{4.1}$$

The observations of the non-plunging jet impinging at α = 30° to 60°, has been described by (Rajaratnam and Mazurek, 2002) as:

$$\frac{\varepsilon_m}{L_i} = 0.73\frac{F_o}{(L_i/d)} - 0.10 \tag{4.2}$$

and for jet impact angle 7.5° and 15°, the maximum scour depth has been described as:

$$\frac{\varepsilon_m}{L_i} = 0.77\frac{F_o}{(L_i/d)} - 0.20 \tag{4.3}$$

Equation (4.2) has been found to agree with the data of the present study for α = 30° and 45° while equation (4.3) is not validated by the present data set.

Thus, the present study aims to develop an expression taking all the jet impinging angles into consideration (15° < α < 90°) for the non-plunging case and it is described by:

$$\frac{\varepsilon_m}{L_i} = 0.63\left(\frac{F_o}{L_i/d}\right) - 0.08 \tag{4.4}$$

In order to prove the accuracy of the proposed equation, a comparison has been done with the experimental and the predicted results of the present study using equation 4.4 (Figure 4.14a). The experimental and predicted results of Rajaratnam and Mazurek (2002) using Equation 4.4 is also included. It is seen that the prediction based on the equation proposed in the present study is appropriate for a wide range of jet impinging angles.

From the observations made in the present study, an attempt has been made to predict the scour expression for the plunging case for 15° < α < 90° (since for α = 0°, ε_m/L_i = 0). Equation for the plunging case shows that:

$$\frac{\varepsilon_m}{L_i} = 0.43\left(\frac{F_o}{L_i / d}\right) + 0.01 \qquad (4.5)$$

A comparison has been made between the experimental and the predicted values (Figure 4.14b). The result shows that the prediction is appropriate for a wide range of jet impinging angles.

Overall, one can conclude that L_i is an important parameter for the prediction of scour for non-plunging and plunging condition. This is because L_i has a strong dependence on the angle at which the jet impinges on the sand surface. Thus, both equations 4.4 and 4.5 provide better predictions of the scour at asymptotic condition for the non-plunging and plunging conditions respectively.

4.6.2 Variation of scour parameters with time

Figures 4.15, 4.16, 4.17, 4.18, 4.19 show the dependence of the normalized scour parameters on the dimensionless time ratio (U_0t/b_0) for the plunging and the non-plunging cases. All the parameters increase with time up to the asymptotic state. It should be remarked that it was not visually possible to actually obtain the maximum depth of the scour during the test. Consequently, only the data at an asymptotic condition after the flow was stopped is shown in the figures.

Figure 4.15(a-c) shows that the maximum scour depth is greater for the plunging case than the non-plunging case for $\alpha = 0°$ to 30° for all time instants. For $\alpha = 45°$ and 90°, it is noticed that the non-plunging condition produces greater scour than plunging condition for the all time instants (Figure 4.15d,e). This is because the non-plunging jet is weakly deflected, and there is not much sediment in suspension within the scour hole while the jet is flowing to settle down in the scour hole when the jet is stopped

(Rajaratnam and Mazurek, 2003). On the other hand, for the plunging case, a large amount of sand remains in suspension within the scour hole during the jet flow and deposited in the hole when the jet is stopped. This accounts for a reduction in scour depth. The corresponding ridge height also shows similar behaviour for $\alpha = 0°$ to 90° for all time instants, t = 1 to 72 hours (Figure 4.16).

Figure 4.17 shows that except for $\alpha = 0°$, the length/radius of the scour hole is greater for the non-plunging case than the plunging case for all jet impinging angles. Further, the scour width is larger for the plunging case than the non-plunging case for $\alpha =$ 0° to 30° and almost merges for $\alpha = 45°$ (Figure 4.18). The volume of the scour seem to increase for the plunging case than the non-plunging case for $\alpha = 0°$ to 30°, and decrease for $\alpha = 45°$ and 90° for all time instants (Figure 4.19).

Thus, it is quite evident that there is a dependence of all the scour parameters on the tailwater depth. It is important to recognize that for small jet impingement angles ($15° < \alpha < 30°$) the influence of the tailwater depth is prominent. However, with the increase of the jet impinging angles ($\alpha > 45°$), the dependence of the scour parameters on the tailwater depth is reduced.

The proposed prediction of the scour profile along the nozzle invert at any particular time for a given U_o has been described herein. It has been found that for the plunging and non-plunging cases, linear approach was the best representation for the dependence of the scour depth on time. The present study found that there exists a strong correlation between time and the scour depth and are expressed in the forms:

(a) Non-plunging case

For $\alpha = 15°$

$$\varepsilon_m/b_o = 1.09 \log_{10}(U_o t/b_o) - 4.39 \quad (4.6a)$$

For $\alpha = 30°$

$$\varepsilon_m/b_o = 0.51 \log_{10}(U_o t/b_o) + 1.65 \quad (4.6b)$$

For $\alpha = 45°$

$$\varepsilon_m/b_o = 0.75 \log_{10}(U_o t/b_o) + 0.38 \quad (4.6c)$$

For $\alpha = 90°$

$$\varepsilon_m/b_o = 0.55 \log_{10}(U_o t/b_o) - 1.43 \quad (4.6d)$$

Combining equations (4.6a, 4.6b, 4.6c, 4.6d), a logarithmic relation is found for the jet impinging angle (α) and the maximum scour depth (ε_m/b_o) at any particular time at the given U_o.

$$\varepsilon_m/b_o = A \log_{10}(U_o t/b_o) + B \quad (4.7)$$

where,

$$A = 0.002\,\alpha^2 - 0.12\,\alpha + 2.51 \qquad 15° \le \alpha \le 45°$$

$$B = -0.016\,\alpha^2 + 1.14 - 17.76 \qquad 15° \le \alpha \le 45°$$

The above equation is used to find out the parameters "A" and "B" and respective correlation coefficients R^2 are 1 and 1.

and,

$$A = -0.0003\,\alpha^2 + 0.04\,\alpha - 0.44 \qquad 30° \le \alpha \le 90°$$

$$B = 0.0013\,\alpha^2 - 0.18\alpha + 6.00 \qquad 30° \le \alpha \le 90°$$

The above equation is used to find out the parameters "A" and "B" and respective correlation coefficients R^2 are 1 and 1.

The parameters "A" and "B" are plotted against the jet impinging angle in Figure 4.20c and 4.20d. The curve indicates that the maximum scour depth is very sensitive to different jet impinging angles with time.

(b) Plunging case:

For $\alpha = 0°$

$$\varepsilon_m/b_o = 0.74 \log_{10}(U_o t/b_o) - 0.62 \quad (4.8a)$$

For $\alpha = 15°$

$$\varepsilon_m/b_o = 0.68 \log_{10}(U_o t/b_o) + 0.20 \quad (4.8b)$$

For $\alpha = 30°$

$$\varepsilon_m/b_o = 0.51 \log_{10}(U_o t/b_o) + 1.51 \quad (4.8c)$$

For $\alpha = 45°$

$$\varepsilon_m/b_o = 0.90 \log_{10}(U_o t/b_o) - 0.88 \quad (4.8d)$$

For $\alpha = 90°$

$$\varepsilon_m/b_o = 0.47 \log_{10}(U_o t/b_o) - 1.0 \quad (4.8e)$$

Combining equations (4.8a, 4.8b, 4.8c, 4.8d, 4.8e), a logarithmic relation is found for the jet impinging angle (α) and the maximum scour depth (ε_m/b_o) at any particular time at the given U_o.

$$\varepsilon_m/b_o = A \log_{10}(U_o t/b_o) + B \quad (4.9)$$

where,

$$A = -0.008\,\alpha + 0.76 \quad 0° \leq \alpha < 30°$$

$$B = 0.07\,\alpha - 0.80 \quad 0° \leq \alpha < 30°$$

The above equation is used to find out the parameters "A" and "B" and respective correlation coefficients R^2 are 0.93 and 0.98.

and

$$A = -0.001\,\alpha^2 + 0.07\,\alpha - 1.08\ , \qquad 30° \le \alpha \le 90°$$

$$B = -0.003\,\alpha^2 - 0.36\,\alpha + 9.85\ , \qquad 30° \le \alpha \le 90°$$

The polynomial equations are used to find out the parameters "A" and "B". The parameters "A" and "B" are plotted against the jet impinging angle in Figure 4.20 (a,b). The curve indicates that the scour depth is sensitive to the different jet impinging angles with time.

Figure 4.1: Pictorial representation of the time development of the scour geometry for non-plunging case for $\alpha = 15°$

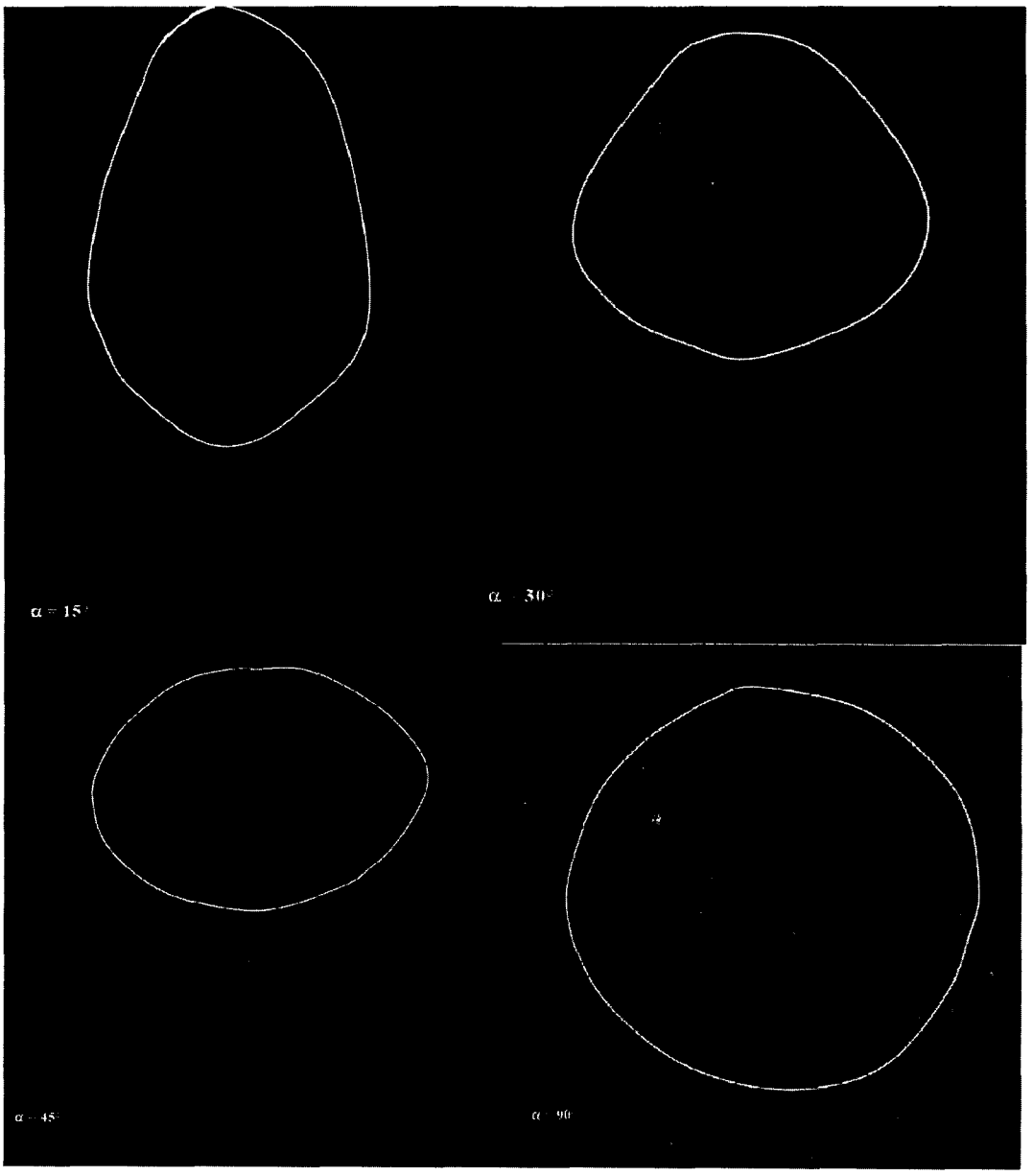

Figure 4.2: Photographs showing the change of scour hole shape at t = 6 hours for non-plunging condition.

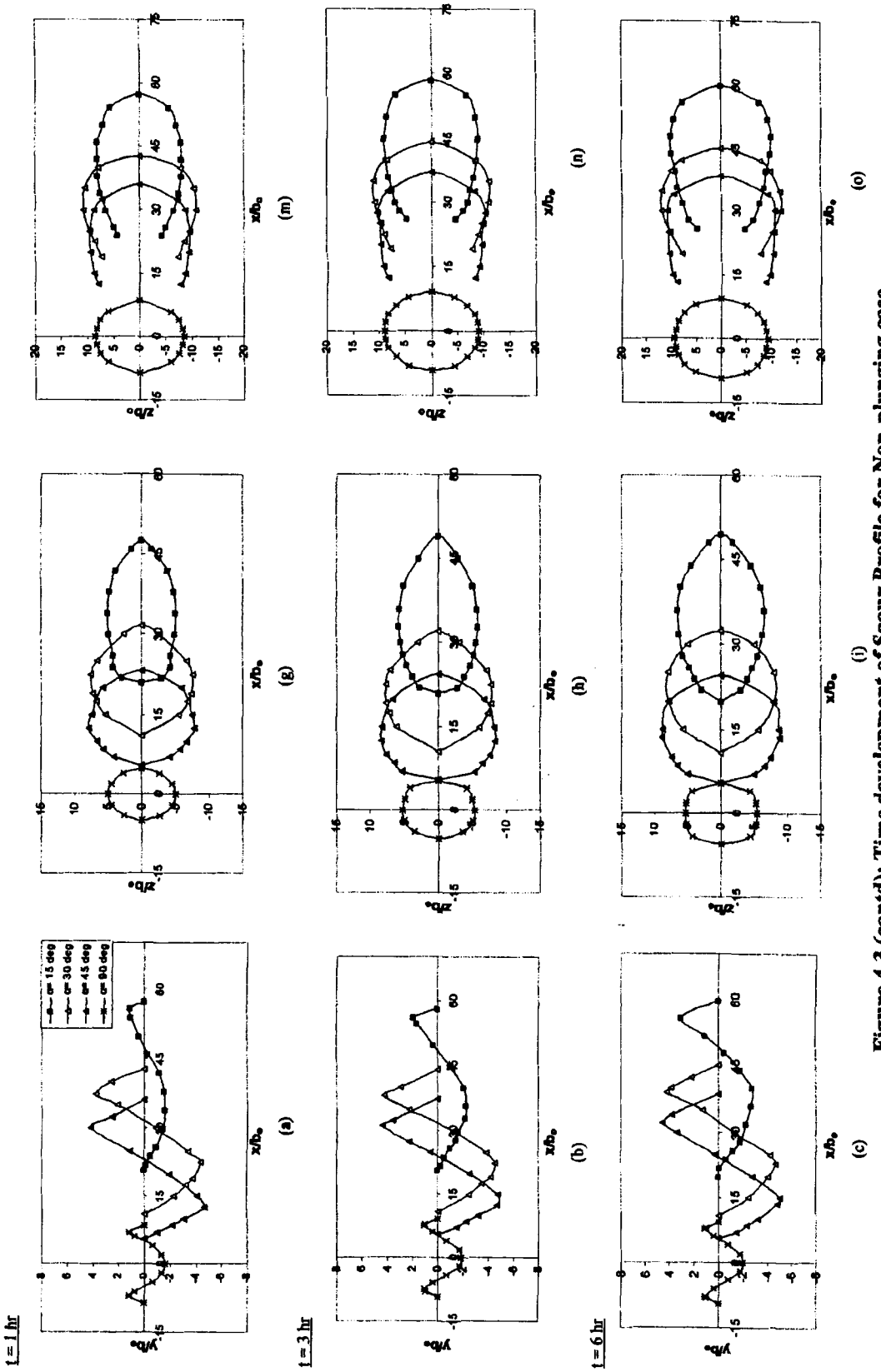

Figure 4.3 (contd): Time development of Scour Profile for Non-plunging case

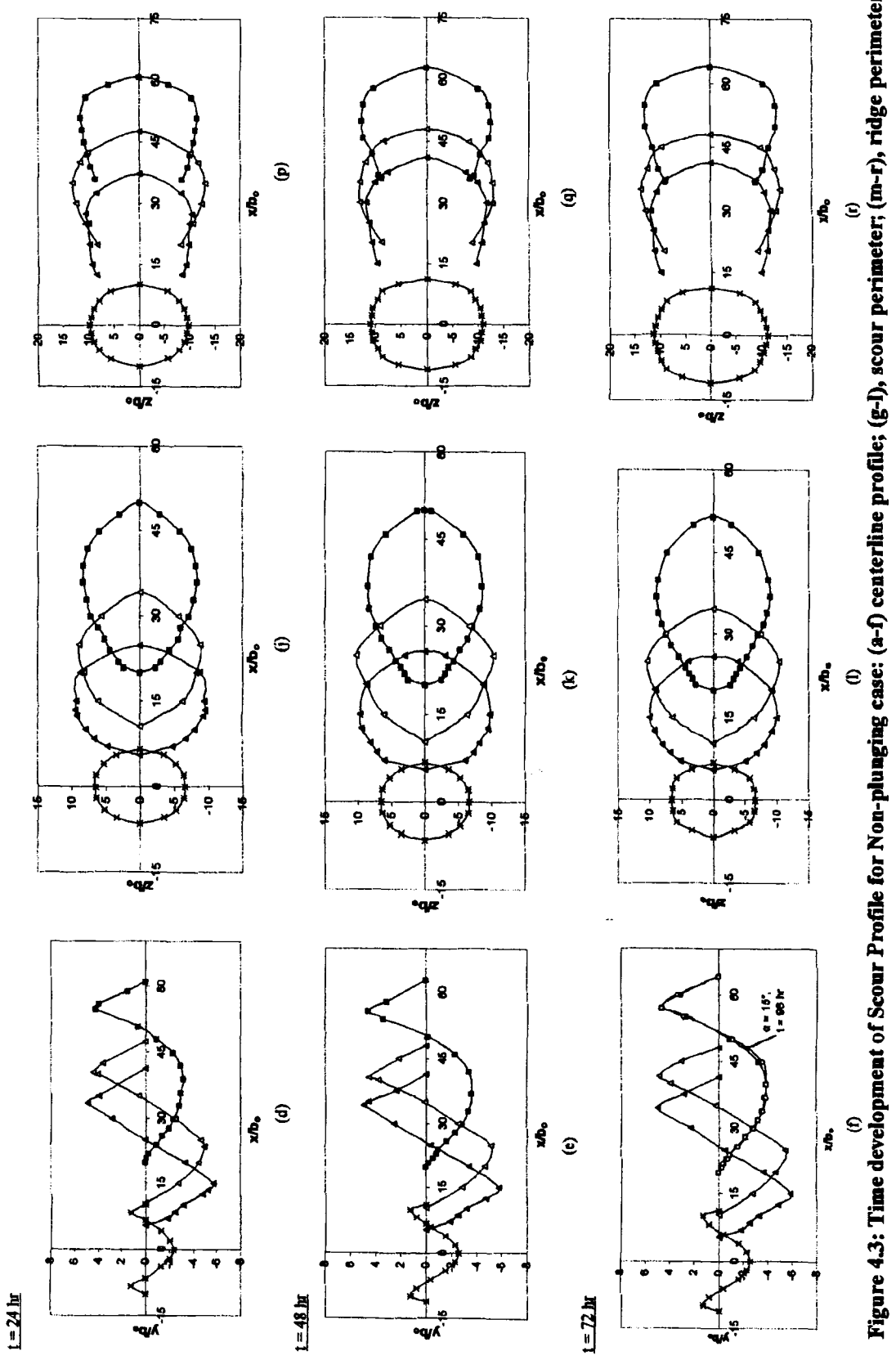

Figure 4.3: Time development of Scour Profile for Non-plunging case: (a-f) centerline profile; (g-l), scour perimeter; (m-r), ridge perimeter

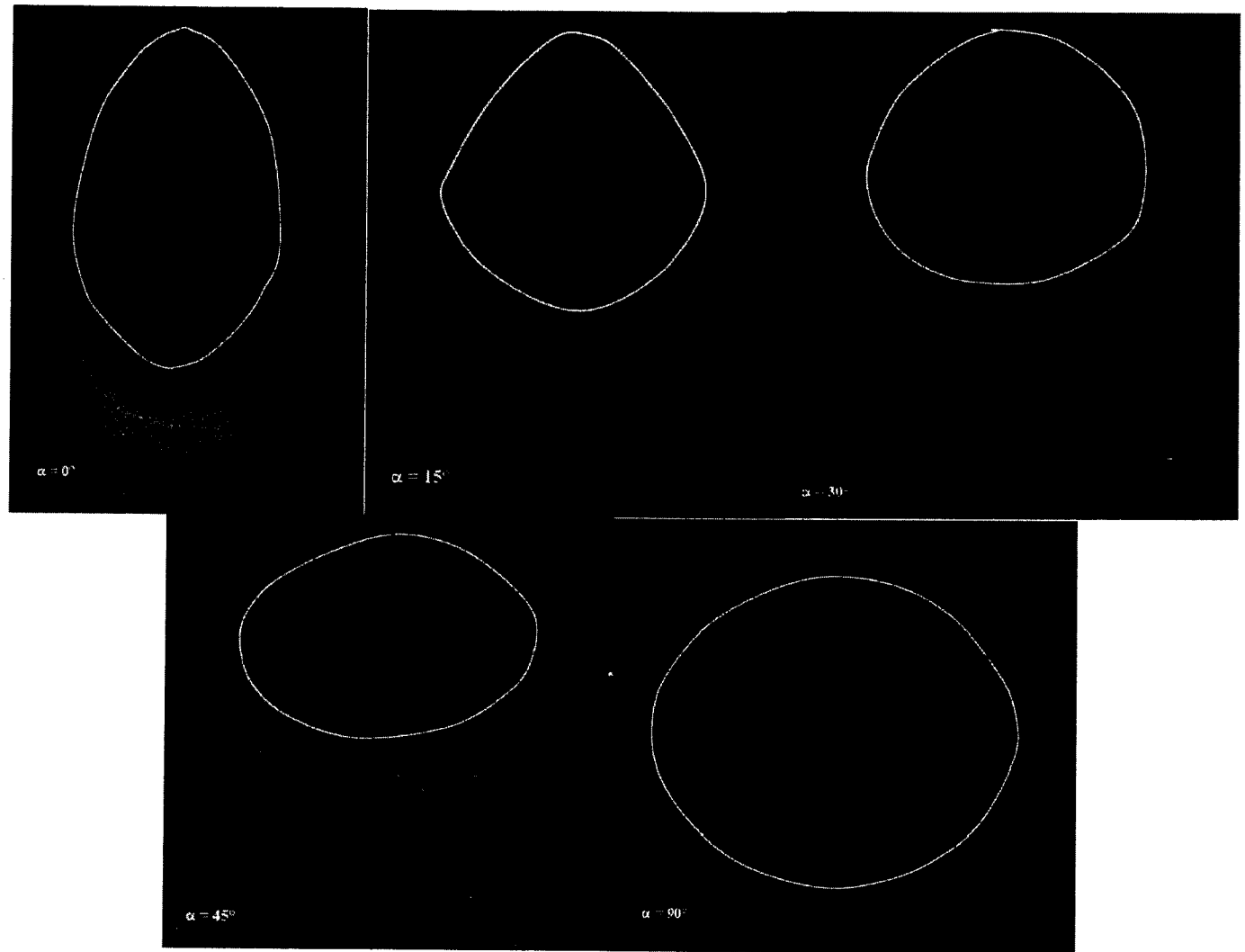

Figure 4.4: Pictorial representation of the change of the scour hole shape for α = 0° to 90° (t = 6 hours) for plunging case

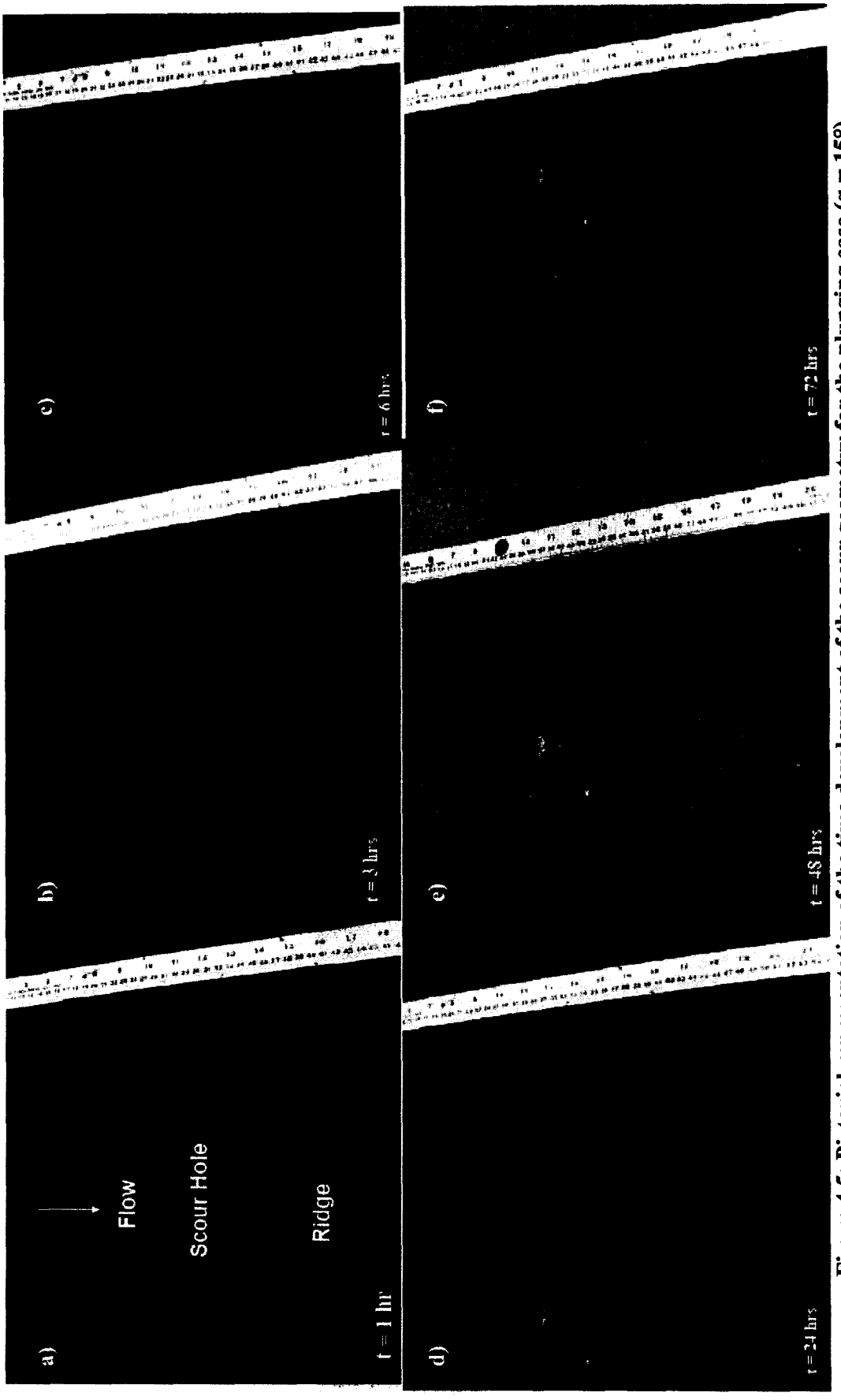

Figure 4.5: Pictorial representation of the time development of the scour geometry for the plunging case ($\alpha = 15°$)

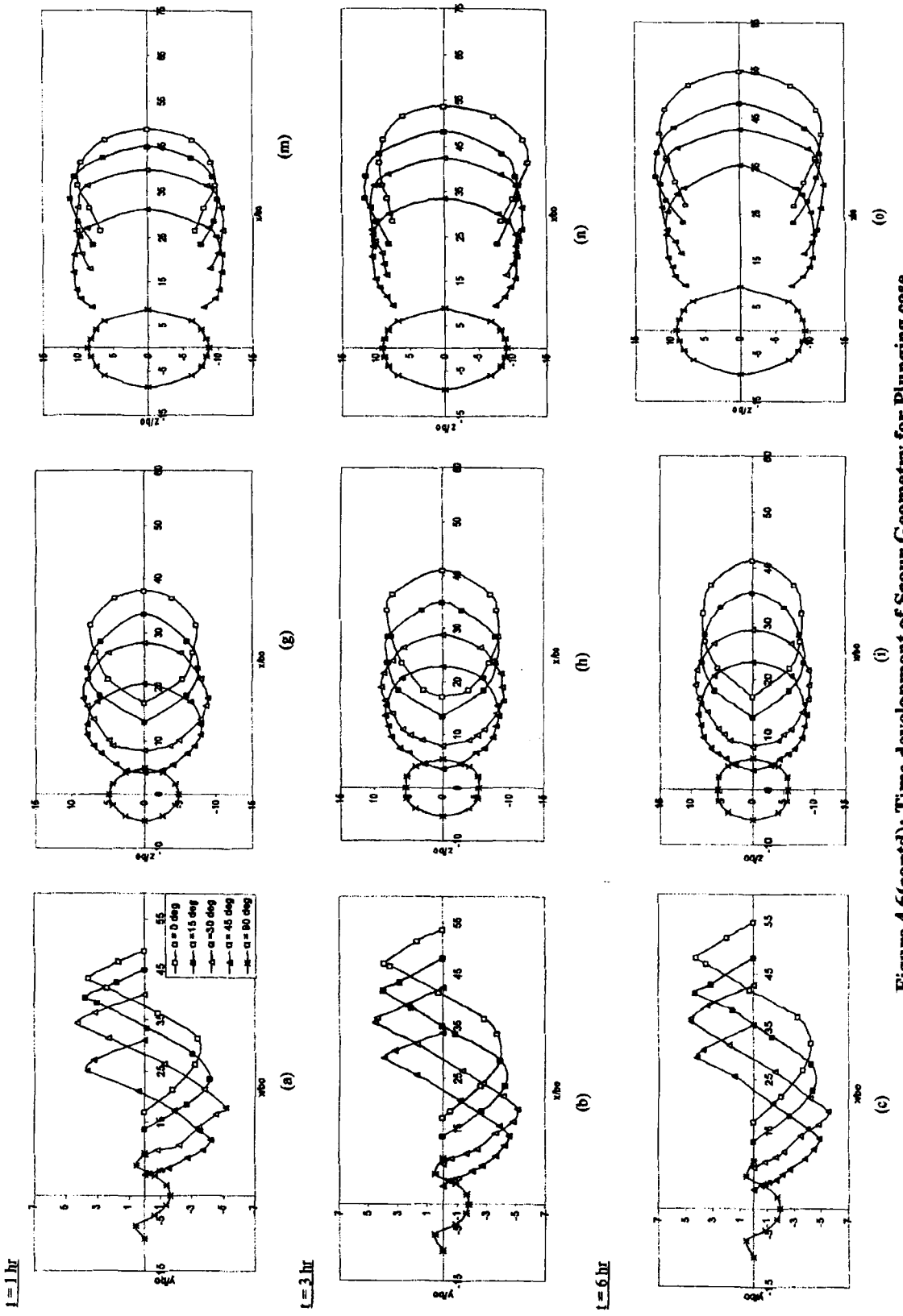

Figure 4.6(contd): Time development of Scour Geometry for Plunging case

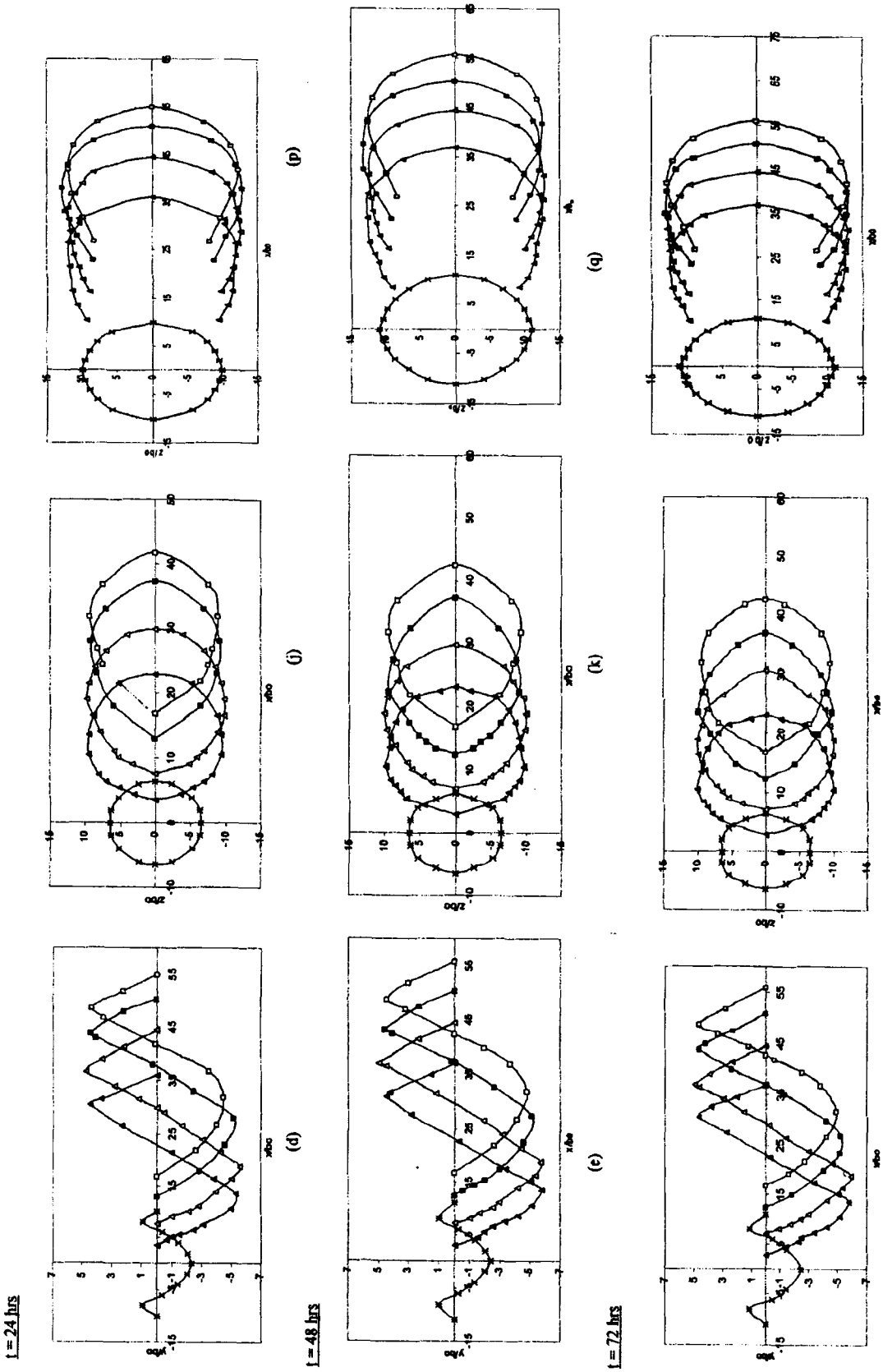

Figure 4.6: Time development of Scour Geometry for Plunging case: (a-f), centerline profile; (g-l), scour perimeter; (m-r), ridge perimeter

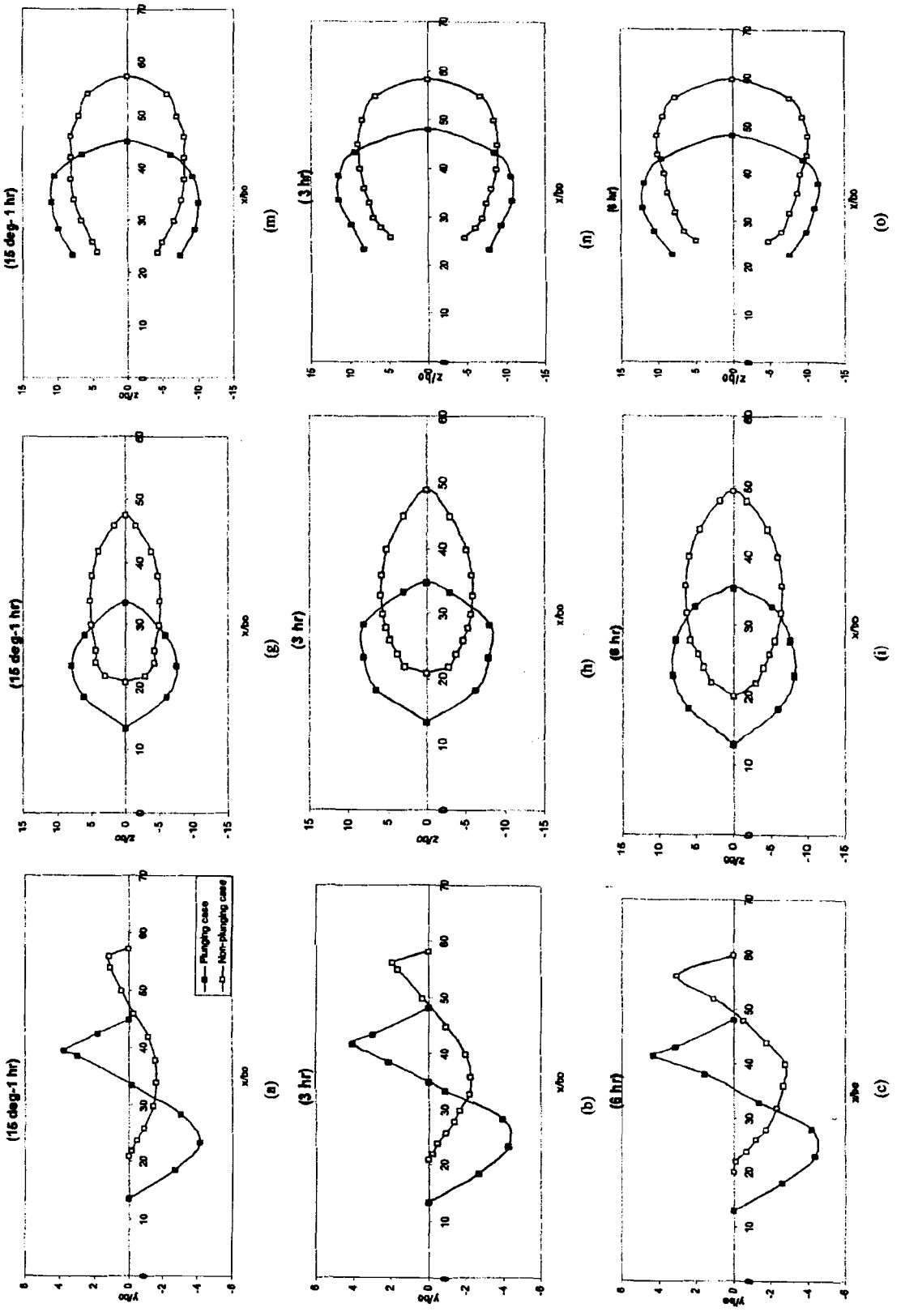

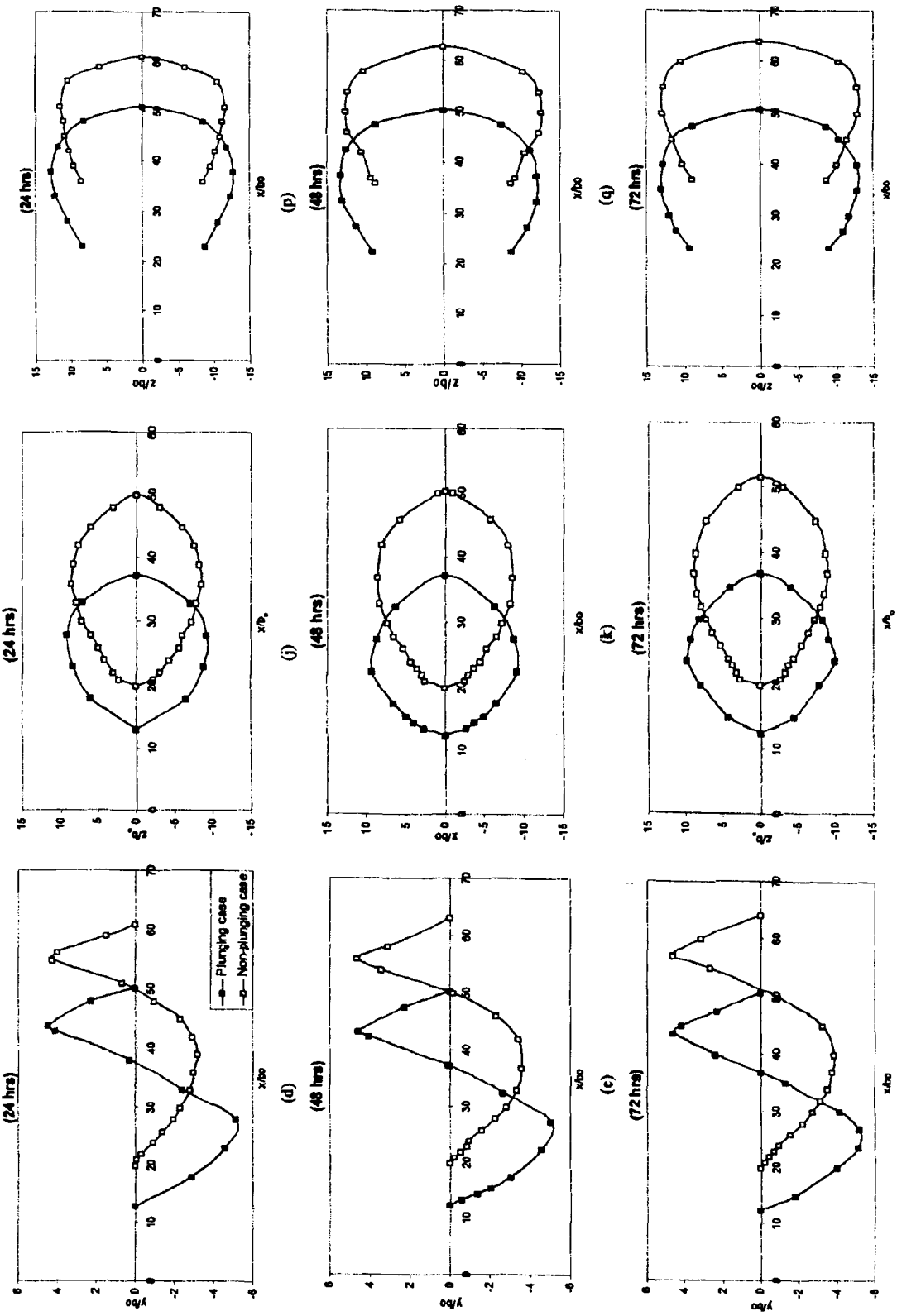

Figure 4.7: Comparison of scour profile between plunging and non-plunging case for $\alpha = 15°$

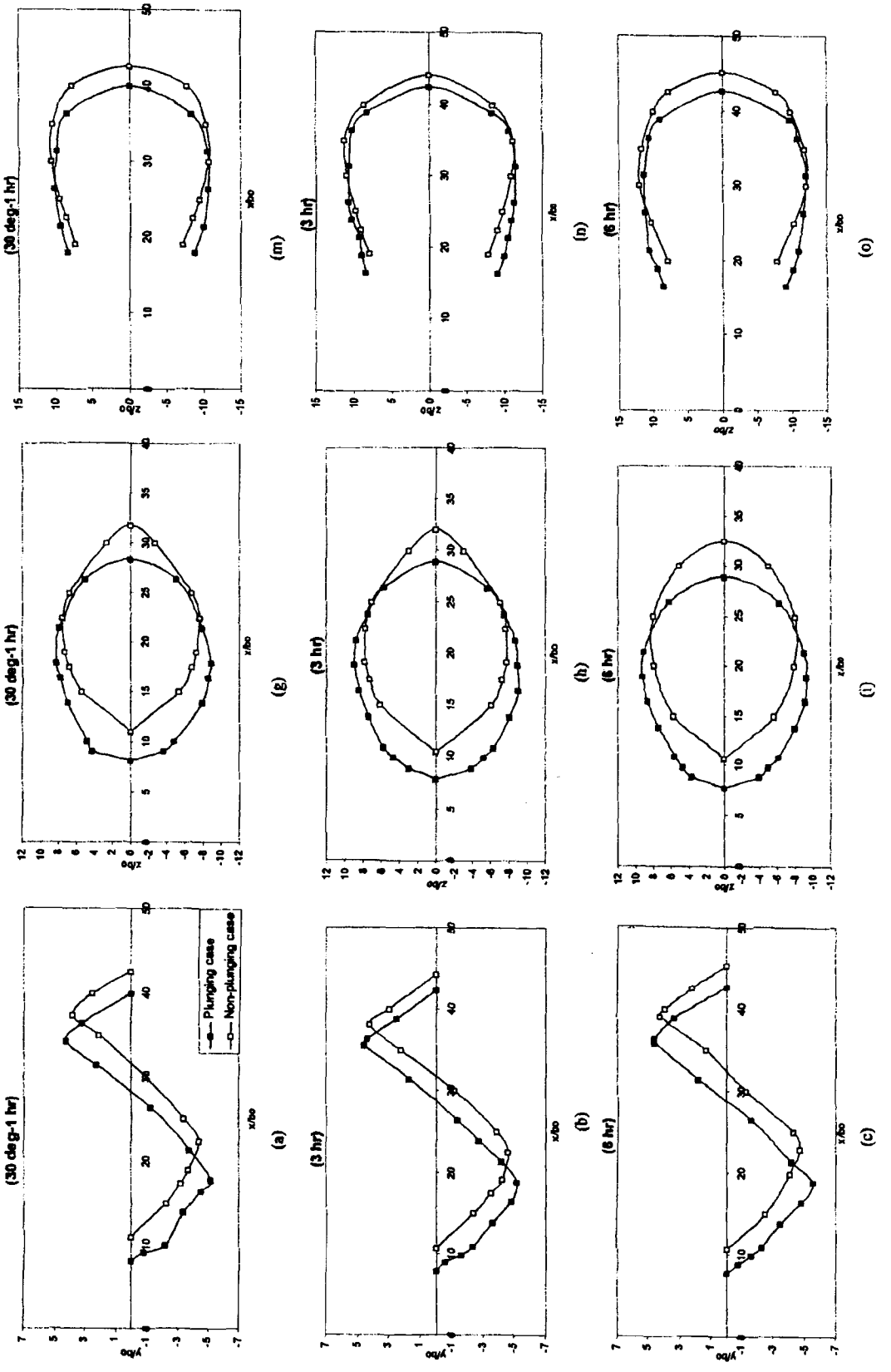

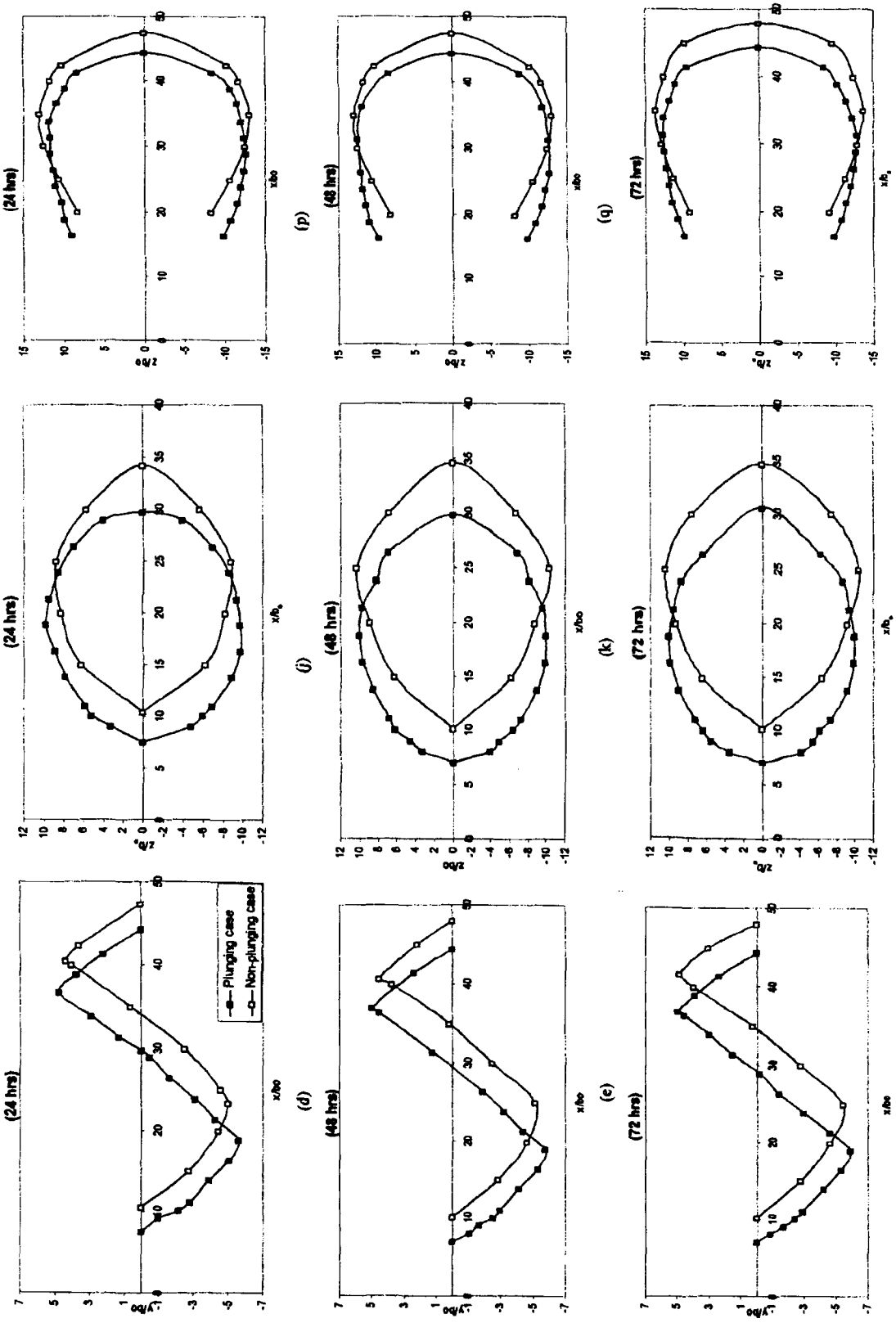

Figure 4.8: Comparison of scour profile between plunging and non-plunging case for $\alpha = 30°$

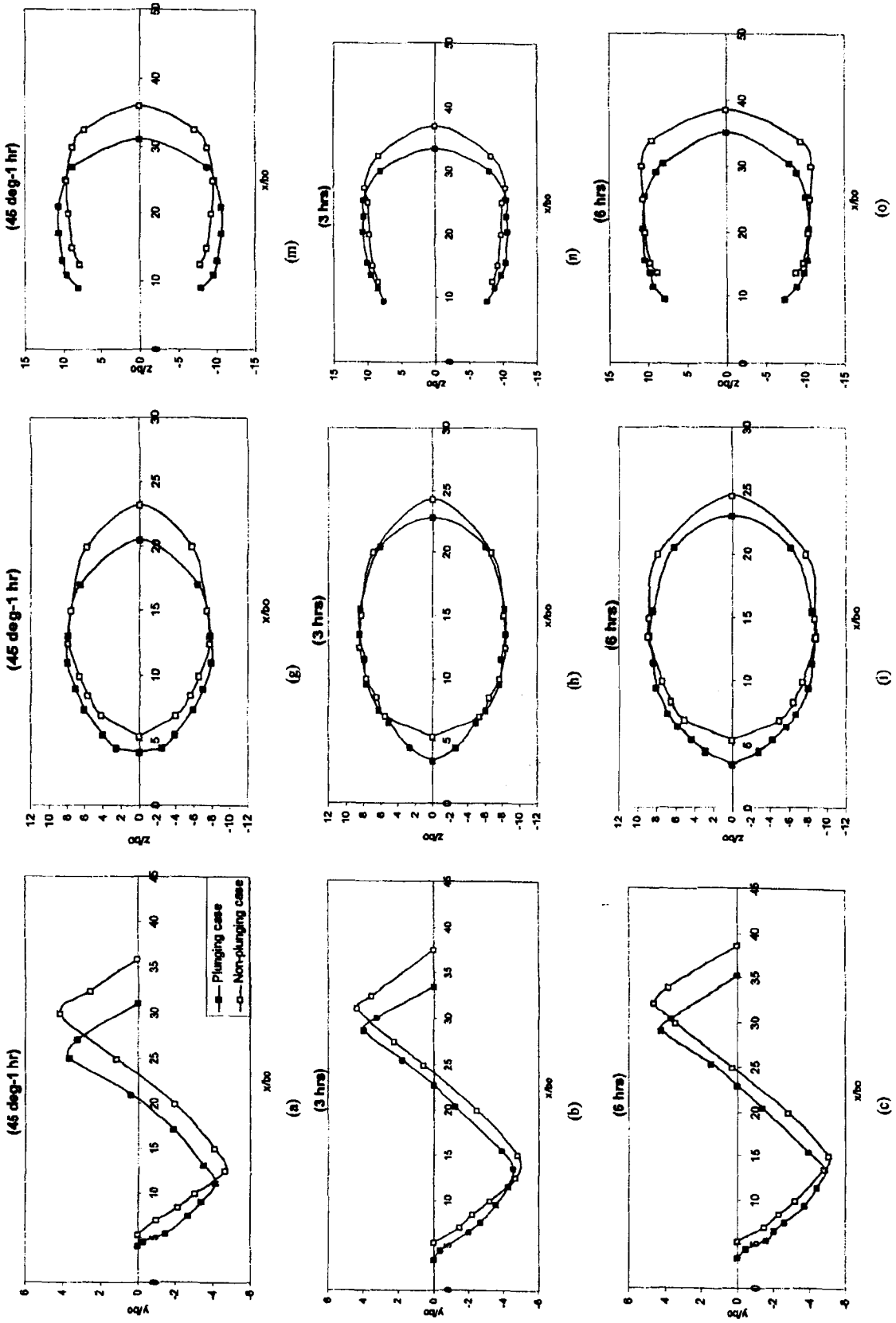

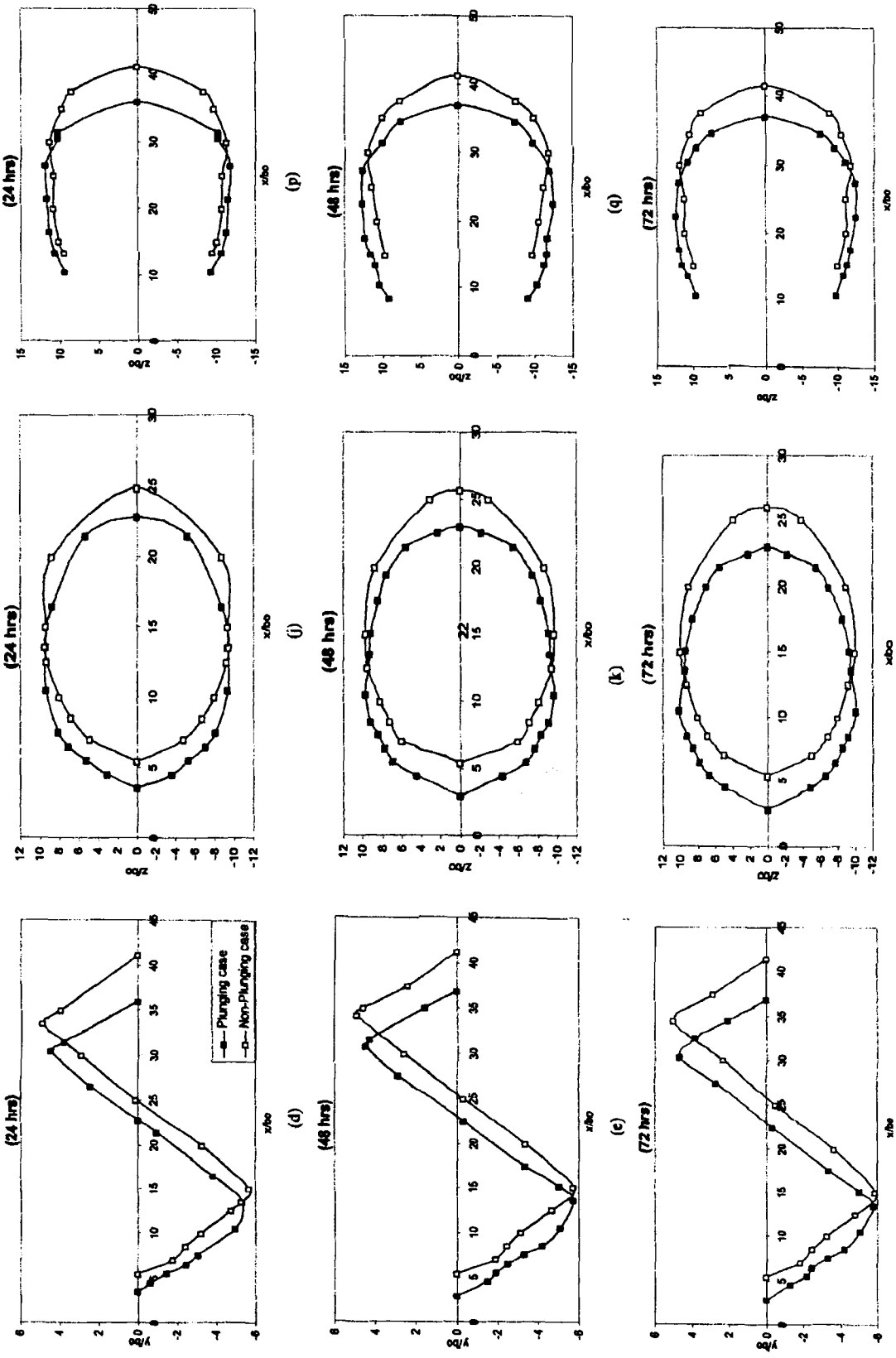

Figure 4.9: Comparison of scour profile between plunging and non-plunging case for $\alpha = 45°$

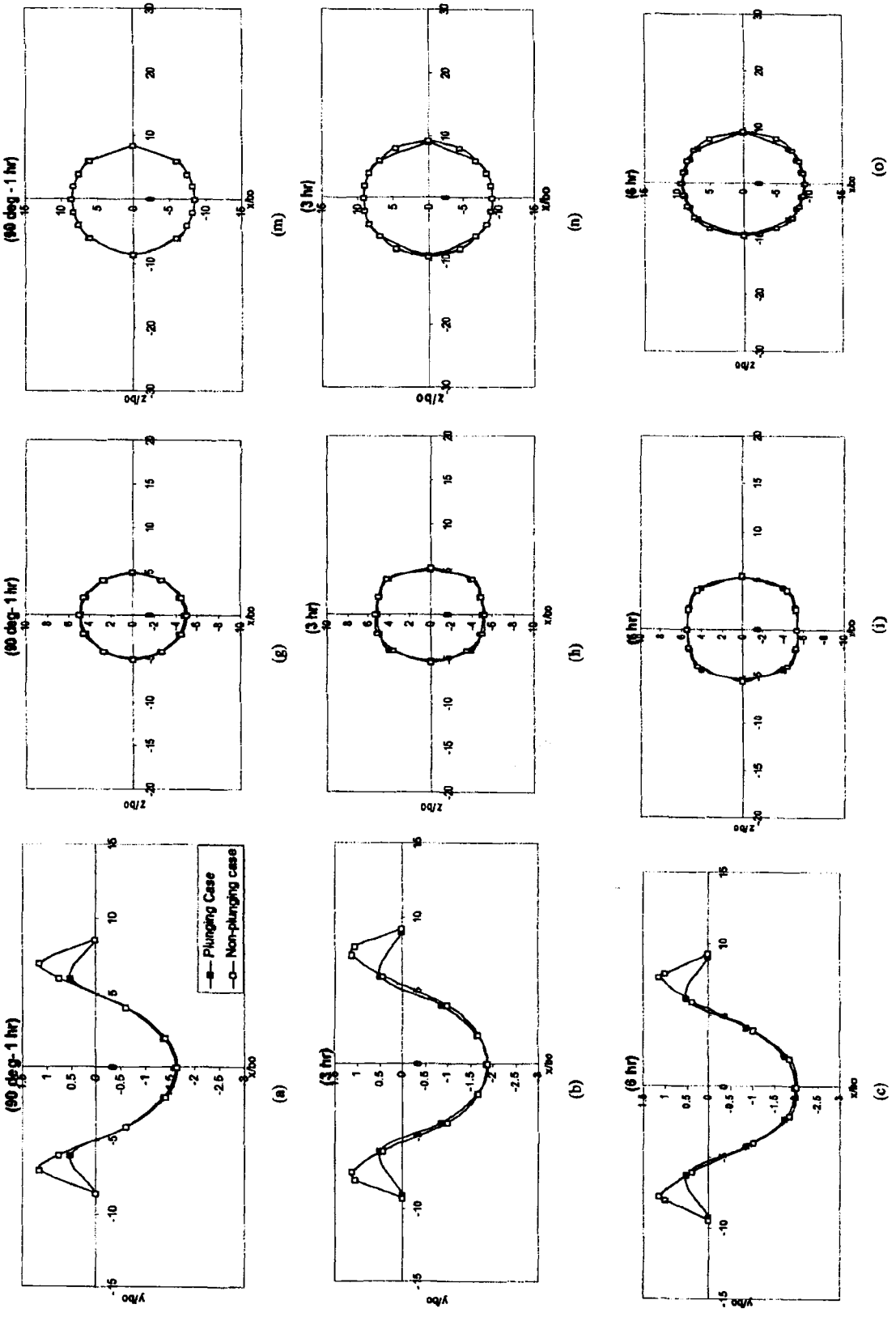

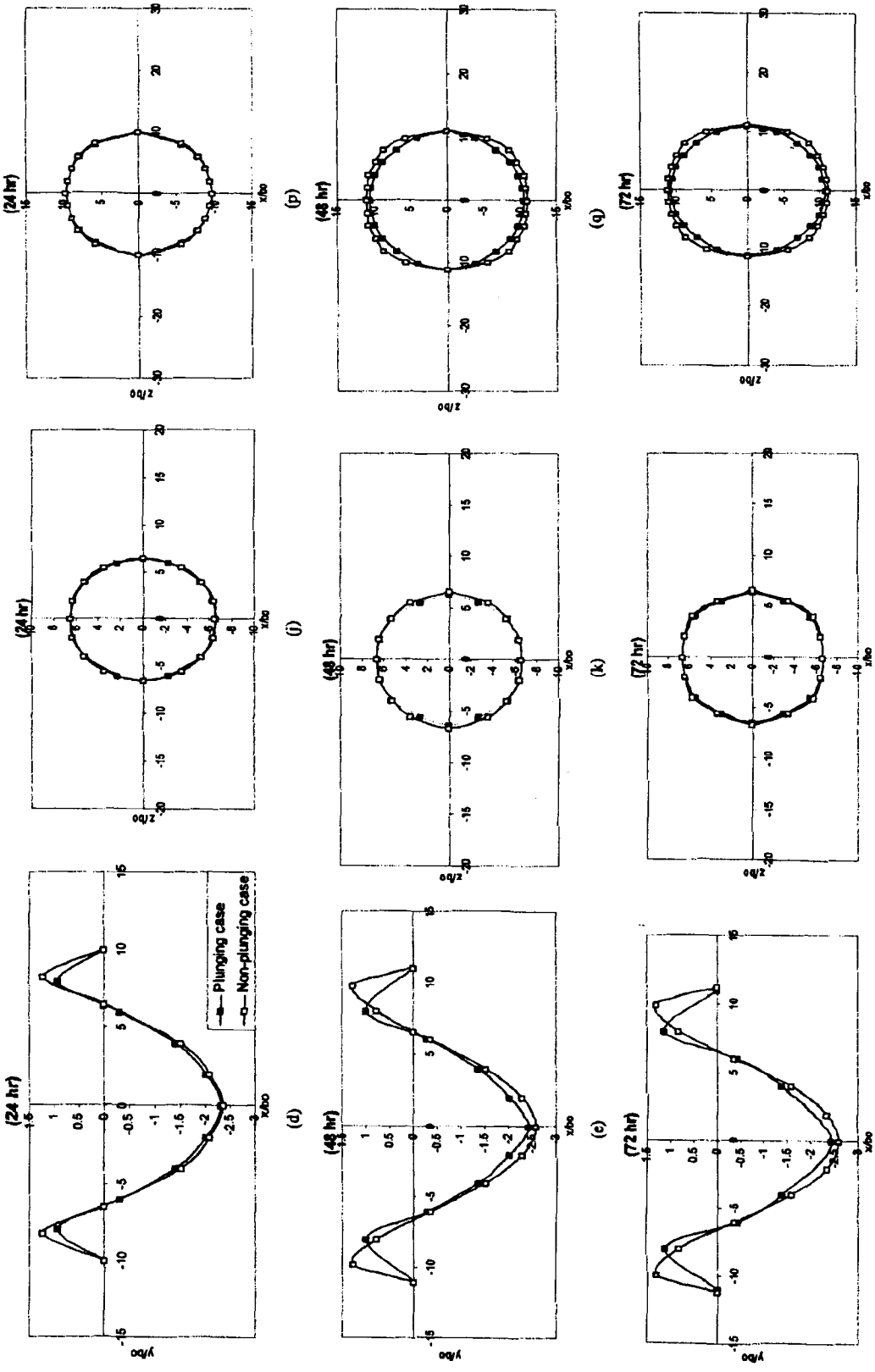

Figure 4.10: Comparison of scour profile between plunging and non-plunging case for $\alpha = 90°$

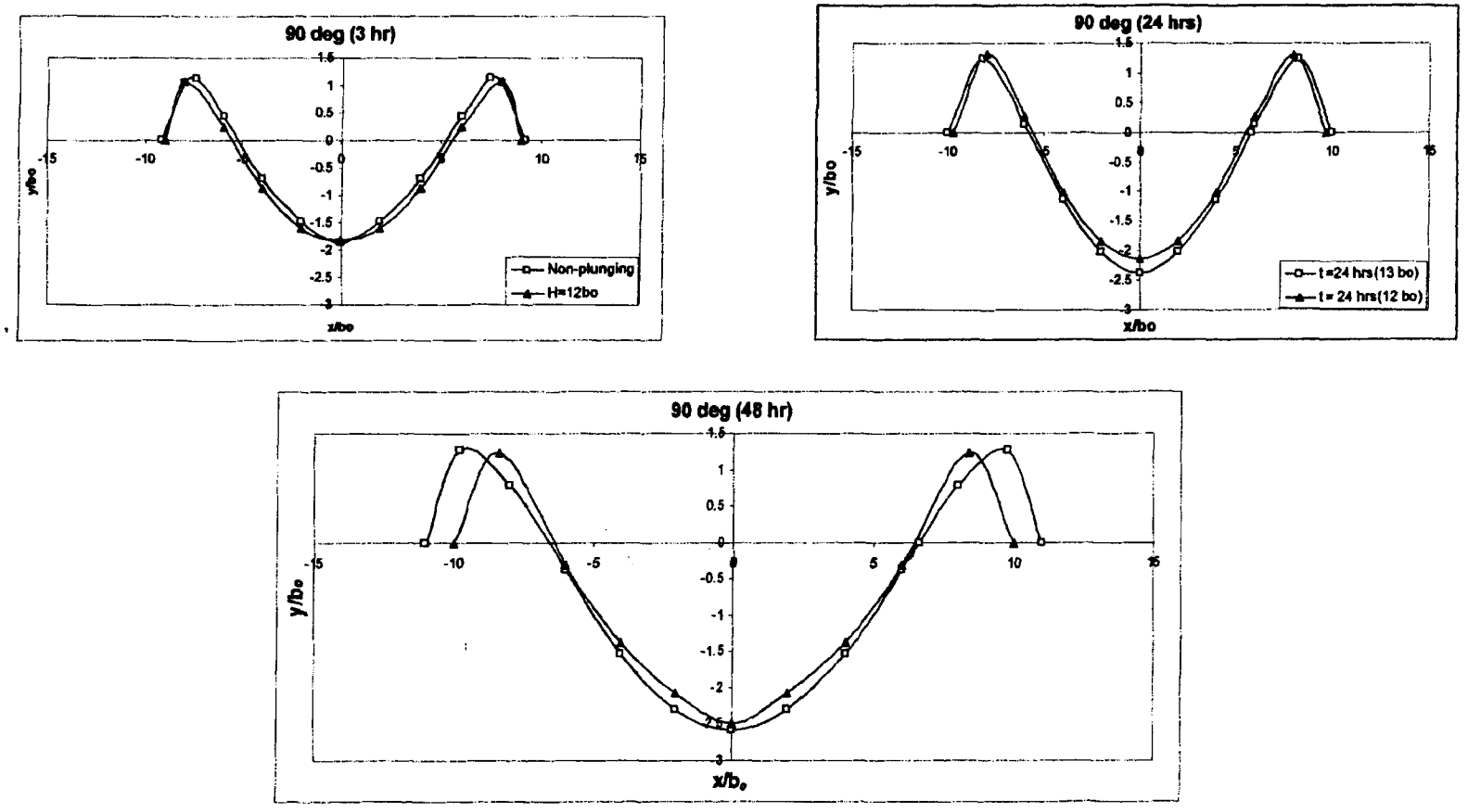

Figure 4.11: Comparison between centerline scour profile for non-plunging case (H/b_o =13) and H/b_o = 12.

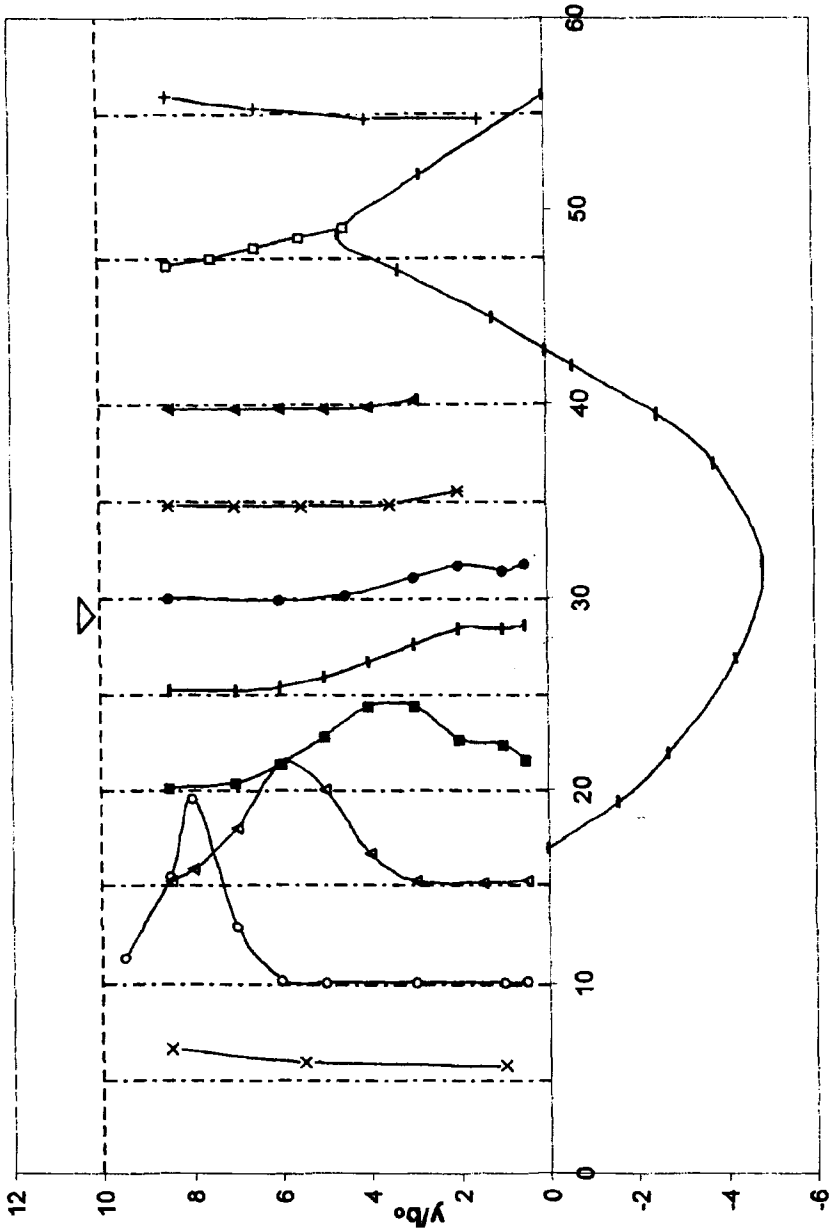

Figure 4.12: Longitudinal mean velocity profiles at different sections at asymptotic state for the Plunging case for $\alpha = 0°$,

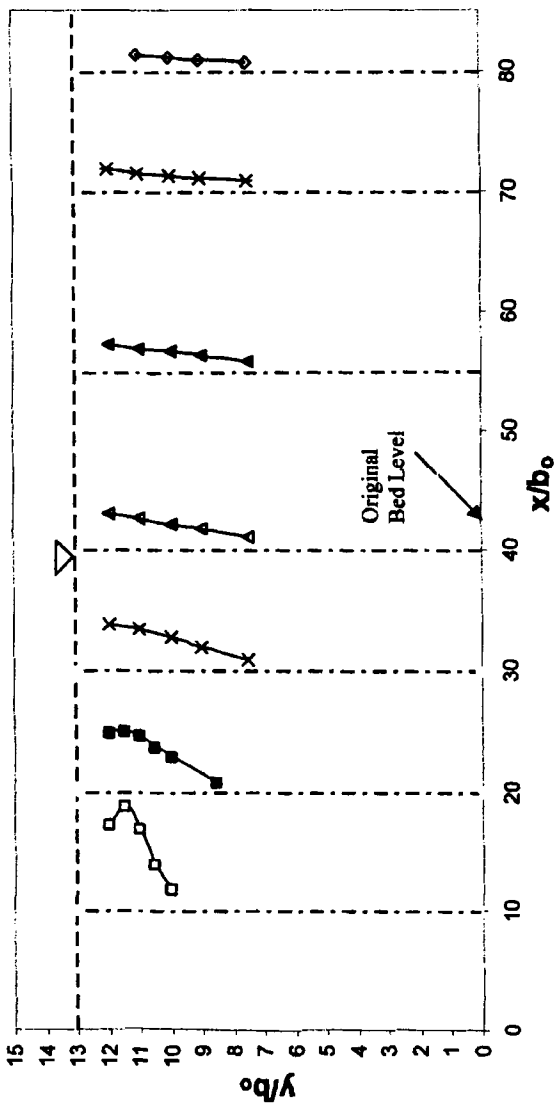

Figure 4.13: Longitudinal mean velocity profiles at different sections at asymptotic state for the non-plunging case for $\alpha = 0°$,

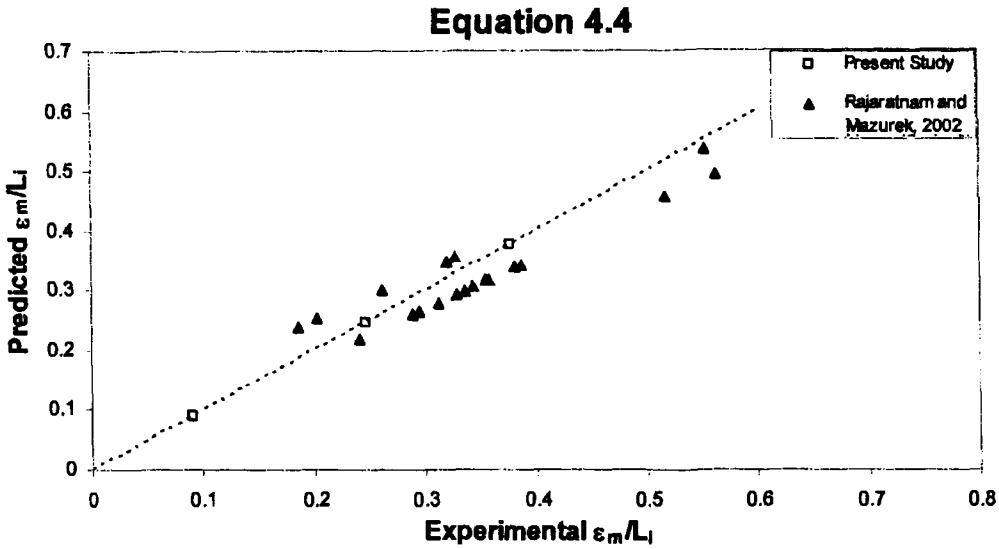

(a)

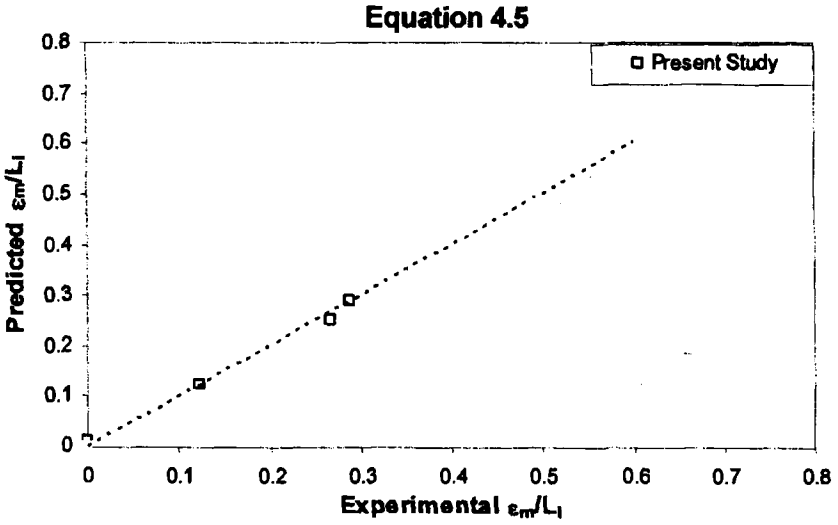

(b)

Figure 4.14: Comparison between the experimental and the predicted results
(a) Non-plunging case
(b) Plunging case

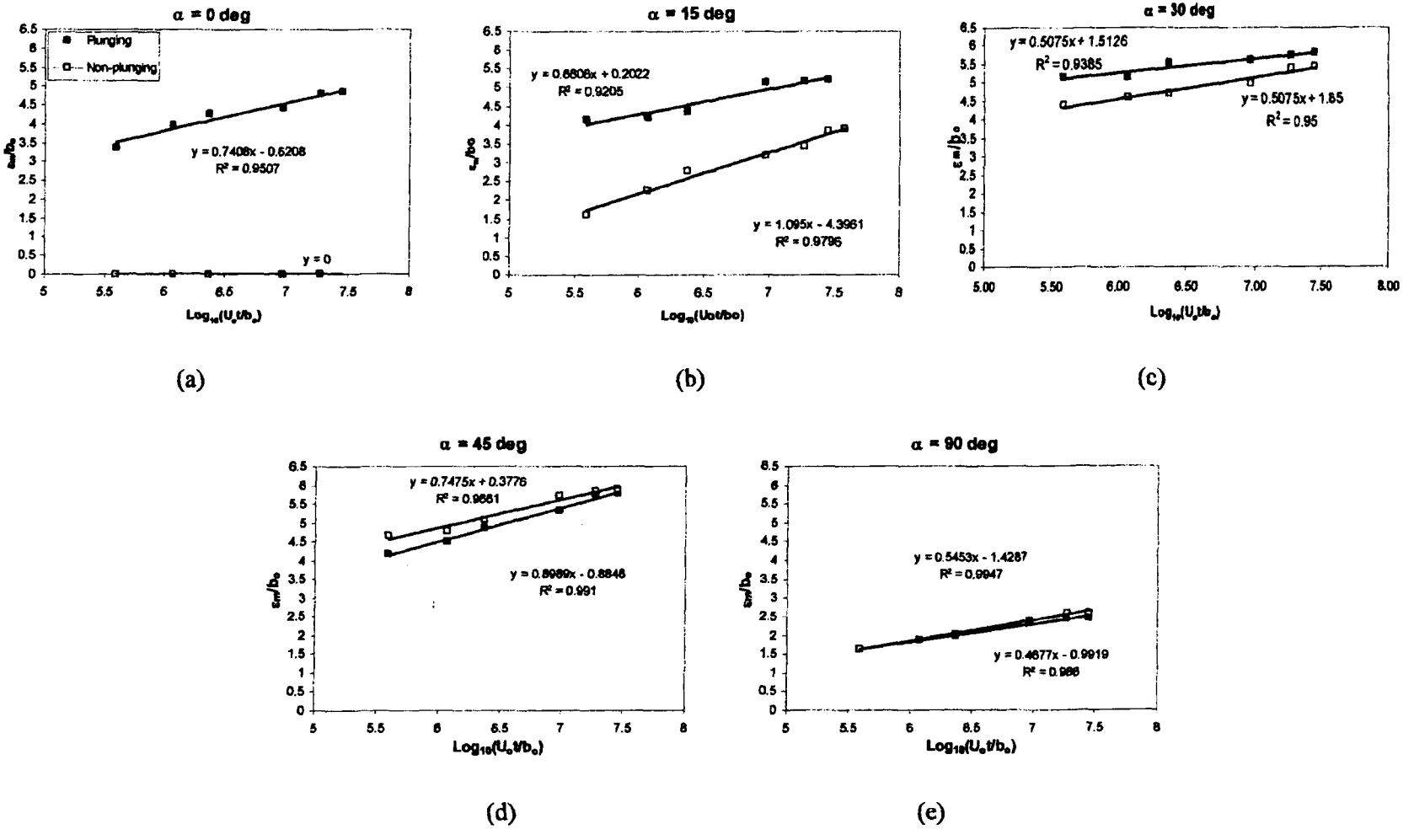

Figure 4.15: Variation of the maximum scour depth with time.

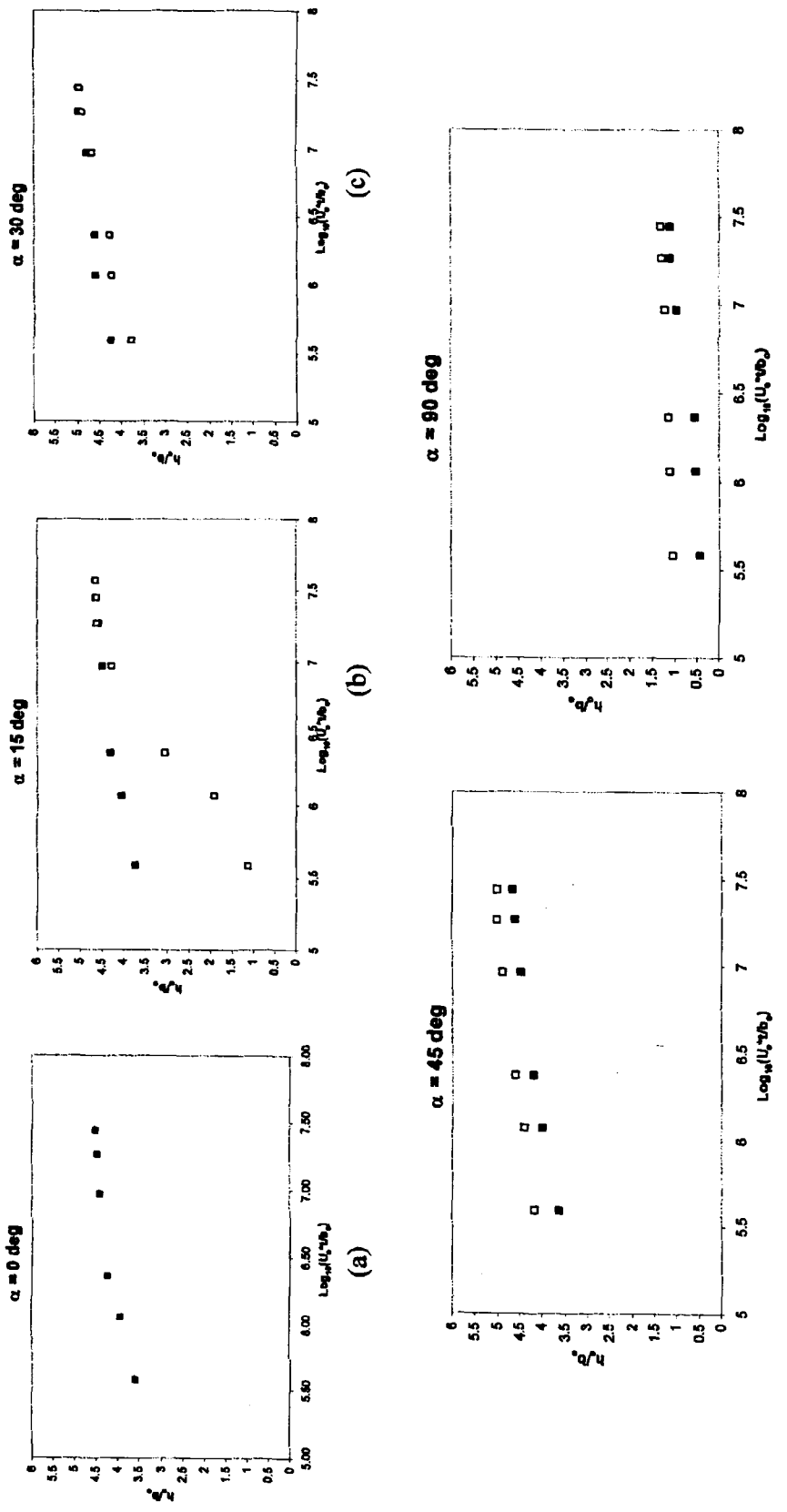

Figure 4.16: Variation of height of ridge with time.

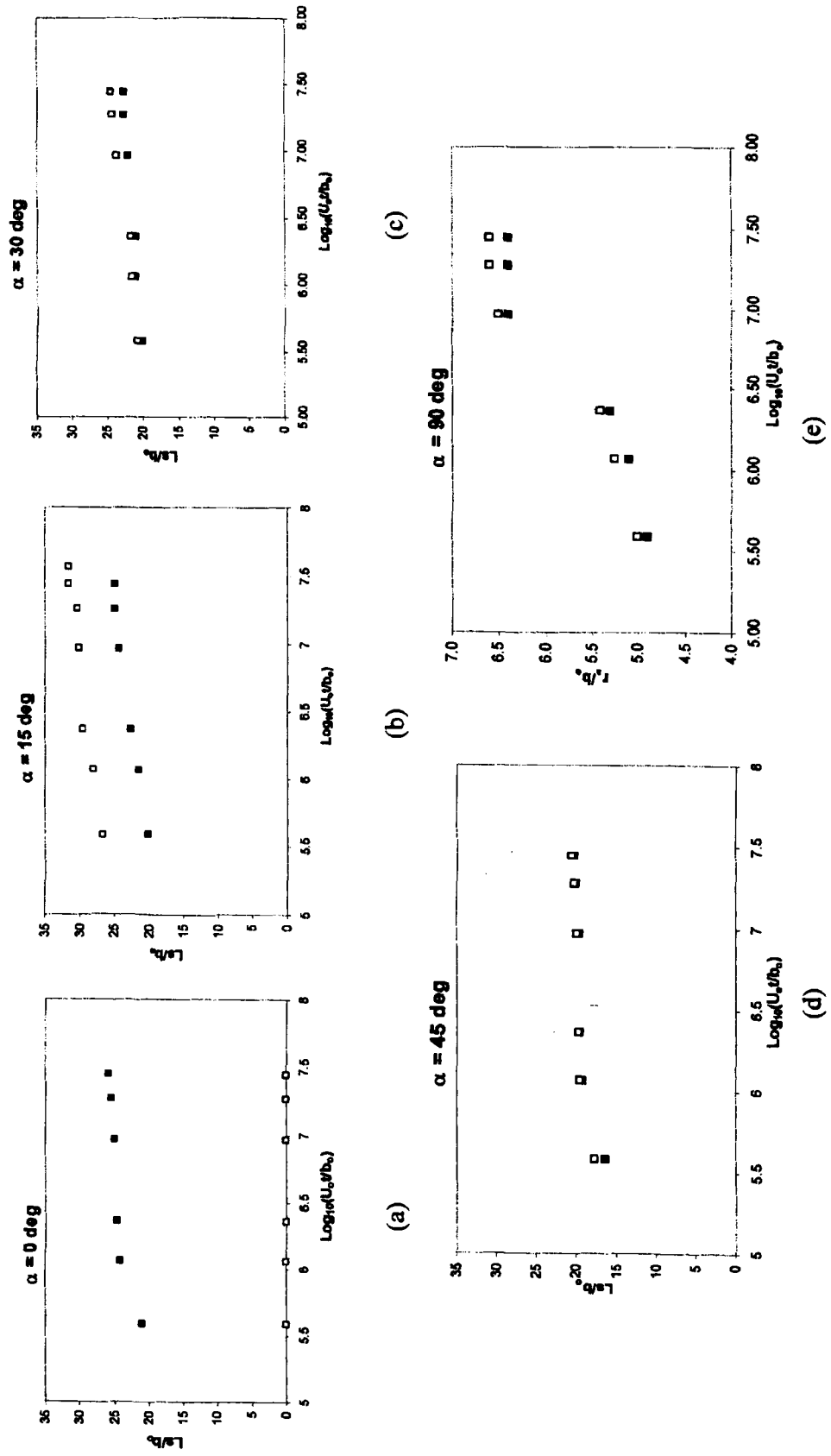

Figure 4.17: Variation of the length of scour with time.

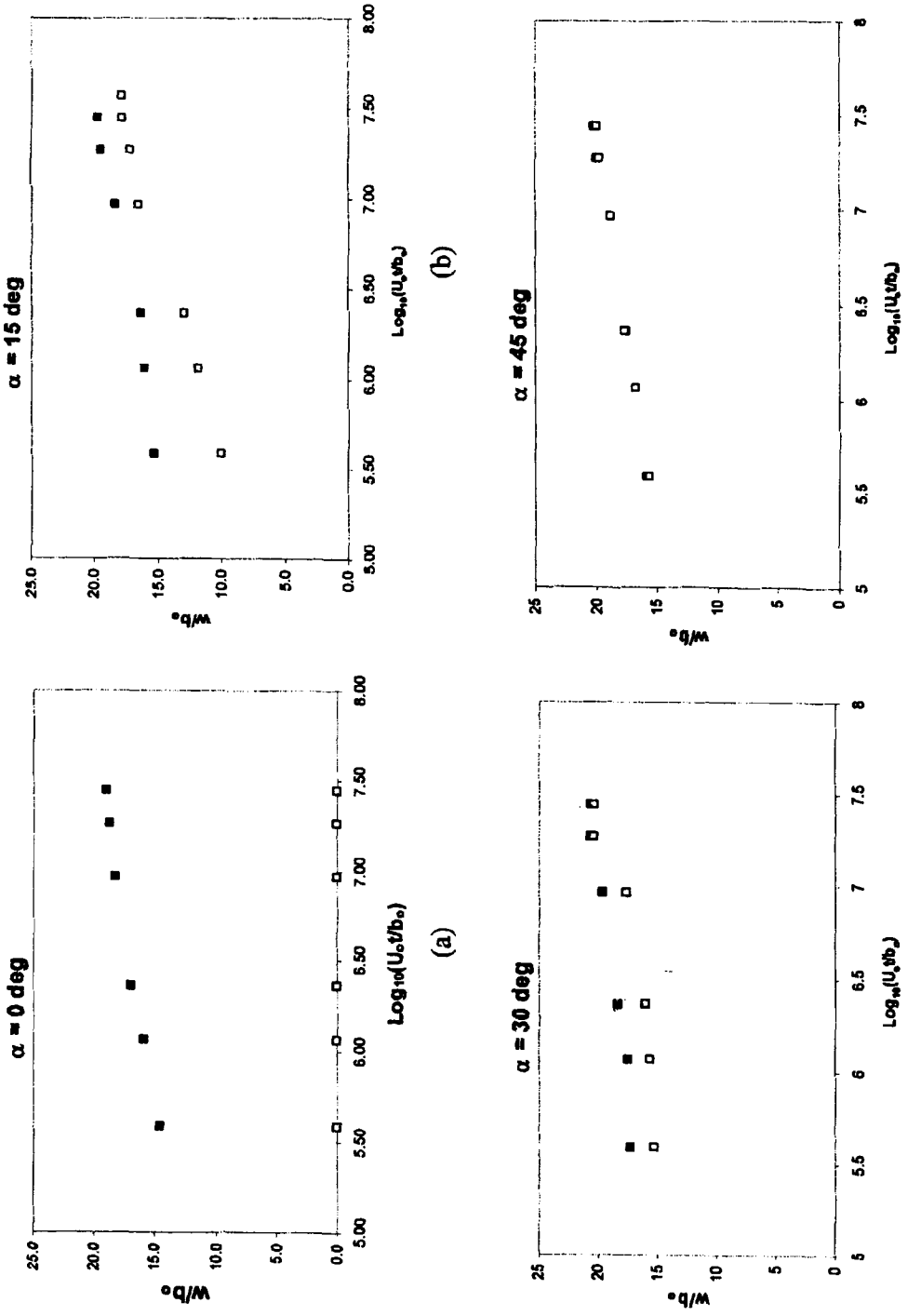

Figure 4.18: Variation of width of scour with time.

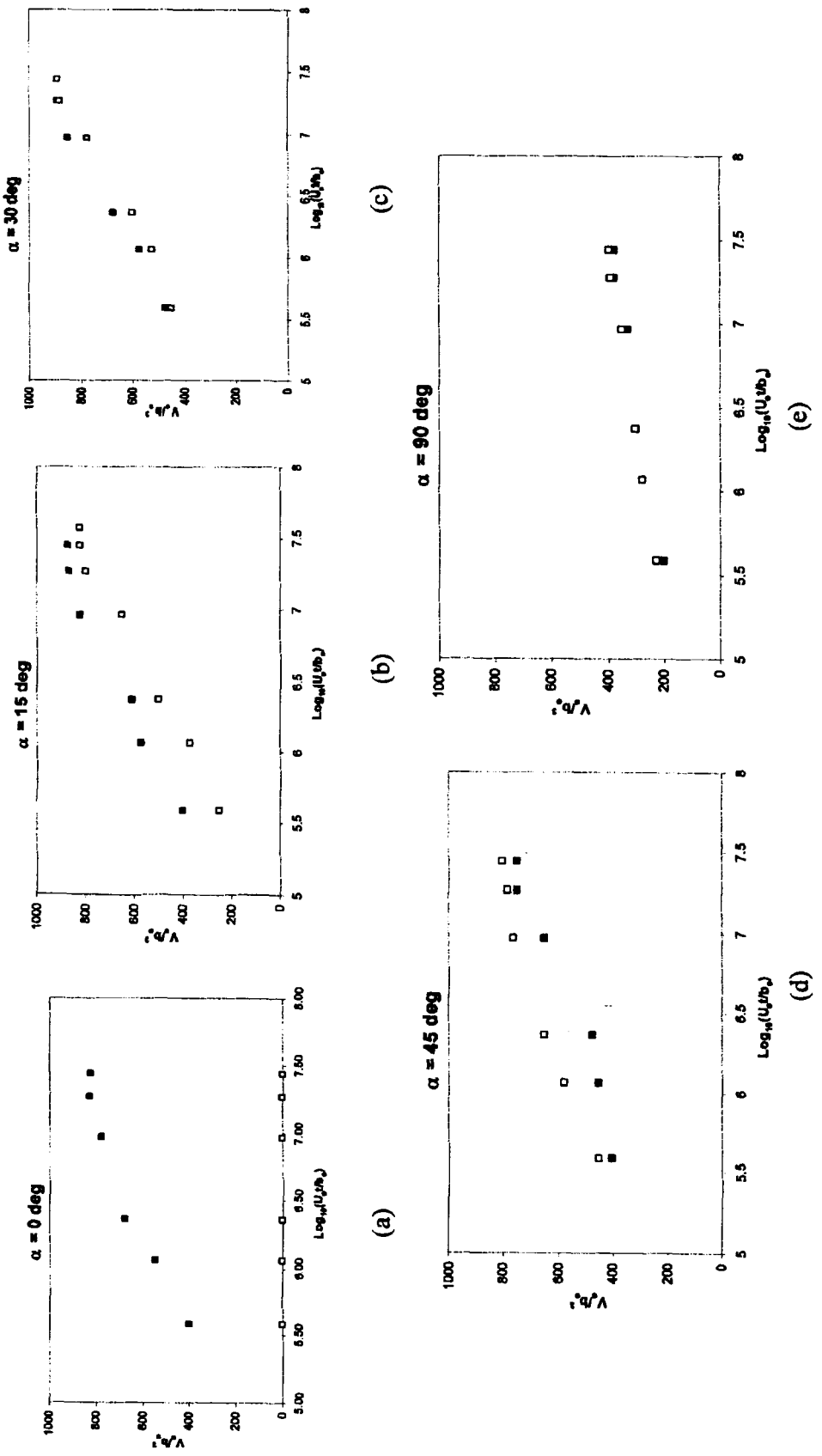

Figure 4.19: Variation of scour volume with time.

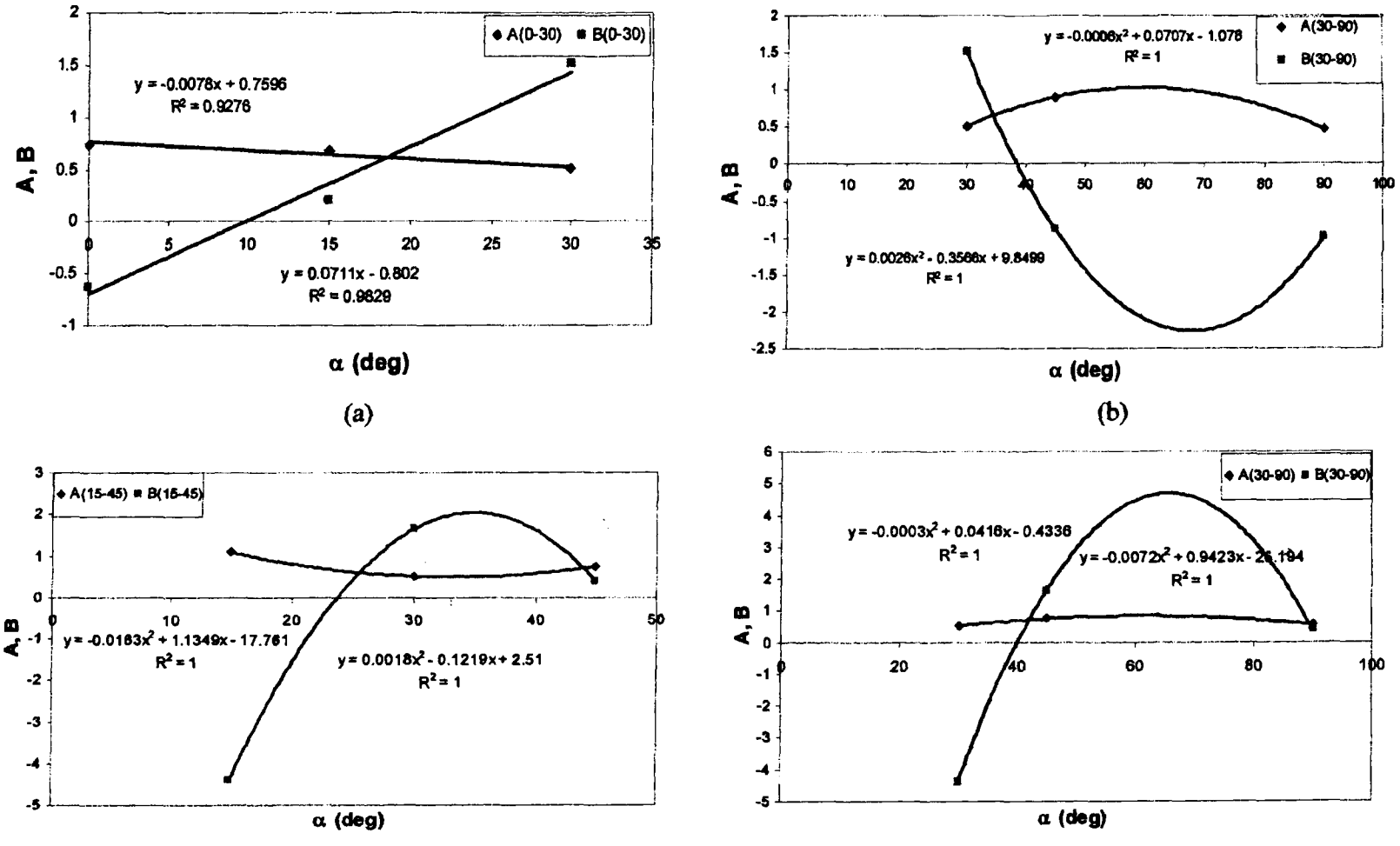

Figure 4.20: Variation of curve fit parameters (A and B) with α; (a, b) Plunging case (c,d) Non-plunging case

CHAPTER 5
CONCLUSIONS AND RECOMMENDATIONS

5.1 Conclusions

The present study deals with local scour caused by square turbulent impinging jets. The series of experiments cover two tailwater depths corresponding to the plunging and non-plunging condition. The tests were conducted for five jet impinging angles ($0° < \alpha < 90°$) with the same densimetric Froude number and sand sample. All tests were conducted until an asymptotic state of scour is reached.

The major conclusions of the study are:

1. The present study has identified the evolution of the scour process for both the plunging and the non-plunging jet conditions.

2. The dependence of the scour parameters on time has been quantitatively identified. It should be noted that for the plunging case, the asymptotic state is reached at t = 72 hours for all jet impinging angles. On the other hand, for the non-plunging case for $\alpha = 0°$, no scour formation has been noticed even after 24 hours of testing. Further, in case of the non-plunging condition, for $\alpha = 15°$, the asymptotic state is attained at t = 96 hours unlike other jet impinging angles ($15° < \alpha < 90°$) where the asymptotic state is attained at t = 72 hours.

3. It can be concluded that for small jet impingement angles ($15° < \alpha < 30°$) the difference in the scour geometry between the non-plunging and the plunging condition is more pronounced. It is evident that for $\alpha > 45°$, the difference in the scour geometry between the non-plunging and the plunging condition is further reduced.

4. The vertical jet flow case shows some distinct characteristics for both the plunging and non-plunging conditions. It should be noted that the trend seen in the present study is similar to the earlier observation made by Rajaratnam and Mazurek (2003) on vertical jets. The jet remains in Strongly Deflected Jet Regime for the plunging case and Weakly Deflected Jet Regime for the non-plunging case as defined by Aderibigbe and Rajaratnam (1996).

5. In an effort to provide useful but simplified scour predicting equations at asymptotic condition, an attempt has been made to combine all jet impinging angles ($15° < \alpha < 90°$) for both the plunging and non-plunging conditions. In order to prove the accuracy of the equation, a comparison has been made between the experimental and the predicted results and it has been found that the prediction based on the present study are more appropriate for a wide range of jet impinging angles.

5.2 Recommendations for future studies

The present study has provided extensive observations of the scouring process due to a three-dimensional square turbulent impinging jet on cohesionless sand bed for plunging and non-plunging conditions. To further expand the scope, studies need to be carried out at higher densimetric Froude number ($F_o > 10$) and small impingement distance ($h_{imp} < 5.5d$). To clarify the effect of the grain size distribution, coarser bed material need to be used in future studies. This will assist in understanding the role of particle size separation.

REFERENCES

Ade, F. and Rajaratnam, N. (1998), "Generalized study of erosion by circular horizontal turbulent jets." Journal of Hydraulic Research, Vol. 36, No. 4, pp.613-635.

Aderibigbe, O. and Rajaratnam, N. (1998), "Effect of sediment gradation on erosion by plane turbulent wall jets." Journal of Hydraulic Engineering, Vol. 124, No. 10, pp.1034-1042.

Aderibigbe, O. and Rajaratnam, N. (1996), "Erosion of loose beds by submerged circular impinging vertical turbulent jets.", Journal of Hydraulic Research, Vol. 34, No. 1, pp.19-33.

Afify, A. and Urroz, G. (1994), "Plunge-Pool Scour by Inclined Jets.", Proc. National Conference on Hydraulic Engineering, Vol. 2, pp.1040-1044.

Ahsan, M. and Mazurek, K. (2003), "Submergence effects on interaction of flow with the sediment bed in local scour.", Annual Conference of the Canadian Society of Civil Engineering, Nouveau-Brunswick, Canada, pp.1- 10.

Akashi, N. and Saitou, T. (1986), "Influence of water surface on scour from vertical submerged jet.", Journal of Hydroscience and Hydraulic Engineering, Vol. 4, No. 2, pp.55-69.

Ali, K.H.M and Lim, S.Y (1986), "Local scour caused by submerged wall jets.", Proc. of the Inst. of Civil Engineers, Part 2, 81, pp. 607-645.

Ali, K.H.M and Neyshabouri, S.A.A. (1991), "Localized scour downstream of a deeply submerged horizontal jet.", Proc. of the Inst. of Civil Engineers, Part 2, 91, 1-18.

Anderson, C.L. and Blaisdell, F.W. (1982), "Plunge Pool Energy Dissipator for Pipe Spillways.", Proceedings- Conference Applying Research to Hydraulic Practice Jackson, New York, pp. 289-298.

Azuma, R., Sekiguchi, H. and Ono, T. (2006), "Performance of Levee System at Flood Stage.", Annuals of Disas. Prev. Res. Inst., Kyoto Univ., No. 49 C, pp. 225-235.

Balachandar, R. and Kells, J.A. (1997), "Local channel scour in uniformly graded sediments: the time scale problem.", Canadian Journal of Civil Engineering, Vol. 24, pp.799-807.

Balachandar, R., Kells, J.A. and Thiessen, R.J. (2000), "The effect of tailwater depth on the dynamics of local scour.", Canadian Journal of Civil Engineering, Vol. 27, pp.138-150.

Bey, A., Faruque, M. A. A., and Balachandar, R. (2006), "Two dimensional scour hole problem: Role of fluid structures.", ASCE Journal of Hydraulic Engineering, Vol. 133, No. 4, pp. 414-430.

Bormann, N.E and Julien, P.Y. (1991), "Scour downstream of Grade-Control structures.", Journal of Hydraulic Engineering, Vol. 117, No. 5, pp.579-594.

Blaisdell, F.W and Anderson, C.L. (1991), "Pipe plunge pool energy dissipater.", ASCE, Journal of Hydraulic Engineering Vol. 117, No. 3, pp. 303-323.

Breusers, H. N. C., and Raudkivi, A. J. (1991), "Scouring.", Int. Assoc. of Hydraulic Research-Hydraulic Structure Design Manual. A. A. Balkem, Rotterdam, The Netherlands.

Canepa, S. and Hager, W.H. (2003), "Effect of air jet content on plunge pool scour.", Journal of Hydraulic Engineering, Vol. 128, No. 5, pp.358-365.

Chiew, Y.M. and Lim, S.Y. (1996), "Local scour by a deeply submerged horizontal circular jet.", Journal of Hydraulic Engineering, pp.529-532.

Deshpande, N.P., Balachandar, R. and Mazurek, K.A.(2007), "Effects of Submergence and Test start-up conditions on local scour by Plane Turbulent Wall Jets.", Journal of Hydraulic Research, Vol. 45, No. 3, pp. 370-387.

Faruque, M.A.A., Sarathi, P. and Balachandar, R. (2006), "Clear water local scour by submerged three-dimensional wall jets: Effect of tailwater depth.", ASCE Journal of Hydraulic Engineering, Vol.132, No. 6, pp.575-580.

Figliola and Beasley (1995), "Theory and Design for Mechanical Measurements", 2nd. Ed., John Wiley and Sons, Inc., New York, NY.

Hager, W.H., Oliveto, G., Pagliara, S. and Unger, J. (2004), "Recent advances in scour hydraulics.", River Flow 2004 conference, London, pp. 3-12.

Karki, R., Faruque, M.A.A. and Balachandar, R. (2007), "Local Scour by submerged offset jets.", Submitted to the Water Management Journal, Proc. of the Institution of Civil Engineers (December 2005).

Laursen, E.M. (1952), "Observations on the nature of scour.", Proc. of the fifth Hydraulics Conference, Iowa city, Iowa, pp. 179-197.

Lim, S. Y. (1995), "Scour below unsubmerged full-flowing culvert outlets.", Proc. of the Institution of Civil Engineers, Water Maritime and Energy, Vol. 112, No. 2, pp. 136-149.

Mih, W.C. and Kabir, J. (1983), "Impingement of Water Jets on nonuniform Streambed.", Journal of Hydraulic Engineering, Vol. 109, No. 4, pp.536-548.

Mih, W.C. (1982), "Scouring Effects of Water Jets Impinging on Non-uniform Streambeds.", Proc. Conference Applying Research to Hydraulic Practice, Jackson, New York, pp. 270-279.

Minor, H., Hager, W.H. and Canepa, S. (2002), "Does an aerated water jet reduce plunge pool scour?", Proc. Conference Applying Research to Hydraulic Practice, Jackson, New York, pp. 117-124.

Pagliara, S., Hager, W.H. and Minor, H.E. (2004), "Plunge pool scour in prototype and laboratory.", International Conference Hydraulics of Dams and River Structures, Tehran, pp. 165-172.

Pagliara, S., Hager, W.H., Minor, H.E. (2006), "Hydraulics of plane plunge pool scour.", Journal of Hydraulic Engineering, Vol. 132, No. 5, pp.450-461.

Rajaratnam, N. (1976), "Turbulent Jets.", Elsevier Scientific Publishing Company, Amsterdam.

Rajaratnam, N. (1981), "Erosion by plane turbulent jets.", Journal of Hydraulic Research, Vol. 19, No. 4, pp. 339-358.

Rajaratnam, N. and Berry, B. (1977), "Erosion by circular turbulent wall jets.", Journal of Hydraulic Research, Vol. 15, No. 3, pp. 277-289.

Rajaratnam, N. and Macdougall, R.K. (1983), "Erosion by plane wall jets with minimum tailwater.", Journal of Hydraulic Engineering, Vol. 109, No. 7, pp.1061-1064.

Rajaratnam, N. and Mazurek, K.A. (2002), "Erosion of a polystyrene bed by obliquely impinging circular turbulent air jets.", Journal of Hydraulic Research, Vol. 40, No. 6, pp. 709-716.

Rajaratnam, N. and Mazurek, K.A. (2003), "Erosion of Sand by Circular Impinging Water Jets with Small Tailwater.", Journal of Hydraulic Engineering, Vol. 129, No. 3, pp.225-229.

Rajaratnam, N. and Aderibigbe, O. (1995), "Erosion of sand beds by oblique plane water jets.", Proc. of the Institution of Civil Engineers, Water Maritime and Energy, Vol. 112, No. 1, pp 31-38.

Rajaratnam, N. and Beltaos, S. (1977), "Erosion by Impinging Circular Turbulent Jets.", Journal of Hydraulic Engineering, Vol. 103, No. 10, pp.1191-1205.

Rajaratnam, N. and Diebel, M. (1981), "Erosion below culvert-like structure.", Proc., 5th Canadian Hydotechnical Conference, CSCE, pp. 469-484

Rouse, H. (1939), "Criterion for Similarity in Sediment Transport.", Proc. of the Hydraulic Conference, Iowa State University, Studies in Engineering, Bulletin 20, pp. 33 – 49

Sankar, G. (2005), "Characteristics of confined square jets in the vicinity of a free surface.", M. A. Sc. Thesis, University of Windsor, Windsor, Canada.

Sarathi, P., Faruque, M.A.A. and Balachandar, R. (2007), "Influence of tailwater depth, sediment size and densimetric Froude number on scour by submerged square wall jets.", To appear in the Journal of Hydraulic Research.

Sarma, K.V.N. and Sivasankar, R. (1968), "Scour under vertical circular jets.", The Institution of Engineers (India), Bangalore, pp.568 -579.

Tarapore, Z.S. (1956). "Scour below a submerged sluice gate.", MSc Thesis, Dept. of civil Engineering, University of Minneapolis, Minnesota, USA

Westrich, B. and Kobus, H. (1973), "Erosion of a Uniform Sand bed by continuous and pulsating jets.", International Association for Hydraulic Research, Vol.1, Paper no A13, pp. 1-8.

APPENDIX A: Uncertainty analysis and error estimation

A.1 Introduction

In general, the experimental errors can have two components: a fixed (bias) error and a random (precision) error. Experimental results involve various sources of error. Errors could be accidental errors, fixed errors and mistakes. Each of the error exhibits the bias (B) and precision (P) components, which can be calculated by using the root-sum-square (RSS) method as follows:

$$B = \pm \sqrt{B_1^2 + B_2^2 + ...B_n^2}$$

$$P = \pm \sqrt{P_1^2 + P_2^2 + ...P_n^2}$$

where n is the total number of error sources. In the RSS method the combining of bias and precision errors can be done by the following equation:

$$E = \pm \sqrt{B^2 + P^2}$$

The calculations used in estimating the errors involved in different measurements are described. Considering a quantity to be measured such as x_o units and recorded as x units, one can write the error (e) in x_o as,

$$\begin{aligned} x &= x_o + e \\ &= x_o(1+f) \end{aligned}$$

where $f = e/x_o$ and can be referred as the fractional error in x_o, or percentage error after multiplying by 100 ($= 100e/x_o$).

If measurements such as x, y,....are used to calculate R = R(x,y,....), the uncertainty in the R (W_R) can be estimated using the formula given in Figliola and Beasley (1995) as follows:

$$W_R = \pm\sqrt{(\frac{\partial R}{\partial x}w_x)^2 + (\frac{\partial R}{\partial y}w_y)^2}$$

where, w_x is the uncertainty in x and w_y is the uncertainty in y. The most likely uncertainty percentage is calculated as $100w_R/R$.

Thus, we see that uncertainties in a measured variable are propagated through another measured variable in a predictable way.

Table A.1 summarises the maximum uncertainties in the measured and derived quantities used in this thesis.

Parameters	Maximum uncertainty (± %)
x	0.4
b_o	7.1
d_{50}	3.5
F_o	4.0
ε_m	3.5
w	0.5
V_o	3.0
ε_m/b_o	7.4
w/b_o	7.1
x/b_o	0.7
V_o/b_o^3	4.0
U_o	6.0

APPENDIX B: Experimental data

Table B.1: Scour parameters at different times

Plunging case:

$\alpha = 0°$

Time, t (hr)	$Log_{10}(U_o*t/b_o)$	ε_m (mm)	ε_m/b_o	h_o (mm)	h_o/b_o	w (mm)	w/b_o	L_s (mm)	L_s/b_o	V_o (c.c)	V_o/b_o^3
1	5.59	33.8	3.38	35.85	3.585	146	14.6	210	21	400	400
3	6.07	39.8	3.98	39.34	3.934	159	15.9	241	24.1	550	550
6	6.37	42.7	4.265	42.34	4.234	170	17.0	246	24.6	675	675
24	6.97	44.2	4.42	43.95	4.395	182	18.2	250	25	775	775
48	7.27	48	4.796	44.57	4.457	188	18.8	257	25.7	825	825
72	7.45	48.02	4.802	45	4.5	190	19.0	258	25.8	825	825

$\alpha = 15°$

Time, t (hr)	$Log_{10}(U_o*t/b_o)$	ε_m (mm)	ε_m/b_o	h_o (mm)	h_o/b_o	w (mm)	w/b_o	L_s (mm)	L_s/b_o	V_o (c.c)	V_o/b_o^3
1	5.59	41.5	4.15	37.06	3.706	153	15.3	201	20.1	400	400
3	6.07	43.1	4.31	40.15	4.015	160	16.0	215	21.5	575	575
6	6.37	43.7	4.37	42.85	4.285	164	16.4	226	22.6	610	610
24	6.97	51.4	5.14	44.64	4.464	184	18.4	244	24.4	825	825
48	7.27	51.8	5.18	45.65	4.565	196	19.6	248	24.8	875	875
72	7.45	52.1	5.21	46.26	4.626	196	19.6	248	24.8	875	875

$\alpha = 30°$

Time, t (hr)	$Log_{10}(U_o*t/b_o)$	ε_m (mm)	ε_m/b_o	h_o (mm)	h_o/b_o	w (mm)	w/b_o	L_s (mm)	L_s/b_o	V_o (c.c)	V_o/b_o^3
1	5.59	51.5	5.15	42.28	4.228	172	17.2	201	20.1	475	475
3	6.07	51.5	5.15	45.67	4.567	175	17.5	210	21.0	575	575
6	6.37	55.3	5.53	45.96	4.596	184	18.4	211	21.1	675	675
24	6.97	55.9	5.59	47.78	4.778	196	19.6	221	22.1	850	850
48	7.27	57.5	5.75	49.62	4.962	200	20.0	227	22.7	890	890
72	7.45	59	5.9	49.65	4.965	200	20.0	228	22.8	890	890

$\alpha = 45°$

Time, t (hr)	$Log_{10}(U_o*t/b_o)$	ε_m (mm)	ε_m/b_o	h_o (mm)	h_o/b_o	w (mm)	w/b_o	L_s (mm)	L_s/b_o	V_o (c.c)	V_o/b_o^3
1	5.59	41.7	4.174	36.01	3.601	158	15.8	164	16.4	400	400
3	6.07	45.2	4.519	39.69	3.969	168	16.8	193	19.3	450	450
6	6.37	48.7	4.872	41.77	4.177	176	17.6	195	19.5	475	475
24	6.97	53.2	5.316	44.81	4.481	188	18.8	195	19.5	650	650
48	7.27	57.5	5.75	45.99	4.599	202	20.2	202	20.2	750	750
72	7.45	57.8	5.778	46.55	4.655	202	20.2	202	20.2	750	750

$\alpha = 90°$

Time, t (hr)	$Log_{10}(U_o*t/b_o)$	ε_m (mm)	ε_m/b_o	h_o (mm)	h_o/b_o	r_s (mm)	r_s/b_o	V_o (c.c)	V_o/b_o^3
1	5.59	16.2	1.619	4.18	0.418	49	4.9	175	175
3	6.07	18.5	1.853	4.89	0.489	51	5.1	275	275
6	6.37	19.6	1.959	5.23	0.523	53	5.3	300	300
24	6.97	23.3	2.332	9.45	0.945	64	6.4	325	325
48	7.27	24.3	2.432	10.98	1.098	64	6.4	375	375
72	7.45	24.4	2.438	11.08	1.108	64	6.4	375	375

Non-plunging case:

$\alpha = 15°$

Time, t (hr)	$Log_{10}(U_o*t/b_o)$	ε_m (mm)	ε_m/b_o	h_o (mm)	h_o/b_o	w (mm)	w/b_o	L_s (mm)	L_s/b_o	V_o (c.c)	V_o/b_o^3
1	5.59	16.19	1.619	11.07	1.107	100.6	10.1	267	26.7	250	250
3	6.07	22.74	2.274	19.03	1.903	118	11.8	280	28.0	375	375
6	6.37	27.88	2.788	30.21	3.021	130	13.0	294	29.4	500	500
24	6.97	31.82	3.182	42.74	4.274	166	16.6	301	30.1	650	650
48	7.27	34.31	3.431	46.08	4.608	172	17.2	302	30.2	800	800
72	7.45	38.51	3.851	46.15	4.615	178	17.8	315	31.5	825	825
96	7.58	38.88	3.888	46.33	4.633	178	17.8	315	31.5	825	825

$\alpha = 30°$

Time, t (hr)	$Log_{10}(U_o*t/b_o)$	ε_m (mm)	ε_m/b_o	h_o (mm)	h_o/b_o	w (mm)	w/b_o	L_s (mm)	L_s/b_o	V_o (c.c)	V_o/b_o^3
1	5.59	44.02	4.402	37.54	3.754	152.2	15.22	207.0	20.7	450	450
3	6.07	45.95	4.595	42.13	4.213	156	15.6	215.0	21.5	525	525
6	6.37	47.03	4.703	42.6	4.26	160	16	218.0	21.8	600	600
24	6.97	49.75	4.975	46.5	4.65	176	17.6	237.0	23.7	775	775
48	7.27	53.98	5.398	48.5	4.9	206	20.6	244.0	24.4	885	885
72	7.45	54.36	5.436	49.5	4.95	207	20.7	245.0	24.5	890	890

$\alpha = 45°$

Time, t (hr)	$Log_{10}(U_o*t/b_o)$	ε_m (mm)	ε_m/b_o	h_o (mm)	h_o/b_o	w (mm)	w/b_o	L_s (mm)	L_s/b_o	V_o (c.c)	V_o/b_o^3
1	5.59	46.63	4.663	41.4	4.14	156	15.6	178.0	17.8	450	450
3	6.07	47.75	4.775	43.8	4.38	168	16.8	195.0	19.5	575	575
6	6.37	50.84	5.084	45.89	4.589	177	17.7	197.0	19.7	650	650
24	6.97	57.08	5.708	48.89	4.889	188.6	18.86	199.0	19.9	760	760
48	7.27	58.5	5.85	49.21	4.98	197	19.7	204.0	20.4	800	800
72	7.45	58.89	5.889	50.01	5.001	197	19.7	205.0	20.5	800	800

$\alpha = 90°$

Time, t (hr)	$Log_{10}(U_o*t/b_o)$	ε_m (mm)	ε_m/b_o	h_o (mm)	h_o/b_o	r_s (mm)	r_s/b_o	V_o (c.c)	V_o/b_o^3
1	5.59	16.33	1.633	10.48	1.048	50.0	5	225	225
3	6.07	18.76	1.876	11.02	1.102	52.5	5.25	275	275
6	6.37	20.24	2.024	11.28	1.128	54.0	5.4	300	300
24	6.97	23.78	2.378	12.13	1.213	65.0	6.5	350	350
48	7.27	25.86	2.586	12.75	1.275	66.0	6.6	390	390
72	7.45	25.99	2.599	12.89	1.289	66.0	6.6	390	390

Table B.2: Scour profiles

Plunging case:

α = 0°

t = 1 hr

x (mm)	x/bo	y (mm)	y/bo
170	17	0	0
215	21.5	-17.95	-1.795
265	26.5	-32.27	-3.227
315	31.5	-33.8	-3.38
365	36.5	-8.74	-0.874
415	41.5	24.38	2.438
433	43.3	35.85	3.585
465	46.5	16.64	1.664
489	48.9	0	0

t = 3 hr

x (mm)	x/bo	y (mm)	y/bo
172	17.2	0	0
185	18.5	-5.36	0.536
235	23.5	-26.52	2.652
285	28.5	-39.35	3.935
335	33.5	-37.72	3.772
365	36.5	-28.7	-2.87
415	41.5	2.57	0.257
465	46.5	35.51	3.551
471	47.1	39.34	3.934
515	51.5	17	1.7
537	53.7	0	0

t = 6 hr

x (mm)	x/bo	y (mm)	y/bo
169	16.9	0	0
219	21.9	-20.49	-2.049
269	26.9	-36.22	-3.622
319	31.9	-42.65	-4.265
369	36.9	-32.68	-3.268
419	41.9	2.86	0.286
469	46.9	35.29	3.529
481	48.1	42.34	4.234
519	51.9	19.89	1.989
547.5	54.7	0	0

t = 24 hr

x (mm)	x/bo	y (mm)	y/bo
169	16.9	0	0
219	21.9	-26.32	-2.632
269	26.9	-39.77	-3.977
319	31.9	-44.65	-4.465
369	36.9	-34.58	-3.458
419	41.9	0.94	0.094
469	46.9	35.6	3.56
487	48.7	43.95	4.395
519	51.9	22.77	2.277
550	55	0	0

t = 48 hr

x (mm)	x/bo	y (mm)	y/bo
169	16.9	0	0
219	21.9	-26.59	2.659
269	26.9	-41	-4.1
319	31.9	-47.96	4.796
369	36.9	-36.95	3.695
398	39.8	-20	-2
424	42.4	-0.39	0.039
469	46.9	31.8	3.18
489	48.9	44.57	4.457
519	51.9	29.96	2.996
558	55.8	0	0

t = 72 hr

x (mm)	x/bo	y (mm)	y/bo
169	16.9	0	0
194	19.4	-15.62	-1.562
219	21.9	-27.2	-2.72
269	26.9	-42.5	-4.25
319	31.9	-48.72	-4.872
369	36.9	-37.99	-3.799
394	39.4	-24.71	-2.471
419	41.9	-5.96	-0.596
427	42.7	0	0
444	44.4	11.7	1.17
469	46.9	32.94	3.294
488	48.8	46.1	4.61
519	51.9	27.73	2.773
560	56	0	0

$\alpha = 15°$

t = 1 hr

x (mm)	x/bo	y (mm)	y/bo
135	13.5	0	0
185	18.5	-27.11	-2.711
235	23.5	-41.5	-4.15
285	28.5	-30.22	-3.022
335	33.5	-1.77	-0.177
385	38.5	29.81	2.981
395	39.5	37.06	3.706
425	42.5	17.89	1.789
450	45	0	0

t = 3 hr

x (mm)	x/bo	y (mm)	y/bo
135	13.5	0	0
185	18.5	-27.19	2.719
235	23.5	-43.06	4.306
285	28.5	-39.55	3.955
335	33.5	-8.99	0.899
350	35	0	0
385	38.5	21.04	2.104
418	41.8	40.15	4.015
435	43.5	29.06	2.906
482	48.2	0	0

t = 6 hr

x (mm)	x/bo	y (mm)	y/bo
130	13	0	0
180	18	-26.23	-2.623
230	23	-43.71	-4.371
280	28	-42.07	-4.207
330	33	-13.76	-1.376
380	38	15.23	1.523
413	41.3	42.85	4.285
430	43	31.09	3.109
485	48.5	0	0

t = 24 hr

x (mm)	x/bo	y (mm)	y/bo
130	13	0	0
180	18	-28.55	-2.855
230	23	-45.51	-4.551
280	28	-51.43	-5.143
330	33	-24.25	-2.425
380	38	3.02	0.302
430	43	41.1	4.11
439	43.9	44.64	4.464
480	48	22.32	2.232
503	50.3	0	0

t = 48 hr

x (mm)	x/bo	y (mm)	y/bo
125	12.5	0	0
135	13.5	-5.59	0.559
145	14.5	-13.69	1.369
155	15.5	-20.58	2.058
175	17.5	-30.3	-3.03
225	22.5	-45.96	4.596
275	27.5	-50.76	5.076
325	32.5	-26.71	2.671
373	37.3	0	0
375	37.5	1.25	0.125
425	42.5	40.45	4.045
433	43.3	45.65	4.565
475	47.5	22.7	2.27
504	50.4	0	0

t = 72 hr

x (mm)	x/bo	y (mm)	y/bo
125	12.5	0	0
150	15	-18.06	-1.806
200	20	-40.34	-4.034
236	23.6	-51.66	-5.166
270	27	-52.12	-5.212
300	30	-41.71	-4.171
350	35	-12.85	-1.285
369	36.9	0	0
400	40	23.95	2.395
437	43.7	46.26	4.626
450	45	41.55	4.155
475	47.5	22.78	2.278
508	50.8	0	0

$\alpha = 30°$

t = 1 hr				t = 3 hr				t = 6 hr			
x (mm)	x/bo	y (mm)	y/bo	x (mm)	x/bo	y (mm)	y/bo	x (mm)	x/bo	y (mm)	y/bo
82	8.2	0	0	79	7.9	0	0	78	7.8	0	0
91	9.1	-8.07	-0.807	89	8.9	-5.59	0.559	89	8.9	-7.78	-0.778
101	10.1	-22.08	-2.208	99	9.9	-15.99	1.599	99	9.9	-16.15	-1.615
139	13.9	-34.29	-3.429	109	10.9	-23.47	2.347	109	10.9	-22.24	-2.224
164	16.4	-45.47	-4.547	139	13.9	-36.46	3.646	139	13.9	-34.25	-3.425
179	17.9	-51.45	-5.145	164	16.4	-47.84	4.784	164	16.4	-47.98	-4.798
214	21.4	-37.99	-3.799	189	18.9	-51.54	5.154	189	18.9	-55.34	-5.534
264	26.4	-12.76	-1.276	214	21.4	-41.68	4.168	214	21.4	-41.48	-4.148
314	31.4	22.89	2.289	239	23.9	-27.37	2.737	264	26.4	-15.88	-1.588
343	34.3	42.28	4.228	264	26.4	-13.48	1.348	314	31.4	17.87	1.787
364	36.4	31.39	3.139	314	31.4	16.72	1.672	359	35.9	45.96	4.596
				356	35.6	45.67	4.567	364	36.4	45.8	4.58
				364	36.4	43.88	4.388	389	38.9	33.58	3.358
				389	38.9	24.5	2.45	427	42.7	0	0
				424	42.4	0	0				

t = 24 hr				t = 48 hr				t = 72 hr			
x	x/bo	y	y/bo	x (mm)	x/bo	y (mm)	y/bo	x (mm)	x/bo	y (mm)	y/bo
76	7.6	0	0	71	7.1	0	0	-71	7.1	0	-0
91	9.1	-9.49	-0.949	81	8.1	-10.36	1.036	81	8.1	-8.54	-0.854
101	10.1	-21.27	-2.127	91	9.1	-16.58	1.658	91	9.1	-16.89	-1.689
111	11.1	-27.72	-2.772	101	10.1	-25.35	2.535	101	10.1	-23.85	-2.385
139	13.9	-39.11	-3.911	111	11.1	-29.87	2.987	111	11.1	-29.32	-2.932
164	16.4	-50.26	-5.026	139	13.9	-41.7	-4.17	139	13.9	-42.4	-4.24
189	18.9	-55.93	-5.593	164	16.4	-53.55	5.355	164	16.4	-53.31	-5.331
214	21.4	-42.88	-4.288	189	18.9	-57.45	5.745	189	18.9	-59.03	-5.903
239	23.9	-30.99	-3.099	214	21.4	-44.18	4.418	214	21.4	-46.5	-4.65
264	26.4	-16.46	-1.646	239	23.9	-32.28	3.228	239	23.9	-29.74	-2.974
289	28.9	-4.66	-0.466	264	26.4	-18.98	1.898	264	26.4	-14.29	-1.429
297	29.7	0	0	314	31.4	12.13	1.213	289	28.9	-1.94	-0.194
314	31.4	12.49	1.249	364	36.4	45.03	4.503	314	31.4	14.98	1.498
339	33.9	28.72	2.872	369	36.9	49.62	4.962	339	33.9	29.57	2.957
367	36.7	47.78	4.778	414	41.4	23.58	2.358	364	36.4	46.02	4.602
389	38.9	37.24	3.724	444	44.4	0	0	369	36.9	49.65	4.965
414	41.4	22.06	2.206					389	38.9	38.95	3.895
444	44.4	0	0					414	41.4	23.2	2.32
								444	44.4	0	0

$\alpha = 45°$

t = 1 hr				t = 3 hr				t = 6 hr			
x (mm)	x/bo	y (mm)	y/bo	x (mm)	x/bo	y (mm)	y/bo	x (mm)	x/bo	y (mm)	y/bo
41	4.1	0	0	35	3.5	0	0	35	3.5	0	0
45	4.5	-2.72	-0.272	45	4.5	-4.19	0.419	45	4.5	-5.23	-0.523
55	5.5	-15.13	-1.513	65	6.5	-20.11	2.011	55	5.5	-16.48	-1.648
75	7.5	-27.09	-2.709	75	7.5	-27.2	-2.72	65	6.5	-20.61	-2.061
91	9.1	-33.86	-3.386	95	9.5	-36	-3.6	75	7.5	-26.52	-2.652
111	11.1	-41.74	-4.174	115	11.5	-42.45	4.245	95	9.5	-37.53	-3.753
131	13.1	-34.86	-3.486	135	13.5	-45.19	4.519	115	11.5	-44.28	-4.428
171	17.1	-19.2	-1.92	155	15.5	-38.96	3.896	135	13.5	-48.72	-4.872
211	21.1	3.75	0.375	205	20.5	-12.46	1.246	155	15.5	-39.78	-3.978
251	25.1	36.01	3.601	228	22.8	0	0	205	20.5	-14.37	-1.437
271	27.1	31.94	3.194	255	25.5	17.59	1.759	230	23	0	0
311	31.1	0	0	287	28.7	39.69	3.969	255	25.5	14.22	1.422
				301	30.1	32.09	3.209	291	29.1	41.77	4.177
				336	33.6	0	0	305	30.5	36.77	3.677
								353	35.3	0	0

t = 24 hr				t = 48 hr				t = 72 hr			
x	x/bo	y	y/bo	x	x/bo	y	y/bo	x (mm)	x/bo	y (mm)	y/bo
35	3.5	0	0	30	3	0	0	28	2.8	0	0
45	4.5	-6.42	-0.642	45	4.5	-15.71	1.571	45	4.5	-13.32	-1.332
55	5.5	-14.91	-1.491	55	5.5	-19.64	1.964	55	5.5	-22.36	-2.236
65	6.5	-24.66	-2.466	65	6.5	-25.64	2.564	65	6.5	-24.55	-2.455
75	7.5	-30.66	-3.066	75	7.5	-33.02	3.302	75	7.5	-33.56	-3.356
105	10.5	-49.63	-4.963	85	8.5	-42.18	4.218	85	8.5	-42.23	-4.223
135	13.5	-53.16	-5.316	105	10.5	-51.16	5.116	105	10.5	-51.17	-5.117
165	16.5	-38.25	-3.825	135	13.5	-57.5	-5.75	135	13.5	-57.78	-5.778
215	21.5	-9.71	-0.971	151	15.1	-50.65	5.065	151	15.1	-50.55	-5.055
228	22.8	0	0	175	17.5	-33.73	3.373	175	17.5	-33.9	-3.39
265	26.5	23.96	2.396	225	22.5	-3.43	0.343	225	22.5	-3.22	-0.322
305	30.5	44.88	4.488	275	27.5	28.58	2.858	275	27.5	27.13	2.713
315	31.5	37.69	3.769	308	30.8	44.81	4.481	304	30.4	46.55	4.655
360	36	0	0	315	31.5	42.79	4.279	325	32.5	37.88	3.788
				350	35	15.33	1.533	345	34.5	20.33	2.033
				369	36.9	0	0	369	36.9	0	0

$\alpha = 90°$

t = 1 hr				t = 3 hr				t = 6 hr			
x (mm)	x/bo	y (mm)	y/bo	x (mm)	x/bo	y (mm)	y/bo	x (mm)	x/bo	y (mm)	y/bo
-86	8.6	0	0	-90	9	0	0	92	9.2	0	0
60	6	5.18	0.518	60	6	4.89	0.489	62	6.2	5.23	0.523
40	4	-6.07	-0.607	40	4	-8.72	0.872	42	4.2	-8.73	-0.873
20	2	-13.77	-1.377	20	2	-16.54	1.654	22	2.2	-17.29	-1.729
0	0	-16.19	-1.619	0	0	-18.53	1.853	0	0	-19.59	-1.959
-20	-2	-13.77	-1.377	-20	-2	-16.54	1.654	-22	-2.2	-17.29	-1.729
-40	-4	-6.07	-0.607	-40	-4	-8.72	0.872	-42	-4.2	-8.73	-0.873
-60	-6	5.18	0.518	-60	-6	4.89	0.489	-62	-6.2	5.23	0.523
-86	-8.6	0	0	-90	-9	0	0	-92	-9.2	0	0

t = 24 hr				t = 48 hr				t = 72 hr			
x (mm)	x/bo	y (mm)	y/bo	x (mm)	x/bo	y (mm)	y/bo	x (mm)	x/bo	y (mm)	y/bo
100	10	0	0	110	11	0	0	110	11	0	0
80	8	9.45	0.945	80	8	10.04	1.004	80	8	11.18	1.118
64	6.4	0	0	60	6	-3.02	0.302	60	6	-4.5	-0.45
60	6	-3.15	-0.315	40	4	-13.68	1.368	40	4	-13.88	-1.388
40	4	-14.15	-1.415	20	2	-20.33	2.033	0	0	-24.32	-2.432
20	2	-20.32	-2.032	0	0	-24.38	2.438	-40	-4	-13.88	-1.388
0	0	-23.32	-2.332	-20	-2	-20.33	2.033	-60	-6	-4.5	-0.45
-20	-2	-20.32	-2.032	-40	-4	-13.68	1.368	-80	-8	11.18	1.118
-40	-4	-14.15	-1.415	-60	-6	-3.02	0.302	-110	-11	0	0
-60	-6	-3.15	-0.315	-80	-8	10.04	1.004				
-80	-8	9.45	0.945	-110	-11	0	0				
-100	-10	0	0								

Non-plunging case:

$\alpha = 15°$

t = 1 hr

x (mm)	x/bo	y (mm)	y/bo
210	21	0	0
220	22	-1.64	-0.164
240	24	-5	-0.5
260	26	-8.92	-0.892
300	30	-14.29	-1.429
340	34	-16.19	-1.619
380	38	-15.57	-1.557
420	42	-11.74	-1.174
460	46	-2.91	-0.291
500	50	4.13	0.413
540	54	10.7	1.07
560	56	11.07	1.107
573	57.3	0	0

t = 3 hr

x (mm)	x/bo	y (mm)	y/bo
210	21	0	0
220	22	-2.66	0.266
240	24	-5.28	0.528
260	26	-9.63	0.963
280	28	-14.2	-1.42
300	30	-16.45	1.645
330	33	-22.22	2.222
360	36	-22.74	2.274
400	40	-20.21	2.021
450	45	-9.79	0.979
500	50	3.15	0.315
550	55	16.32	1.632
563	56.3	19.03	1.903
583	58.3	0	0

t = 6 hr

x (mm)	x/bo	y (mm)	y/bo
200	20	0	0
220	22	-1.32	-0.132
240	24	-6.8	-0.68
260	26	-12.3	-1.23
280	28	-17.56	-1.756
320	32	-23	-2.3
360	36	-26.88	-2.688
400	40	-27.88	-2.788
440	44	-18.04	-1.804
480	48	-5.4	-0.54
520	52	10.89	1.089
560	56	30.21	3.021
598	59.8	0	0

t = 24 hr

x (mm)	x/bo	y (mm)	y/bo
200	20	0	0
210	21	-0.43	-0.043
220	22	-3.05	-0.305
240	24	-9.26	-0.926
260	26	-14.02	-1.402
280	28	-19.49	-1.949
300	30	-23.08	-2.308
330	33	-27.98	-2.798
360	36	-29.82	-2.982
390	39	-31.82	-3.182
420	42	-29.36	-2.936
450	45	-23.01	-2.301
480	48	-9.63	-0.963
510	51	6.55	0.655
548	54.8	42.74	4.274
560	56	39.82	3.982
590	59	15	1.5
609	60.9	0	0

t = 48 hr

x (mm)	x/bo	y (mm)	y/bo
200	20	0	0
210	21	-2.04	0.204
220	22	-5.29	0.529
230	23	-8.24	0.824
240	24	-9.52	0.952
260	26	-15.88	1.588
280	28	-22.68	2.268
300	30	-28.29	2.829
330	33	-33.56	3.356
370	37	-36	-3.6
420	42	-34.31	3.431
460	46	-22.93	2.293
500	50	-1.56	0.156
540	54	33.95	3.395
559	55.9	46.08	4.608
580	58	31.23	3.123
630	63	0	0

t = 72 hr

x (mm)	x/bo	y (mm)	y/bo
200	20	0	0
210	21	-2.11	-0.211
220	22	-4.46	-0.446
230	23	-6.82	-0.682
240	24	-9.52	-0.952
260	26	-15.5	-1.55
280	28	-21.88	-2.188
300	30	-27.49	-2.749
320	32	-31.59	-3.159
340	34	-35.19	-3.519
370	37	-37.72	-3.772
400	40	-38.51	-3.851
450	45	-32.8	-3.28
500	50	-9.17	-0.917
550	55	26.7	2.67
570	57	46.15	4.615
600	60	31.38	3.138
640	64	0	0

t = 96 hr

x (mm)	x/bo	y (mm)	y/bo
200	20	0	0
210	21	-3	-0.3
220	22	-4.1	-0.41
230	23	-7.78	-0.778
240	24	-9.52	-0.952
260	26	-16.12	-1.612
280	28	-21.79	-2.179
300	30	-28.48	-2.848
320	32	-31.99	-3.199
340	34	-36.17	-3.617
370	37	-38.73	-3.873
400	40	-38.88	-3.888
450	45	-34.8	-3.48
500	50	-11.17	-1.117
550	55	28.7	2.87
570	57	46.33	4.633
600	60	32.98	3.298
640	64	0	0

$\alpha = 30°$

t = 1 hr

x (mm)	x/bo	y (mm)	y/bo
110	11	0	0
150	15	-22.89	-2.289
175	17.5	-32.26	-3.226
190	19	-37.46	-3.746
225	22.5	-44.02	-4.402
250	25	-34.29	-3.429
300	30	-9.23	-0.923
350	35	21.04	2.104
373	37.3	37.54	3.754
400	40	25.5	2.55
426	42.6	0	0

t = 3 hr

x (mm)	x/bo	y (mm)	y/bo
107	10.7	0	0
150	15	-24.36	2.436
175	17.5	-35.13	3.513
192	19.2	-42.29	4.229
225	22.5	-45.95	4.595
250	25	-38.96	3.896
300	30	-12.1	-1.21
350	35	22.42	2.242
382	38.2	42.13	4.213
400	40	29.71	2.971
443	44.3	0	0

t = 6 hr

x (mm)	x/bo	y (mm)	y/bo
107	10.7	0	0
150	15	-24.81	-2.481
200	20	-40.58	-4.058
230	23	-47.03	-4.703
250	25	-43.22	-4.322
300	30	-12.64	-1.264
350	35	12.62	1.262
390	39	42.6	4.26
400	40	39.09	3.909
425	42.5	21.8	2.18
452	45.2	0	0

t = 24 hr				t = 48 hr				t = 72 hr			
x (mm)	x/bo	y (mm)	y/bo	x (mm)	x/bo	y (mm)	y/bo	x (mm)	x/bo	y (mm)	y/bo
105	10.5	0	0	102	10.2	0	0	102	10.2	0	0
150	15	-27.13	-2.713	150	15	-28.51	2.851	150	15	-27.71	-2.771
200	20	-44.36	-4.436	200	20	-46.71	4.671	200	20	-46.37	-4.637
235	23.5	-49.75	-4.975	250	25	-51.3	-5.13	250	25	-54.36	-5.436
250	25	-45.78	-4.578	300	30	-24.71	2.471	300	30	-27.75	-2.775
300	30	-24.69	-2.469	350	35	1.65	0.165	350	35	2.2	0.22
350	35	5.88	0.588	400	40	37.46	3.746	400	40	39.2	3.92
400	40	40.19	4.019	406	40.6	45.5	4.55	416	41.6	48.52	4.852
405	40.5	43.97	4.397	450	45	21.6	2.16	450	45	30.29	3.029
425	42.5	35.78	3.578	480	48	0	0	480	48	0	0
475	47.5	0	0								

$\alpha = 45°$

t = 1 hr				t = 3 hr				t = 6 hr			
x (mm)	x/bo	y (mm)	y/bo	x (mm)	x/bo	y (mm)	y/bo	x (mm)	x/bo	y (mm)	y/bo
54	5.4	0	0	54	5.4	0	0	-54	5.4	0	-0
70	7	-10.05	-1.005	70	7	-14.89	1.489	70	7	-14.95	-1.495
85	8.5	-21.56	-2.156	85	8.5	-22.32	2.232	85	8.5	-23.42	-2.342
100	10	-30.57	-3.057	100	10	-32.47	3.247	100	10	-32.45	-3.245
125	12.5	-46.63	-4.663	125	12.5	-47.12	4.712	135	13.5	-48.49	-4.849
150	15	-40.93	-4.093	150	15	-47.75	4.775	150	15	-50.84	-5.084
200	20	-19.68	-1.968	200	20	-24.98	2.498	200	20	-28.27	-2.827
250	25	11.35	1.135	250	25	5.27	0.527	250	25	2.57	0.257
300	30	41.4	4.14	275	27.5	22.44	2.244	300	30	33.82	3.382
325	32.5	25.26	2.526	312	31.2	43.8	4.38	322	32.2	45.89	4.589
360	36	0	0	325	32.5	35.41	3.541	340	34	38	3.8
				375	37.5	0	0	387	38.7	0	0

t = 24 hr				t = 48 hr				t = 72 hr			
x (mm)	x/bo	y (mm)	y/bo	x (mm)	x/bo	y (mm)	y/bo	x (mm)	x/bo	y (mm)	y/bo
54	5.4	0	0	54	5.4	0	0	54	5.4	0	0
70	7	-17.68	-1.768	70	7	-18.93	1.893	70	7	-18.48	-1.848
85	8.5	-24.34	-2.434	85	8.5	-25.11	2.51	85	8.5	-24.78	-2.478
100	10	-32.04	-3.204	100	10	-31.76	3.176	100	10	-32.67	-3.267
125	12.5	-47.53	-4.753	125	12.5	-47.02	4.702	125	12.5	-48.11	-4.811
135	13.5	-52.49	-5.249	150	15	-57.49	5.749	150	15	-58.89	-5.889
150	15	-57.08	-5.708	200	20	-33.8	-3.38	200	20	-36.52	-3.652
200	20	-32.82	-3.282	250	25	-3.66	0.366	250	25	-5.33	-0.533
250	25	0.88	0.088	300	30	25.89	2.589	260	26	0	0
300	30	28.8	2.88	342	34.2	49.21	4.921	300	30	23.26	2.326
335	33.5	48.89	4.889	350	35	45.89	4.589	344	34.4	50.01	5.001
350	35	39.43	3.943	375	37.5	23.79	2.379	375	37.5	28.66	2.866
412	41.2	0	0	413	41.3	0	0	415	41.5	0	0

$\alpha = 90°$

t = 1 hr				t = 3 hr				t = 6 hr			
x (mm)	x/bo	y (mm)	y/bo	x (mm)	x/bo	y (mm)	y/bo	x (mm)	x/bo	y (mm)	y/bo
85	8.5	0	0	92	9.2	0	0	94	9.4	0	0
70	7	11.48	1.148	80	8	10.47	1.047	80	8	10	1
60	6	7.56	0.756	74	7.4	11.25	1.125	77	7.7	11.28	1.128
40	4	-6.03	-0.603	60	6	4.24	0.424	60	6	3.69	0.369
20	2	-13.22	-1.322	40	4	-7.06	0.706	40	4	-8.24	-0.824
0	0	-16.33	-1.633	20	2	-14.76	1.476	20	2	-15.53	-1.553
-20	-2	-13.22	-1.322	0	0	-18.76	1.876	0	0	-20.24	-2.024
-40	-4	-6.03	-0.603	-20	-2	-14.76	1.476	-20	-2	-15.53	-1.553
-60	-6	7.56	0.756	-40	-4	-7.06	0.706	-40	-4	-8.24	-0.824
-70	-7	11.48	1.148	-60	-6	4.24	0.424	-60	-6	3.69	0.369
-85	-8.5	0	0	-74	-7.4	11.25	1.125	-77	-7.7	11.28	1.128
				-80	-8	10.47	1.047	-80	-8	10	1
				-92	-9.2	0	0	-94	-9.4	0	0

t = 24 hr				t = 48 hr				t = 72 hr			
x (mm)	x/bo	y (mm)	y/bo	x (mm)	x/bo	y (mm)	y/bo	x (mm)	x/bo	y (mm)	y/bo
100	10	0	0	110	11	0	0	112	11.2	0	0
82.5	8.25	12.39	1.239	98	9.8	12.69	1.269	99.5	9.95	12.89	1.289
60	6	1.43	0.143	80	8	7.79	0.779	80	8	8.23	0.823
58	5.8	0	0	60	6	-3.69	0.369	60	6	-3.78	-0.378
40	4	-15.23	-1.532	40	4	-15.23	1.523	40	4	-15.9	-1.59
20	2	-20.24	-2.024	20	2	-22.95	2.295	20	2	-23.33	-2.333
0	0	-23.78	-2.378	0	0	-25.86	2.586	0	0	-25.99	-2.599
-20	-2	-20.24	-2.024	-20	-2	-22.95	2.295	-20	-2	-23.33	-2.333
-40	-4	-15.23	-1.532	-40	-4	-15.23	1.523	-40	-4	-15.9	-1.59
-60	-6	1.43	0.143	-60	-6	-3.69	0.369	-60	-6	-3.78	-0.378
-82.5	-8.25	12.39	1.239	-80	-8	7.79	0.779	-80	-8	8.23	0.823
-100	-10	0	0	-98	-9.8	12.69	1.269	-99.5	9.95	12.89	1.289
				-110	-11	0	0	-112	11.2	0	0

Table B.3: Scour hole perimeters

Plunging case:

$\alpha = 0°$

t = 1 hr				t = 3 hr				t =6 hr			
x (mm)	x/b_o	z (mm)	z/b_o	x (mm)	x/b_o	z (mm)	z/b_o	x (mm)	x/b_o	z (mm)	z/b_o
170	17	0	0	169	16.9	0	0	169	16.9	0	0
215	21.5	-53	-5.3	219	21.9	-54	-5.4	219	21.9	-59	-5.9
265	26.5	-67	-6.7	269	26.9	-69	-6.9	269	26.9	-77	-7.7
315	31.5	-72	-7.2	319	31.9	-76	-7.6	319	31.9	-80	-8
365	36.5	-40	-4	369	36.9	-63	-6.3	369	36.9	-67	-6.7
379	37.9	0	0	411	41.1	0	0	415	41.5	0	0
365	36.5	40	4	369	36.9	60	6	369	36.9	66	6.6
315	31.5	74	7.4	319	31.9	83	8.3	319	31.9	80	8
265	26.5	67	6.7	269	26.9	76	7.6	269	26.9	77	7.7
215	21.5	50	5	219	21.9	53	5.3	219	21.9	57	5.7
170	17	0	0	169	16.9	0	0	169	16.9	0	0

t = 24 hr				t = 48 hr				t = 72 hr			
x (mm)	x/b_o	z (mm)	z/b_o	x (mm)	x/b_o	z (mm)	z/b_o	x (mm)	x/b_o	z (mm)	z/b_o
169	16.9	0	0	169	16.9	0	0	169	16.9	0	0
219	21.9	-60	-6	219	21.9	-63	-6.3	219	21.9	-65	-6.5
269	26.9	-80	-8	269	26.9	-83	-8.3	269	26.9	-86	-8.6
319	31.9	-89	-8.9	319	31.9	-93	-9.3	319	31.9	-96	-9.6
369	36.9	-71	-7.1	369	36.9	-80	-8	369	36.9	-83	-8.3
417	41.7	0	0	424	42.4	0	0	419	41.9	-28	-2.8
369	36.9	71	7.1	369	36.9	80	8	427	42.7	0	0
319	31.9	91	9.1	319	31.9	94	9.4	419	41.9	30	3
269	26.9	84	8.4	269	26.9	82	8.2	369	36.9	83	8.3
219	21.9	66	6.6	219	21.9	63	6.3	319	31.9	94	9.4
169	16.9	0	0	169	16.9	0	0	269	26.9	88	8.8
								219	21.9	70	7
								169	16.9	0	0

$\alpha = 15°$

t = 1 hr				t = 3 hr				t =6 hr			
x (mm)	x/b_o	z (mm)	z/b_o	x (mm)	x/b_o	z (mm)	z/b_o	x (mm)	x/b_o	z (mm)	z/b_o
135	13.5	0	0	135	13.5	0	0	130	13	0	0
185	18.5	-60	-6	185	18.5	-63	-6.3	180	18	-59	-5.9
235	23.5	-75	-7.5	235	23.5	-79	-7.9	230	23	-82	-8.2
285	28.5	-59	-5.9	285	28.5	-80	-8	280	28	-76	-7.6
336	33.6	0	0	335	33.5	-30	-3	330	33	-51.4	-5.14
285	28.5	59	5.9	350	35	0	0	356	35.6	0	0
235	23.5	78	7.8	335	33.5	30	3	330	33	51.4	5.14
185	18.5	61	6.1	285	28.5	80	8	280	28	77	7.7
135	13.5	0	0	235	23.5	81	8.1	230	23	82	8.2
				185	18.5	64	6.4	180	18	61	6.1
				135	13.5	0	0	130	13	0	0

t = 24 hr				t = 48 hr				t = 72 hr			
x (mm)	x/b_o	z (mm)	z/b_o	x (mm)	x/b_o	z (mm)	z/b_o	x (mm)	x/b_o	z (mm)	z/b_o
130	13	0	0	125	12.5	0	0	125	12.5	0	0
180	18	-65	-6.5	135	13.5	-27	-2.7	150	15	-44	-4.4
230	23	-88	-8.8	145	14.5	-37	-3.7	200	20	-78	-7.8
280	28	-92	-9.2	155	15.5	-50	-5	236	23.6	-98	-9.8
330	33	-70	-7	175	17.5	-65	-6.5	270	27	-91	-9.1
374	37.4	0	0	225	22.5	-91	-9.1	300	30	-82	-8.2
330	33	70	7	275	27.5	-86.5	-8.65	350	35	-40	-4
280	28	92	9.2	325	32.5	-62.4	-6.24	369	36.9	0	0
230	23	83	8.3	373	37.3	0	0	350	35	40	4
180	18	60	6	325	32.5	62.4	6.24	300	30	82	8.2
130	13	0	0	275	27.5	86.5	8.65	270	27	93	9.3
				225	22.5	94	9.4	236	23.6	99	9.9
				175	17.5	65	6.5	200	20	80	8
				155	15.5	50	5	150	15	43	4.3
				145	14.5	40	4	125	12.5	0	0
				135	13.5	27	2.7				
				125	12.5	0	0				

$\alpha = 30°$

t = 1 hr				t = 3 hr				t =6 hr			
x (mm)	x/b_o	z (mm)	z/b_o	x (mm)	x/b_o	z (mm)	z/b_o	x (mm)	x/b_o	z (mm)	z/b_o
82	8.2	0	0	79	7.9	0	0	78	7.8	0	0
91	9.1	-36	-3.6	89	8.9	-39	-3.9	89	8.9	-40	-4
101	10.1	-48	-4.8	99	9.9	-52.5	-5.25	99	9.9	-50.5	-5.05
139	13.9	-79	-7.9	109	10.9	-63	-6.3	109	10.9	-62	-6.2
164	16.4	-86	-8.6	139	13.9	-81	-8.1	139	13.9	-80	-8
179	17.9	-89	-8.9	164	16.4	-91	-9.1	164	16.4	-91	-9.1
214	21.4	-79	-7.9	189	18.9	-89	-8.9	189	18.9	-92	-9.2
264	26.4	-50	-5	214	21.4	-87.34	8.734	214	21.4	-90.3	-9.03
283	28.3	0	0	239	23.9	-74.32	7.432	264	26.4	-62	-6.2
264	26.4	50	5	264	26.4	-56.75	5.675	289	28.9	0	0
214	21.4	79	7.9	289	28.9	0	0	264	26.4	62	6.2
179	17.9	83	8.3	264	26.4	56.75	5.675	214	21.4	90.3	9.03
164	16.4	78	7.8	239	23.9	74.32	7.432	189	18.9	92	9.2
139	13.9	-79	-7.9	214	21.4	87.34	8.734	164	16.4	86	8.6
101	10.1	-48	-4.8	189	18.9	89	8.9	139	13.9	73	7.3
91	9.1	-36	-3.6	164	16.4	84	8.4	109	10.9	56	5.6
82	8.2	0	0	139	13.9	74	7.4	99	9.9	46	4.6
				109	10.9	57.5	5.75	89	8.9	37	3.7
				99	9.9	46	4.6	78	7.8	0	0
				89	8.9	30	3				
				79	7.9	0	0				

t = 24 hr				t = 48 hr				t = 72 hr			
x (mm)	x/b_o	z (mm)	z/b_o	x (mm)	x/b_o	z (mm)	z/b_o	x (mm)	x/b_o	z (mm)	z/b_o
76	7.6	0	0	71	7.1	0	0	71	7.1	0	0
91	9.1	-48.5	-4.85	81	8.1	-40	-4	81	8.1	-42	-4.2
101	10.1	-60	-6	91	9.1	-50	-5	91	9.1	-55	-5.5
111	11.1	-70	-7	101	10.1	-65	-6.5	101	10.1	-62	-6.2
139	13.9	-89	-8.9	111	11.1	-73	-7.3	111	11.1	-74	-7.4
164	16.4	-98	-9.8	139	13.9	-90	-9	139	13.9	-92	-9.2
189	18.9	-98	-9.8	164	16.4	-99	-9.9	164	16.4	-99	-9.9
214	21.4	-94	-9.4	189	18.9	-100	-10	189	18.9	-100	-10
239	23.9	-86	-8.6	214	21.4	-96.5	-9.65	214	21.4	-94.6	-9.46
264	26.4	-70	-7	239	23.9	-82	-8.2	239	23.9	-87	-8.7
289	28.9	-40	-4	264	26.4	-68.7	-6.87	264	26.4	-63.5	-6.35
297	29.7	0	0	298	29.8	0	0	306	30.6	0	0
289	28.9	40	4	264	26.4	68.7	6.87	264	26.4	63.5	6.35
264	26.4	70	7	239	23.9	82	8.2	239	23.9	87	8.7
239	23.9	86	8.6	214	21.4	96.5	9.65	214	21.4	94.6	9.46
214	21.4	94	9.4	189	18.9	100	10	189	18.9	100	10
189	18.9	98	9.8	164	16.4	96.5	9.65	164	16.4	99	9.9
164	16.4	89	8.9	139	13.9	85	8.5	139	13.9	89	8.9
139	13.9	78	7.8	111	11.1	68	6.8	111	11.1	72	7.2
111	11.1	58	5.8	101	10.1	61	6.1	101	10.1	63	6.3
101	10.1	51.5	5.15	91	9.1	45	4.5	91	9.1	55	5.5
91	9.1	32	3.2	81	8.1	32.5	3.25	81	8.1	-42	-4.2
76	7.6	0	0	71	7.1	0	0	71	7.1	0	0
				71	7.1	0	0				

$\alpha = 45°$

t = 1 hr				t = 3 hr				t =6 hr			
x (mm)	x/b_o	z (mm)	z/b_o	x (mm)	x/b_o	z (mm)	z/b_o	x (mm)	x/b_o	z (mm)	z/b_o
41	4.1	0	0	35	3.5	0	0	35	3.5	0	0
45	4.5	-25	-2.5	45	4.5	-27	-2.7	45	4.5	-28	-2.8
55	5.5	-40	-4	65	6.5	-50	-5	55	5.5	-43	-4.3
75	7.5	-60	-6	75	7.5	-62	-6.2	65	6.5	-57	-5.7
91	9.1	-70	-7	95	9.5	-76	-7.6	75	7.5	-68	-6.8
111	11.1	-79	-7.9	115	11.5	-79	-7.9	95	9.5	-80	-8
131	13.1	-78.2	-7.82	135	13.5	-84	-8.4	115	11.5	-84	-8.4
171	17.1	-65.2	-6.52	155	15.5	-83	-8.3	135	13.5	-88	-8.8
205	20.5	0	0	205	20.5	-60.2	-6.02	155	15.5	-84	-8.4
171	17.1	65.2	6.52	228	22.8	0	0	205	20.5	-62	-6.2
131	13.1	78.2	7.82	205	20.5	60.2	6.02	230	23	0	0
111	11.1	79	7.9	155	15.5	83	8.3	205	20.5	62	6.2
91	9.1	70	7	135	13.5	84	8.4	155	15.5	84	8.4
75	7.5	60	6	115	11.5	79	7.9	135	13.5	88	8.8
55	5.5	40	4	95	9.5	76	7.6	115	11.5	84	8.4
45	4.5	25	2.5	75	7.5	62	6.2	95	9.5	80	8
41	4.1	0	0	65	6.5	50	5	75	7.5	68	6.8
				45	4.5	27	2.7	65	6.5	57	5.7
				35	3.5	0	0	55	5.5	43	4.3
								45	4.5	28	2.8

t = 24 hr				t = 48 hr				t = 72 hr			
x (mm)	x/b_o	z (mm)	z/b_o	x (mm)	x/b_o	z (mm)	z/b_o	x (mm)	x/b_o	z (mm)	z/b_o
35	3.5	0	0	30	3	0	0	28	2.8	0	0
45	4.5	-36	-3.6	45	4.5	-44	-4.4	45	4.5	-49	-4.9
55	5.5	-53	-5.3	55	5.5	-69	-6.9	55	5.5	-67	-6.7
65	6.5	-70	-7	65	6.5	-77	-7.7	65	6.5	-78	-7.8
75	7.5	-81	-8.1	75	7.5	-84	-8.4	75	7.5	-86	-8.6
105	10.5	-94	-9.4	85	8.5	-91	-9.1	85	8.5	-92	-9.2
135	13.5	-94	-9.4	105	10.5	-97	-9.7	105	10.5	-101	-10.1
165	16.5	-87.5	-8.75	135	13.5	-93	-9.3	135	13.5	-95	-9.5
215	21.5	-52	-5.2	151	15.1	-91	-9.1	151	15.1	-93.3	-9.33
228	22.8	0	0	175	17.5	-84	-8.4	175	17.5	-86	-8.6
215	21.5	52	5.2	195	19.5	-75	-7.5	200	20	-70	-7
165	16.5	87.5	8.75	215	21.5	-55	-5.5	215	21.5	-55	-5.5
135	13.5	94	9.4	225	22.5	-22	-2.2	225	22.5	-22	-2.2
105	10.5	94	9.4	230	23	0	0	230	23	0	0
75	7.5	81	8.1	225	22.5	22	2.2	225	22.5	22	2.2
65	6.5	70	7	215	21.5	55	5.5	215	21.5	55	5.5
55	5.5	51	5.1	195	19.5	75	7.5	200	20	70	7
45	4.5	30	3	175	17.5	84	8.4	175	17.5	86	8.6
35	3.5	0	0	151	15.1	91	9.1	151	15.1	93.3	9.33
				135	13.5	93	9.3	135	13.5	95	9.5
				105	10.5	97	9.7	105	10.5	101	10.1
				85	8.5	91	9.1	85	8.5	92	9.2
				75	7.5	84	8.4	75	7.5	86	8.6
				65	6.5	77	7.7	65	6.5	78	7.8
				55	5.5	69	6.9	55	5.5	67	6.7
				45	4.5	-44	-4.4	45	4.5	49	4.9
				30	3	0	0	28	2.8	0	0

$\alpha = 90°$

t = 1 hr				t = 3 hr				t =6 hr			
x (mm)	x/b_o	z (mm)	z/b_o	x (mm)	x/b_o	z (mm)	z/b_o	x (mm)	x/b_o	z (mm)	z/b_o
49	4.9	0	0	51	5.1	0	0	53	5.3	0	0
40	4	26	2.6	40	4	39	3.9	42	4.2	40	4
20	2	43	4.3	20	2	54	5.4	22	2.2	56	5.6
0	0	48	4.8	0	0	56	5.6	0	0	60	6
-20	-2	43	4.3	-20	-2	54	5.4	-22	-2.2	56	5.6
-40	-4	26	2.6	-40	-4	39	3.9	-42	-4.2	40	4
-49	-4.9	0	0	-51	-5.1	0	0	-53	-5.3	0	0
-40	-4	-26	-2.6	-40	-4	-39	-3.9	-42	-4.2	-40	-4
-20	-2	-43	-4.3	-20	-2	-54	-5.4	-22	-2.2	-56	-5.6
0	0	-48	-4.8	0	0	-56	-5.6	0	0	-60	-6
20	2	-43	-4.3	20	2	-54	-5.4	22	2.2	-56	-5.6
40	4	-26	-2.6	40	4	-39	-3.9	42	4.2	-40	-4
49	4.9	0	0	51	5.1	0	0	53	5.3	0	0
								53	5.3	0	0

t = 24 hr				t = 48 hr				t = 72 hr			
x (mm)	x/b_o	z (mm)	z/b_o	x (mm)	x/b_o	z (mm)	z/b_o	x (mm)	x/b_o	z (mm)	z/b_o
64	6.4	0	0	64	6.4	0	0	64	6.4	0	0
60	6	23	2.3	55	5.5	27	2.7	55	5.5	30	3
40	4	52	5.2	40	4	53	5.3	40	4	54	5.4
20	2	63	6.3	20	2	63	6.3	20	2	64	6.4
0	0	65.4	6.54	0	0	65.7	6.57	0	0	66	6.6
-20	-2	63	6.3	-20	-2	63	6.3	-20	-2	64	6.4
-40	-4	52	5.2	-40	-4	53	5.3	-40	-4	54	5.4
-60	-6	23	2.3	-55	-5.5	27	2.7	-55	-5.5	30	3
-64	-6.4	0	0	-64	-6.4	0	0	-64	-6.4	0	0
-60	-6	-23	-2.3	-55	-5.5	-27	-2.7	-55	-5.5	-30	-3
-40	-4	-52	-5.2	-40	-4	-53	-5.3	-40	-4	-54	-5.4
-20	-2	-63	-6.3	-20	-2	-63	-6.3	-20	-2	-64	-6.4
0	0	-65.4	-6.54	0	0	-65.7	-6.57	0	0	-66	-6.6
20	2	-63	-6.3	20	2	-63	-6.3	20	2	-64	-6.4
40	4	-52	-5.2	40	4	-53	-5.3	40	4	-54	-5.4
60	6	-23	-2.3	55	5.5	-27	-2.7	55	5.5	-30	-3
64	6.4	0	0	64	6.4	0	0	64	6.4	0	0

Non-plunging case:

α = 15°

t = 1 hr				t = 3 hr				t =6 hr			
x (mm)	x/b_o	z (mm)	z/b_o	x (mm)	x/b_o	z (mm)	z/b_o	x (mm)	x/b_o	z (mm)	z/b_o
210	21	0	0	210	21	0	0	200	20	0	0
220	22	-29	-2.9	220	22	-28	-2.8	220	22	-30	-3
240	24	-43	-4.3	240	24	-38	-3.8	240	24	-40	-4
260	26	-43	-4.3	260	26	-47	-4.7	260	26	-48	-4.8
300	30	-49	-4.9	280	28	-52.6	-5.26	280	28	-55	-5.5
340	34	-50.3	-5.03	300	30	-56	-5.6	320	32	-63	-6.3
380	38	-48	-4.8	330	33	-59	-5.9	360	36	-65	-6.5
420	42	-39	-3.9	360	36	-57	-5.7	400	40	-60	-6
460	46	-15	-1.5	400	40	-51	-5.1	440	44	-45	-4.5
477	47.7	0	0	450	45	-29.5	-2.95	480	48	-18	-1.8
460	46	15	1.5	490	49	0	0	494	49.4	0	0
420	42	39	3.9	450	45	29.5	2.95	480	48	18	1.8
380	38	48	4.8	400	40	51	5.1	440	44	45	4.5
340	34	50.3	5.03	360	36	57	5.7	400	40	60	6
300	30	49	4.9	330	33	59	5.9	360	36	65	6.5
260	26	43	4.3	300	30	56	5.6	320	32	63	6.3
240	24	43	4.3	280	28	52.6	5.26	280	28	58	5.8
220	22	29	2.9	260	26	47	4.7	260	26	48	4.8
210	21	0	0	240	24	38	3.8	240	24	40	4
				220	22	28	2.8	220	22	30	3
				210	21	0	0	200	20	0	0

t = 24 hr				t = 48 hr				t = 72 hr			
x (mm)	x/b_o	z (mm)	z/b_o	x (mm)	x/b_o	z (mm)	z/b_o	x (mm)	x/b_o	z (mm)	z/b_o
200	20	0	0	200	20	0	0	200	20	0	0
210	21	-23	-2.3	210	21	-25	-2.5	210	21	-27	-2.7
220	22	-31	-3.1	220	22	-30	-3	220	22	-32	-3.2
240	24	-43	-4.3	230	23	-36	-3.6	230	23	-36	-3.6
260	26	-56	-5.6	240	24	-44	-4.4	240	24	-43	-4.3
280	28	-60	-6	260	26	-52	-5.2	260	26	-54	-5.4
300	30	-72	-7.2	280	28	-65	-6.5	280	28	-63	-6.3
330	33	-78	-7.8	300	30	-72	-7.2	300	30	-71	-7.1
360	36	-83	-8.3	330	33	-83	-8.3	320	32	-80	-8
390	39	-82	-8.2	370	37	-86	-8.6	340	34	-85	-8.5
420	42	-76	-7.6	420	42	-80	-8	370	37	-89	-8.9
450	45	-59.5	-5.95	460	46	-58	-5.8	400	40	-87	-8.7
480	48	-30	-3	500	50	-10	-1	450	45	-72.3	-7.23
501	50.1	0	0	502	50.2	0	0	500	50	-30	-3
480	48	30	3	500	50	10	1	515	51.5	0	0
450	45	59.5	5.95	460	46	58	5.8	500	50	30	3
420	42	76	7.6	420	42	80	8	450	45	72.3	7.23
390	39	82	8.2	370	37	86	8.6	400	40	87	8.7
360	36	83	8.3	330	33	83	8.3	370	37	89	8.9
330	33	78	7.8	300	30	73	7.3	340	34	85	8.5
300	30	72	7.2	280	28	65	6.5	320	32	80	8
280	28	60	6	260	26	53	5.3	300	30	73	7.3
260	26	51	5.1	240	24	44	4.4	280	28	65	6.5
240	24	43	4.3	230	23	36	3.6	260	26	54	5.4
220	22	31	3.1	220	22	30	3	240	24	43	4.3
210	21	23	2.3	210	21	25	2.5	230	23	38	3.8
200	20	0	0	200	20	0	0	220	22	32	3.2
								210	21	-27	-2.7
								200	20	0	0

t = 96 hr

x (mm)	x/b_o	z (mm)	z/b_o
200	20	0	0
210	21	-27	-2.7
220	22	-32	-3.2
230	23	-36	-3.6
240	24	-43	-4.3
260	26	-54	-5.4
280	28	-65	-6.5
300	30	-73	-7.3
320	32	-83	-8.3
340	34	-87	-8.7
370	37	-89	-8.9
400	40	-87	-8.7
450	45	-76	-7.6
500	50	-30	-3
515	51.5	0	0
500	50	30	3
450	45	76	7.6
400	40	87	8.7
370	37	89	8.9
340	34	87	8.7
320	32	83	8.3
300	30	73	7.3
280	28	65	6.5
260	26	54	5.4
240	24	43	4.3
230	23	38	3.8
220	22	32	3.2
210	21	27	2.7
200	20	0	0
200	20	0	0
210	21	-27	-2.7
200	20	0	0

$\alpha = 30°$

t = 1 hr				t = 3 hr				t =6 hr			
x (mm)	x/b_o	z (mm)	z/b_o	x (mm)	x/b_o	z (mm)	z/b_o	x (mm)	x/b_o	z (mm)	z/b_o
110	11	0	0	105	10.5	0	0	107	10.7	0	0
150	15	-54	-5.4	150	15	-61.5	-6.15	150	15	-57	-5.7
175	17.5	-68	-6.8	175	17.5	-73	-7.3	200	20	-79	-7.9
190	19	-73	-7.3	192	19.2	-78	-7.8	250	25	-80	-8
225	22.5	-76.1	-7.61	225	22.5	-77	-7.7	300	30	-50	-5
250	25	-67	-6.7	250	25	-71	-7.1	325	32.5	0	0
300	30	-27	-2.7	300	30	-30	-3	300	30	50	5
317	31.7	0	0	320	32	0	0	250	25	80	8
300	30	27	2.7	300	30	30	3	200	20	79	7.9
250	25	67	6.7	250	25	71	7.1	150	15	57	5.7
225	22.5	76.1	7.61	225	22.5	77	7.7	107	10.7	0	0
190	19	73	7.3	192	19.2	78	7.8				
175	17.5	68	6.8	175	17.5	73	7.3				
150	15	54	5.4	150	15	61.5	6.15				
110	11	0	0	105	10.5	0	0				

t = 24 hr				t = 48 hr				t = 72 hr			
x (mm)	x/b_o	z (mm)	z/b_o	x (mm)	x/b_o	z (mm)	z/b_o	x (mm)	x/b_o	z (mm)	z/b_o
105	10.5	0	0	102	10.2	0	0	102	10.2	0	0
150	15	-61.8	-6.18	150	15	-62.5	-6.25	150	15	-64.5	-6.45
200	20	-82.3	-8.23	200	20	-88.5	-8.85	200	20	-92	-9.2
250	25	-88	-8.8	250	25	-103	-10.3	250	25	-104	-10.4
300	30	-57	-5.7	300	30	-67.6	-6.76	300	30	-75.3	-7.53
342	34.2	0	0	346	34.6	0	0	347	34.7	0	0
300	30	57	5.7	300	30	67.6	6.76	300	30	75.3	7.53
250	25	88	8.8	250	25	103	10.3	250	25	104	10.4
200	20	82.3	8.23	200	20	88.5	8.85	200	20	92	9.2
150	15	61.8	6.18	150	15	62.5	6.25	150	15	64.5	6.45
105	10.5	0	0	102	10.2	0	0	102	10.2	0	0

$\alpha = 45°$

t = 1 hr				t = 3 hr				t =6 hr			
x (mm)	x/b_o	z (mm)	z/b_o	x (mm)	x/b_o	z (mm)	z/b_o	x (mm)	x/b_o	z (mm)	z/b_o
54	5.4	0	0	54	5.4	0	0	54	5.4	0	0
70	7	-41	-4.1	70	7	-54	-5.4	70	7	-50.5	-5.05
85	8.5	-57	-5.7	85	8.5	-65	-6.5	85	8.5	-65	-6.5
100	10	-66	-6.6	100	10	-76	-7.6	100	10	-74.5	-7.45
125	12.5	-78	-7.8	125	12.5	-84	-8.4	135	13.5	-88.5	-8.85
150	15	-74.5	-7.45	150	15	-82	-8.2	150	15	-87.5	-8.75
200	20	-58	-5.8	200	20	-68	-6.8	200	20	-78	-7.8
232	23.2	0	0	243	24.3	0	0	246	24.6	0	0
200	20	58	5.8	200	20	68	6.8	200	20	78	7.8
150	15	74.5	7.45	150	15	82	8.2	150	15	87.5	8.75
125	12.5	78	7.8	125	12.5	84	8.4	135	13.5	88.5	8.85
100	10	66	6.6	100	10	76	7.6	100	10	74.5	7.45
85	8.5	57	5.7	85	8.5	65	6.5	85	8.5	65	6.5
70	7	41	4.1	70	7	54	5.4	70	7	50.5	5.05
54	5.4	0	0	54	5.4	0	0	54	5.4	0	0

t = 24 hr				t = 48 hr				t = 72 hr			
x (mm)	x/b_o	z (mm)	z/b_o	x (mm)	x/b_o	z (mm)	z/b_o	x (mm)	x/b_o	z (mm)	z/b_o
54	5.4	0	0	54	5.4	0	0	54	5.4	0	0
70	7	-47.8	-4.78	70	7	-60	-6	70	7	-50.5	-5.05
85	8.5	-67.3	-6.73	85	8.5	-72	-7.2	85	8.5	-68.5	-6.85
100	10	-79.3	-7.93	100	10	-82	-8.2	100	10	-80	-8
125	12.5	-92.3	-9.23	125	12.5	-95	-9.5	125	12.5	-92.5	-9.25
135	13.5	-94.3	-9.43	150	15	-97	-9.7	150	15	-99.5	-9.95
150	15	-94	-9.4	200	20	-87	-8.7	200	20	-90	-9
200	20	-87	-8.7	250	25	-30	-3	250	25	-38.5	-3.85
248	24.8	0	0	257	25.7	0	0	260	26	0	0
200	20	87	8.7	250	25	30	3	250	25	38.5	3.85
150	15	94	9.4	200	20	87	8.7	200	20	90	9
135	13.5	94.3	9.43	150	15	97	9.7	150	15	99.5	9.95
125	12.5	92.3	9.23	125	12.5	95	9.5	125	12.5	92.5	9.25
100	10	79.3	7.93	100	10	82	8.2	100	10	80	8
85	8.5	67.3	6.73	85	8.5	72	7.2	85	8.5	68.5	6.85
70	7	47.8	4.78	70	7	60	6	70	7	50.5	5.05
54	5.4	0	0	54	5.4	0	0	54	5.4	0	0

$\alpha = 90°$

t = 1 hr				t = 3 hr				t =6 hr			
x (mm)	x/b_o	z (mm)	z/b_o	x (mm)	x/b_o	z (mm)	z/b_o	x (mm)	x/b_o	z (mm)	z/b_o
50	5	0	0	52.5	5.25	0	0	54	5.4	0	0
40	4	21	2.1	40	4	35	3.5	40	4	38	3.8
20	2	40	4	20	2	51	5.1	20	2	53	5.3
0	0	48	4.8	0	0	53	5.3	0	0	54	5.4
-20	-2	40	4	-20	-2	51	5.1	-20	-2	53	5.3
-40	-4	21	2.1	-40	-4	35	3.5	-40	-4	38	3.8
-50	-5	0	0	-52.5	-5.25	0	0	-54	-5.4	0	0
-40	-4	-21	-2.1	-40	-4	-35	-3.5	-40	-4	-38	-3.8
-20	-2	-40	-4	-20	-2	-51	-5.1	-20	-2	-53	-5.3
0	0	-48	-4.8	0	0	-53	-5.3	0	0	-54	-5.4
20	2	-40	-4	20	2	-51	-5.1	20	2	-53	-5.3
40	4	-21	-2.1	40	4	-35	-3.5	40	4	-38	-3.8
50	5	0	0	52.5	5.25	0	0	54	5.4	0	0

t = 24 hr				t = 48 hr				t = 72 hr			
x (mm)	x/b_o	z (mm)	z/b_o	x (mm)	x/b_o	z (mm)	z/b_o	x (mm)	x/b_o	z (mm)	z/b_o
65	6.5	0	0	66	6.6	0	0	66	6.6	0	0
55	5.5	27	2.7	55	5.5	29	2.9	55	5.5	30	3
40	4	44	4.4	40	4	45	4.5	40	4	46	4.6
20	2	58	5.8	20	2	58	5.8	20	2	60	6
0	0	62	6.2	0	0	62	6.2	0	0	65	6.5
-20	-2	58	5.8	-20	-2	58	5.8	-20	-2	60	6
-40	-4	44	4.4	-40	-4	45	4.5	-40	-4	46	4.6
-55	-5.5	27	2.7	-55	-5.5	29	2.9	-55	-5.5	30	3
-65	-6.5	0	0	-66	-6.6	0	0	-66	-6.6	0	0
-55	-5.5	-27	-2.7	-55	-5.5	-29	-2.9	-55	-5.5	-30	-3
-40	-4	-44	-4.4	-40	-4	-45	-4.5	-40	-4	-46	-4.6
-20	-2	-58	-5.8	-20	-2	-58	-5.8	-20	-2	-60	-6
0	0	-62	-6.2	0	0	-62	-6.2	0	0	-65	-6.5
20	2	-58	-5.8	20	2	-58	-5.8	20	2	-60	-6
40	4	-44	-4.4	40	4	-45	-4.5	40	4	-46	-4.6
55	5.5	-27	-2.7	55	5.5	-29	-2.9	55	5.5	-30	-3
65	6.5	0	0	66	6.6	0	0	66	6.6	0	0

Table B.4: Ridge perimeters

Plunging case:

$\alpha = 0°$

t = 1 hr				t = 3 hr				t =6 hr			
x (mm)	x/b_o	z (mm)	z/b_o	x (mm)	x/b_o	z (mm)	z/b_o	x (mm)	x/b_o	z (mm)	z/b_o
265	26.5	-67	-6.7	269	26.9	-76	-7.6	269	26.9	-77	-7.7
315	31.5	-81	-8.1	319	31.9	-84	-8.4	319	31.9	-92	-9.2
365	36.5	-97	-9.7	369	36.9	-100	-10	369	36.9	-108	-10.8
415	41.5	-90	-9	419	41.9	-108	-10.8	419	41.9	-117	-11.7
465	46.5	-64	-6.4	469	46.9	-100	-10	469	46.9	-110	-11
489	48.9	0	0	520	52	-53	-5.3	519	51.9	-74	-7.4
465	46.5	61	6.1	537	53.7	0	0	547.5	54.75	0	0
415	41.5	94	9.4	520	52	59	5.9	519	51.9	72	7.2
365	36.5	99	9.9	469	46.9	104	10.4	469	46.9	106	10.6
315	31.5	83	8.3	419	41.9	112	11.2	419	41.9	115	11.5
265	26.5	67	6.7	369	36.9	103	10.3	369	36.9	105	10.5
				319	31.9	87	8.7	319	31.9	92	9.2
				269	26.9	76	7.6	269	26.9	77	7.7

t = 24 hr				t = 48 hr				t = 72 hr			
x (mm)	x/b_o	z (mm)	z/b_o	x (mm)	x/b_o	z (mm)	z/b_o	x (mm)	x/b_o	z (mm)	z/b_o
269	26.9	-82	-8.2	269	26.9	-83	-8.3	269	26.9	-86	-8.6
319	31.9	-97	-9.7	319	31.9	-100	-10	319	31.9	-104	-10.4
369	36.9	-113	-11.3	369	36.9	-120	-12	369	36.9	-123	-12.3
419	41.9	-123	-12.3	419	41.9	-126	-12.6	419	41.9	-128	-12.8
469	46.9	-112	-11.2	469	46.9	-118	-11.8	469	46.9	-120	-12
519	51.9	-74	-7.4	519	51.9	-90	-9	519	51.9	-92	-9.2
551	55.1	0	0	558	55.8	0	0	560	56	0	0
519	51.9	77	7.7	519	51.9	89	8.9	519	51.9	90	9
469	46.9	111	11.1	469	46.9	118	11.8	469	46.9	119	11.9
419	41.9	119	11.9	419	41.9	125	12.5	419	41.9	128	12.8
369	36.9	113	11.3	369	36.9	117	11.7	369	36.9	120	12
319	31.9	97	9.7	319	31.9	100	10	319	31.9	103	10.3
269	26.9	82	8.2	269	26.9	83	8.3	269	26.9	88	8.8

$\alpha = 15°$

t = 1 hr				t = 3 hr				t =6 hr			
x (mm)	x/b_o	z (mm)	z/b_o	x (mm)	x/b_o	z (mm)	z/b_o	x (mm)	x/b_o	z (mm)	z/b_o
235	23.5	-75	-7.5	235	23.5	-79	-7.9	230	23	-76	-7.6
285	28.5	-95	-9.5	285	28.5	-94	-9.4	280	28	-98	-9.8
335	33.5	-100	-10	335	33.5	-108	-10.8	330	33	-110	-11
385	38.5	-93	-9.3	385	38.5	-106	-10.6	380	38	-115	-11.5
425	42.5	-62	-6.2	435	43.5	-86	-8.6	430	43	-94	-9.4
450	45	0	0	482	48.2	0	0	480	48	0	0
425	42.5	64	6.4	435	43.5	94	9.4	430	43	94	9.4
385	38.5	104	10.4	385	38.5	114	11.4	380	38	118	11.8
335	33.5	109	10.9	335	33.5	115	11.5	330	33	120	12
285	28.5	99	9.9	285	28.5	99	9.9	280	28	105	10.5
235	23.5	78	7.8	235	23.5	81	8.1	230	23	81	8.1
235	23.5	-75	-7.5	235	23.5	-79	-7.9	230	23	-76	-7.6

t = 24 hr				t = 48 hr				t = 72 hr			
x (mm)	x/b_o	z (mm)	z/b_o	x (mm)	x/b_o	z (mm)	z/b_o	x (mm)	x/b_o	z (mm)	z/b_o
230	23	-88	-8.8	225	22.5	-88	-8.8	236	23.6	-93	-9.3
280	28	-106	-10.6	275	27.5	-108	-10.8	270	27	-110	-11
330	33	-124	-12.4	325	32.5	-121	-12.1	300	30	-118	-11.8
380	38	-128	-12.8	375	37.5	-121	-12.1	350	35	-128	-12.8
430	43	-118	-11.8	425	42.5	-113	-11.3	400	40	-128	-12.8
480	48	-85	-8.5	475	47.5	-75.5	-7.55	450	45	-104	-10.4
509	50.9	0	0	504	50.4	0	0	475	47.5	-87	-8.7
480	48	82	8.2	475	47.5	88	8.8	508	50.8	0	0
430	43	118	11.8	425	42.5	125	12.5	475	47.5	89	8.9
380	38	128	12.8	375	37.5	132	13.2	450	45	115	11.5
330	33	122	12.2	325	32.5	131	13.1	400	40	128	12.8
280	28	105	10.5	275	27.5	113	11.3	350	35	130	13
230	23	-88	-8.8	225	22.5	91	9.1	300	30	120	12
				225	22.5	-88	-8.8	270	27	110	11
								236	23.6	93	9.3

$\alpha = 30°$

t = 1 hr				t = 3 hr				t =6 hr			
x (mm)	x/b_o	z (mm)	z/b_o	x (mm)	x/b_o	z (mm)	z/b_o	x (mm)	x/b_o	z (mm)	z/b_o
17.9	-89	-8.9	17.9	164	16.4	-91	-9.1	164	16.4	-91	-9.1
21.4	-100	-10	21.4	189	18.9	-100	-10	189	18.9	-102	-10.2
26.4	-107	-10.7	26.4	214	21.4	-105	-10.5	214	21.4	-109	-10.9
31.4	-106	-10.6	31.4	239	23.9	-109.5	10.95	264	26.4	-116	-11.6
36.4	-85	-8.5	36.4	264	26.4	-113	-11.3	314	31.4	-120	-12
40	0	0	40	314	31.4	-114.5	11.45	364	36.4	-108	-10.8
36.4	85	8.5	36.4	364	36.4	-106	-10.6	389	38.9	-97.5	-9.75
31.4	99	9.9	31.4	389	38.9	-84	-8.4	427	42.7	0	0
26.4	101	10.1	26.4	424	42.4	0	0	389	38.9	95	9.5
21.4	94	9.4	21.4	389	38.9	81	8.1	364	36.4	108	10.8
17.9	83	8.3	17.9	364	36.4	101	10.1	314	31.4	118	11.8
				314	31.4	107	10.7	264	26.4	116	11.6
				264	26.4	106	10.6	214	21.4	107	10.7
				239	23.9	102	10.2	189	18.9	100	10.0
				214	21.4	92	9.2	164	16.4	90	9.0
				189	18.9	100	-10				
				164	16.4	91	-9.1				

t = 24 hr				t = 48 hr				t = 72 hr			
x (mm)	x/b_o	z (mm)	z/b_o	x (mm)	x/b_o	z (mm)	z/b_o	x (mm)	x/b_o	z (mm)	z/b_o
164	16.4	-98	-9.8	164	16.4	-99	-9.9	164	16.4	-99	-9.9
189	18.9	-108	-10.8	189	18.9	-110	-11	189	18.9	-109	-10.9
214	21.4	-115	-11.5	214	21.4	-118	-11.8	214	21.4	-115	-11.5
239	23.9	-119	-11.9	239	23.9	-122	-12.2	239	23.9	-121	-12.1
264	26.4	-123	-12.3	264	26.4	-127	-12.7	264	26.4	-125	-12.5
289	28.9	-126	-12.6	314	31.4	-126.5	12.65	289	28.9	-127	-12.7
314	31.4	-124	-12.4	364	36.4	-118	-11.8	314	31.4	-129	-12.9
339	33.9	-120	-12	414	41.4	-88	-8.8	339	33.9	-123	-12.3
367	36.7	-114	-11.4	444	44.4	0	0	364	36.4	-114	-11.4
389	38.9	-106	-10.6	414	41.4	83	8.3	389	38.9	-103	-10.3
414	41.4	-84	-8.4	364	36.4	119	11.9	414	41.4	-85	-8.5
444	44.4	0	0	314	31.4	124	12.4	444	44.4	0	0
414	41.4	83	8.3	264	26.4	121	12.1	414	41.4	95	9.5
389	38.9	106	10.6	239	23.9	118	11.8	389	38.9	111	11.1
367	36.7	114	11.4	214	21.4	113.5	11.35	364	36.4	119	11.9
339	33.9	120	12	189	18.9	108	10.8	339	33.9	126	12.6
314	31.4	123	12.3	164	16.4	96.5	9.65	314	31.4	126	12.6
289	28.9	125	12.5	164	16.4	-99	-9.9	289	28.9	125	12.5
264	26.4	120	12	189	18.9	-110	-11	264	26.4	123	12.3
239	23.9	117	11.7	214	21.4	-118	-11.8	239	23.9	119	11.9
214	21.4	114	11.4	239	23.9	-122	-12.2	214	21.4	114	11.4
189	18.9	107	10.7	264	26.4	-127	-12.7	189	18.9	107	10.7
164	16.4	98	9.8	314	31.4	-126.5	12.65	164	16.4	99	9.9

$\alpha = 45°$

t = 1 hr				t = 3 hr				t =6 hr			
x (mm)	x/b_o	z (mm)	z/b_o	x (mm)	x/b_o	z (mm)	z/b_o	x (mm)	x/b_o	z (mm)	z/b_o
91	9.1	-80	-8	95	9.5	-76	-7.6	95	9.5	-74	-7.4
111	11.1	-96	-9.6	115	11.5	-88	-8.8	115	11.5	-90	-9
131	13.1	-101	-10.1	135	13.5	-97	-9.7	135	13.5	-99	-9.9
171	17.1	-106	-10.6	155	15.5	-104	-10.4	155	15.5	-102	-10.2
211	21.1	-106	-10.6	205	20.5	-106	-10.6	205	20.5	-105	-10.5
251	25.1	-97	-9.7	228	22.8	-105	-10.5	255	25.5	-101	-10.1
271	27.1	-87	-8.7	255	25.5	-105	-10.5	291	29.1	-89	-8.9
311	31.1	0	0	301	30.1	-80	-8	305	30.5	-80	-8
271	27.1	87	8.7	336	33.6	0	0	353	35.3	0	0
251	25.1	97	9.7	301	30.1	80	8	305	30.5	80	8
211	21.1	106	10.6	255	25.5	105	10.5	291	29.1	89	8.9
171	17.1	106	10.6	228	22.8	105	10.5	255	25.5	104	10.4
131	13.1	101	10.1	205	20.5	106	10.6	205	20.5	106	10.6
111	11.1	96	9.6	155	15.5	100	10	155	15.5	104	10.4
91	9.1	80	8	135	13.5	95	9.5	135	13.5	98	9.8
				115	11.5	88	-8.8	115	11.5	93	9.3
				95	9.5	76	7.6	95	9.5	79	7.9

t = 24 hr				t = 48 hr				t = 72 hr			
x (mm)	x/b_o	z (mm)	z/b_o	x (mm)	x/b_o	z (mm)	z/b_o	x (mm)	x/b_o	z (mm)	z/b_o
105	10.5	-94	-9.4	85	8.5	-91	-9.1	105	10.5	-97	-9.7
135	13.5	-107	-10.7	105	10.5	-103	-10.3	135	13.5	-107	-10.7
165	16.5	-113	-11.3	135	13.5	-112.5	11.25	151	15.1	-113	-11.3
215	21.5	-116	-11.6	151	15.1	-116	-11.6	175	17.5	-117	-11.7
265	26.5	-118	-11.8	175	17.5	-117	-11.7	225	22.5	-125	-12.5
305	30.5	-103	-10.3	225	22.5	-125	-12.5	275	27.5	-125	-12.5
315	31.5	-103	-10.3	275	27.5	-120	-12	304	30.4	-110	-11
360	36	0	0	315	31.5	-98	-9.8	325	32.5	-95	-9.5
315	31.5	103	10.3	345	34.5	-75	-7.5	345	34.5	-75	-7.5
305	30.5	103	10.3	369	36.9	0	0	369	36.9	0	0
265	26.5	118	11.8	345	34.5	75	7.5	345	34.5	75	7.5
215	21.5	116	11.6	315	31.5	99	9.9	325	32.5	95	9.5
165	16.5	113	11.3	275	27.5	125	12.5	304	30.4	108	10.8
135	13.5	107	10.7	225	22.5	125	12.5	275	27.5	120	12
105	10.5	94	9.4	175	17.5	123	12.3	225	22.5	123	12.3
				151	15.1	116	11.6	175	17.5	120	12
				135	13.5	109	10.9	151	15.1	115	11.5
				105	10.5	103	10.3	135	13.5	107	10.7
				85	8.5	91	9.1	105	10.5	97	9.7

$\alpha = 90°$

t = 1 hr				t = 3 hr				t =6 hr			
x (mm)	x/b_o	z (mm)	z/b_o	x (mm)	x/b_o	z (mm)	z/b_o	x (mm)	x/b_o	z (mm)	z/b_o
86	8.6	0	0	90	9	0	0	92	9.2	0	0
60	6	62	6.2	60	6	68	6.8	62	6.2	68	6.8
40	4	75	7.5	40	4	83	8.3	42	4.2	81	8.1
20	2	83	8.3	20	2	89	8.9	22	2.2	88	8.8
0	0	86	8.6	0	0	91	9.1	0	0	92.5	9.25
-20	-2	83	8.3	-20	-2	89	8.9	-22	-2.2	88	8.8
-40	-4	75	7.5	-40	-4	83	8.3	-42	-4.2	81	8.1
-60	-6	62	6.2	-60	-6	68	6.8	-62	-6.2	68	6.8
-86	-8.6	0	0	-90	-9	0	0	-92	-9.2	0	0
-60	-6	-62	-6.2	-60	-6	-68	-6.8	-62	-6.2	-68	-6.8
-40	-4	-75	-7.5	-40	-4	-83	-8.3	-42	-4.2	-81	-8.1
-20	-2	-83	-8.3	-20	-2	-89	-8.9	-22	-2.2	-88	-8.8
0	0	-86	-8.6	0	0	-91	-9.1	0	0	-92.5	-9.25
20	2	-83	-8.3	20	2	-89	-8.9	22	2.2	-88	-8.8
40	4	-75	-7.5	40	4	-83	-8.3	42	4.2	-81	-8.1
60	6	-62	-6.2	60	6	-68	-6.8	62	6.2	-68	-6.8
86	8.6	0	0	90	9	0	0	92	9.2	0	0

t = 24 hr				t = 48 hr				t = 72 hr			
x (mm)	x/b_o	z (mm)	z/b_o	x (mm)	x/b_o	z (mm)	z/b_o	x (mm)	x/b_o	z (mm)	z/b_o
100	10	0	0	110	11	0	0	110	11	0	0
80	8	57	5.7	100	10	40	4	100	10	42	4.2
60	6	78	7.8	80	8	68	6.8	80	8	70	7
40	4	88	8.8	60	6	87	8.7	60	6	88	8.8
20	2	95	9.5	40	4	98	9.8	40	4	99	9.9
0	0	97	9.7	20	2	104	10.4	20	2	104	10.4
-20	-2	95	9.5	0	0	105	10.5	0	0	109	10.9
-40	-4	88	8.8	-20	-2	104	10.4	-20	-2	104	10.4
-60	-6	78	7.8	-40	-4	98	9.8	-40	-4	99	9.9
-80	-8	57	5.7	-60	-6	87	8.7	-60	-6	88	8.8
-100	-10	0	0	-80	-8	68	6.8	-80	-8	70	7
-80	-8	-57	-5.7	-100	-10	40	4	-100	-10	42	4.2
-60	-6	-78	-7.8	-110	-11	0	0	-110	-11	0	0
-40	-4	-88	-8.8	-100	-10	-40	-4	-100	-10	-42	-4.2
-20	-2	-95	-9.5	-80	-8	-68	-6.8	-80	-8	-70	-7
0	0	-97	-9.7	-60	-6	-87	-8.7	-60	-6	-88	-8.8
20	2	-95	-9.5	-40	-4	-98	-9.8	-40	-4	-99	-9.9
40	4	-88	-8.8	-20	-2	-104	-10.4	-20	-2	-104	-10.4
60	6	-78	-7.8	0	0	-105	-10.5	0	0	-109	-10.9
80	8	-57	-5.7	20	2	-104	-10.4	20	2	-104	-10.4
100	10	0	0	40	4	-98	-9.8	40	4	-99	-9.9
				60	6	-87	-8.7	60	6	-88	-8.8
				80	8	-68	-6.8	80	8	-70	-7
				100	10	-40	-4	100	10	-42	-4.2
				110	11	0	0	110	11	0	0

Non-plunging case:

$\alpha = 15°$

t = 1 hr				t = 3 hr				t =6 hr			
x (mm)	x/b_o	z (mm)	z/b_o	x (mm)	x/b_o	z (mm)	z/b_o	x (mm)	x/b_o	z (mm)	z/b_o
240	24	-43	-4.3	260	26	-47	-4.7	260	26	-48	-4.8
260	26	-50	-5	280	28	-61	-6.1	280	28	-65	-6.5
300	30	-65	-6.5	300	30	-69.5	-6.95	320	32	-76.5	-7.65
340	34	-76	-7.6	330	33	-75.5	-7.55	360	36	-86.5	-8.65
380	38	-80	-8	360	36	-81.5	-8.15	400	40	-90.5	-9.05
420	42	-81	-8.1	400	40	-87.5	-8.75	440	44	-99.5	-9.95
460	46	-80	-8	450	45	-89.5	-8.95	480	48	-100.5	-10.05
500	50	-70	-7	500	50	-84.5	-8.45	520	52	-93.5	-9.35
540	54	-56	-5.6	550	55	-67	-6.7	560	56	-76.5	-7.65
573	57.3	0	0	583	58.3	0	0	598	59.8	0	0
540	54	56	5.6	550	55	67	6.7	560	56	76.5	7.65
500	50	70	7	500	50	84.5	8.45	520	52	93.5	9.35
460	46	80	8	450	45	89.5	8.95	480	48	100.5	10.05
420	42	81	8.1	400	40	87.5	8.75	440	44	99.5	9.95
380	38	80	8	360	36	81.5	8.15	400	40	90.5	9.05
340	34	76	7.6	330	33	75.5	7.55	360	36	86.5	8.65
300	30	65	6.5	300	30	69.5	6.95	320	32	76.5	7.65
260	26	50	5	280	28	61	6.1	280	28	65	6.5
240	24	43	4.3	260	26	47	4.7	260	26	48	4.8

t = 24 hr				t = 48 hr				t = 72 hr			
x (mm)	x/b_o	z (mm)	z/b_o	x (mm)	x/b_o	z (mm)	z/b_o	x (mm)	x/b_o	z (mm)	z/b_o
360	36	-85	-8.5	360	36	-87	-8.7	370	37	-89	-8.9
390	39	-96	-9.6	370	37	-93	-9.3	400	40	-102	-10.2
420	42	-102	-10.2	420	42	-105	-10.5	450	45	-115	-11.5
450	45	-109	-10.9	460	46	-123	-12.3	500	50	-128.5	-12.85
480	48	-112	-11.2	500	50	-126	-12.6	550	55	-128	-12.8
510	51	-116	-11.6	540	54	-123	-12.3	600	60	-104	-10.4
560	56	-105	-10.5	580	58	-103	-10.3	640	64	0	0
590	59	-60	-6	630	63	0	0	600	60	104	10.4
609	60.9	0	0	580	58	103	10.3	550	55	128	12.8
590	59	60	6	540	54	123	12.3	500	50	128.5	12.85
560	56	105	10.5	500	50	126	12.6	450	45	115	11.5
510	51	116	11.6	460	46	123	12.3	400	40	102	10.2
480	48	112	11.2	420	42	105	10.5	370	37	89	8.9
450	45	109	10.9	370	37	93	9.3				
420	42	102	10.2	360	36	87	8.7				
390	39	96	9.6								
360	36	85	8.5								

$\alpha = 30°$

t = 1 hr				t = 3 hr				t =6 hr			
x (mm)	x/b_o	z (mm)	z/b_o	x (mm)	x/b_o	z (mm)	z/b_o	x (mm)	x/b_o	z (mm)	z/b_o
190	19	-73	-7.3	192	19.2	-78	-7.8	200	20	-79	-7.9
225	22.5	-86	-8.6	225	22.5	-90.5	-9.05	250	25	-103	-10.3
250	25	-95	-9.5	250	25	-97.5	-9.75	300	30	-120	-12
300	30	-107	-10.7	300	30	-109.5	10.95	350	35	-118	-11.8
350	35	-104	-10.4	350	35	-111.5	11.15	400	40	-99	-9.9
400	40	-78	-7.8	400	40	-85.5	-8.55	425	42.5	-78	-7.8
426	42.6	0	0	441	44.1	0	0	452	45.2	0	0
400	40	78	7.8	400	40	85.5	8.55	425	42.5	78	7.8
350	35	104	10.4	350	35	111.5	11.15	400	40	99	9.9
300	30	107	10.7	300	30	109.5	10.95	350	35	118	11.8
250	25	95	9.5	250	25	97.5	9.75	300	30	120	12
225	22.5	86	8.6	225	22.5	90.5	9.05	250	25	103	10.3
190	19	73	7.3	192	19.2	78	7.8	200	20	79	7.9

t = 24 hr				t = 48 hr				t = 72 hr			
x (mm)	x/b_o	z (mm)	z/b_o	x (mm)	x/b_o	z (mm)	z/b_o	x (mm)	x/b_o	z (mm)	z/b_o
200	20	-82.3	-8.23	200	20	-88.5	-8.85	200	20	-92	-9.2
250	25	-106.3	-10.63	250	25	-112.5	11.25	250	25	-113	-11.3
300	30	-124.3	-12.43	300	30	-129.5	12.95	300	30	-129	-12.9
350	35	-130.3	-13.03	350	35	-129.5	12.95	350	35	-137	-13.7
400	40	-116.3	-11.63	400	40	-120	-12	400	40	-125	-12.5
425	42.5	-101.8	-10.18	450	45	-83.5	-8.35	450	45	-98	-9.8
475	47.5	0	0	480	48	0	0	480	48	0	0
425	42.5	101.8	10.18	450	45	83.5	8.35	450	45	98	9.8
400	40	116.3	11.63	400	40	120	12	400	40	125	12.5
350	35	130.3	13.03	350	35	129.5	12.95	350	35	137	13.7
300	30	124.3	12.43	300	30	129.5	12.95	300	30	129	12.9
250	25	106.3	10.63	250	25	112.5	11.25	250	25	113	11.3
200	20	82.3	8.23	200	20	88.5	8.85	200	20	92	9.2

$\alpha = 45°$

t = 1 hr				t = 3 hr				t =6 hr			
x (mm)	x/b_o	z (mm)	z/b_o	x (mm)	x/b_o	z (mm)	z/b_o	x (mm)	x/b_o	z (mm)	z/b_o
125	12.5	-78	-7.8	125	12.5	-84	-8.4	135	13.5	-88.5	-8.85
150	15	-87	-8.7	150	15	-92	-9.2	150	15	-97.5	-9.75
200	20	-93.5	-9.35	200	20	-97	-9.7	200	20	-104.5	-10.45
250	25	-95	-9.5	250	25	-99	-9.9	250	25	-106.5	-10.65
300	30	-88	-8.8	275	27.5	-104	-10.4	300	30	-107.5	-10.75
325	32.5	-72	-7.2	325	32.5	-83.5	-8.35	340	34	-94.5	-9.45
360	36	0	0	372	37.2	0	0	387	38.7	0	0
325	32.5	72	7.2	325	32.5	83.5	8.35	340	34	94.5	9.45
300	30	88	8.8	275	27.5	104	10.4	300	30	107.5	10.75
250	25	95	9.5	250	25	99	9.9	250	25	106.5	10.65
200	20	93.5	9.35	200	20	97	9.7	200	20	104.5	10.45
150	15	87	8.7	150	15	92	9.2	150	15	97.5	9.75
125	12.5	78	7.8	125	12.5	84	8.4	135	13.5	88.5	8.85

t = 24 hr				t = 48 hr				t = 72 hr			
x (mm)	x/b_o	z (mm)	z/b_o	x (mm)	x/b_o	z (mm)	z/b_o	x (mm)	x/b_o	z (mm)	z/b_o
135	13.5	-94.3	-9.43	150	15	-97	-9.7	150	15	-99.5	-9.95
150	15	-101.3	-10.13	200	20	-107	-10.7	200	20	-111.5	-11.15
200	20	-108.3	-10.83	250	25	-113	-11.3	250	25	-112	-11.2
250	25	-107.3	-10.73	300	30	-118	-11.8	300	30	-117.5	-11.75
300	30	-112.8	-11.28	350	35	-100	-10	344	34.4	-105.5	-10.55
350	35	-97.3	-9.73	375	37.5	-77	-7.7	375	37.5	-88.5	-8.85
375	37.5	-84.3	-8.43	412	41.2	0	0	415	41.5	0	0
412	41.2	0	0	375	37.5	77	7.7	375	37.5	88.5	8.85
375	37.5	84.3	8.43	350	35	100	10	344	34.4	105.5	10.55
350	35	97.3	9.73	300	30	118	11.8	300	30	117.5	11.75
300	30	112.8	11.28	250	25	113	11.3	250	25	112	11.2
250	25	107.3	10.73	200	20	107	10.7	200	20	111.5	11.15
200	20	108.3	10.83	150	15	97	9.7	150	15	99.5	9.95
135	13.5	94.3	9.43								
135	13.5	-94.3	-9.43								

$\alpha = 90°$

t = 1 hr				t = 3 hr				t =6 hr			
x (mm)	x/b_o	z (mm)	z/b_o	x (mm)	x/b_o	z (mm)	z/b_o	x (mm)	x/b_o	z (mm)	z/b_o
85	8.5	0	0	92	9.2	0	0	94	9.4	0	0
60	6	60	6	80	8	44.5	4.45	80	8	51	5.1
40	4	75	7.5	60	6	68.5	6.85	60	6	74	7.4
20	2	82	8.2	40	4	82.5	8.25	40	4	85	8.5
0	0	86	8.6	20	2	88.5	8.85	20	2	91	9.1
-20	-2	82	8.2	0	0	90.5	9.05	0	0	94	9.4
-40	-4	75	7.5	-20	-2	88.5	8.85	-20	-2	91	9.1
-60	-6	60	6	-40	-4	82.5	8.25	-40	-4	85	8.5
-85	-8.5	0	0	-60	-6	68.5	6.85	-60	-6	74	7.4
-60	-6	-60	-6	-80	-8	44.5	4.45	-80	-8	51	5.1
-20	-2	-82	-8.2	-92	-9.2	0	0	-94	-9.4	0	0
0	0	-86	-8.6	-80	-8	-44.5	-4.45	-80	-8	-51	-5.1
20	2	-82	-8.2	-60	-6	-68.5	-6.85	-60	-6	-74	-7.4
40	4	-75	-7.5	-40	-4	-82.5	-8.25	-40	-4	-85	-8.5
60	6	-60	-6	-20	-2	-88.5	-8.85	-20	-2	-91	-9.1
85	8.5	0	0	0	0	-90.5	-9.05	0	0	-94	-9.4
				20	2	-88.5	-8.85	20	2	-91	-9.1
				40	4	-82.5	-8.25	40	4	-85	-8.5
				60	6	-68.5	-6.85	60	6	-74	-7.4
				80	8	-44.5	-4.45	80	8	-51	-5.1
				92	9.2	0	0	94	9.4	0	0

t = 24 hr				t = 48 hr				t = 72 hr			
x (mm)	x/b_o	z (mm)	z/b_o	x (mm)	x/b_o	z (mm)	z/b_o	x (mm)	x/b_o	z (mm)	z/b_o
100	10	0	0	110	11	0	0	112	11.2	0	0
82.5	8.25	56.5	5.65	98	9.8	55.5	5.55	99.5	9.95	56.5	5.65
60	6	79.5	7.95	80	8	86	8.6	80	8	86.5	8.65
40	4	88.5	8.85	60	6	96	9.6	60	6	97.5	9.75
20	2	94.5	9.45	40	4	106	10.6	40	4	105	10.5
0	0	97	9.7	20	2	108	10.8	20	2	110	11
-20	-2	94.5	9.45	0	0	110	11	0	0	112	11.2
-40	-4	88.5	8.85	-20	-2	108	10.8	-20	-2	110	11
-60	-6	79.5	7.95	-40	-4	106	10.6	-40	-4	105	10.5
-82.5	-8.25	56.5	5.65	-60	-6	96	9.6	-60	-6	97.5	9.75
-100	-10	0	0	-80	-8	86	8.6	-80	-8	86.5	8.65
-82.5	-8.25	-56.5	-5.65	-98	-9.8	55.5	5.55	-99.5	9.95	56.5	5.65
-60	-6	-79.5	-7.95	-110	-11	0	0	-112	11.2	0	0
-40	-4	-88.5	-8.85	-98	-9.8	-55.5	-5.55	-99.5	9.95	-56.5	-5.65
-20	-2	-94.5	-9.45	-80	-8	-86	-8.6	-80	-8	-86.5	-8.65
0	0	-97	-9.7	-60	-6	-96	-9.6	-60	-6	-97.5	-9.75
20	2	-94.5	-9.45	-40	-4	-106	-10.6	-40	-4	-105	-10.5
40	4	-88.5	-8.85	-20	-2	-108	-10.8	-20	-2	-110	-11
60	6	-79.5	-7.95	0	0	-110	-11	0	0	-112	-11.2
82.5	8.25	-56.5	-5.65	20	2	-108	-10.8	20	2	-110	-11
100	10	0	0	40	4	-106	-10.6	40	4	-105	-10.5
				60	6	-96	-9.6	60	6	-97.5	-9.75
				80	8	-86	-8.6	80	8	-86.5	-8.65
				98	9.8	-55.5	-5.55	99.5	9.95	-56.5	-5.65
				110	11	0	0	112	11.2	0	0

VITA AUCTORIS

Piyali Chaudhuri was born in Kolkata, India. She completed a degree in Civil Engineering at Jadavpur University, India in 2002. She has worked as an Assistant Engineer in Consulting Engineering Services, India for three and half years from July 2002 to December 2005. Presently Piyali Chaudhuri is a candidate for Master of Applied Science degree in Civil Engineering with specialization in Water Resources Engineering at the University of Windsor, Windsor, Ontario, Canada and expects to graduate in September 2007.